

Synthesis of Deuterated Benzene for a Circular Deuterium

Economy

by

Benjamin Kappheim

A thesis

presented to the University of Waterloo

in fulfillment of the

thesis requirement for the degree of

Master of Science

in

Chemistry

Waterloo, Ontario, Canada, 2024

© Benjamin Kappheim 2024

Author's Declaration

I hereby declare that I am the sole author of this thesis. This is a true copy of the thesis, including any required final revisions, as accepted by my examiners.

I understand that my thesis may be made electronically available to the public.

Abstract

Deuterium is an important natural isotope; its unique properties can impart significant effects on molecules with emerging applications across electronics and medicinal industries. Aromatic hydrocarbons or arenes are one example of such compounds where deuterium proves advantageous, breaching limitations in commercial organic-based electronics. Current methods introduce deuterium into molecules through direct hydrogen/deuterium (H/D) exchange reactions which depend on a reliable and high supply of deuterium that has been slowly dwindling in recent years. To continue the exploration of deuterium-enriched compounds and their applications, new methods that use deuterium conservatively to achieve efficient H/D exchange are needed. The Canadian company deutraMed™ has responded to this demand by developing a D₂O refinery capable of recycling deuterium waste. Working in partnership, the work herein will discuss the development of an H/D exchange procedure to deuterate benzene that is compatible with the D₂O refinery. Benzene is a simple arene that is a common motif in compounds related to organic electronics and pharmaceuticals. The large-scale production of deuterated benzene fuels the demand for a versatile building block to access an assortment of compounds relevant to these industries. The development of the H/D exchange procedure found success using hydrothermal conditions to achieve 96% deuteration of benzene at laboratory scale. The results of this work will be beneficial in the further development of this process on an industrial scale.

Acknowledgements

Firstly, I would like to thank my supervisor Dr. Graham Murphy. From our first encounter he embraced my enthusiasm and graciously welcomed me to be a part of his research group for the past 3 years. I am grateful for this generosity, in addition to the support, trust, and patience he has given me during this time.

I would also like to thank the members of my advisory committee, Dr. Michael Chong and Dr. Steve Forsey for their time and commitment to my success. I have learned a great deal from their classes and offering of resources to better my knowledge in organic chemistry. I would like to thank Jan Venne, Blossom Yan, and Val Goodfellow for their assistance with NMR and mass spectrometry. I want to further extend my gratitude to Val Goodfellow, for her assistance and companionship during my time both as a teaching assistant and a colleague. Our time spent sharing stories of woodworking, travelling and music have always brought me tremendous joy and I can only hope the feeling is mutual. I would also like to thank Stacey Lavery, for always being a patient, gregarious educator, and an incredible instructor to work for.

To the members of the Murphy group during my time here, you have all been a wonderful bunch to work alongside. I am very thankful to have been surrounded by supportive peers who all do what they can to see each other succeed. To Avery To, Carlee Montgomery, and Fabio Cuzzucoli, you have each added something special to my experience here and have left impressions that will last a lifetime. To the post-docs Dr. Radell Echemendía Perez and Dr. Yulia Vlasenko, I feel so lucky to have met you both and learned so much from your backgrounds and experiences, your passion and motivation to be great chemists is truly inspiring. I would like to thank Tess Fortier and Will LeBeouf for their incredible efforts as co-op students, and for their friendship. Working with you both was an amazing time and brought enrichment I did not know I needed. I wish the best for your futures and goals in life.

Lastly, I would like to thank my family, friends, and significant others. My success would not be what it is without their nurturing and continual support throughout my studies. For whatever comes next, I know they will be there.

Dedication

To my loved ones

Blaire, Mike, Danika, and Alitsia

And to the animals in my life

Sora, Ginger, Penny, Olive, Bruno, and Izzy

Table of Contents

Author's Declaration	ii
Abstract	iii
Acknowledgements	iv
Dedication	v
List of Figures	vii
List of Tables	ix
List of Abbreviations	x
List of Schemes	xii
Chapter 1: Deuterium	1
1.1 Background	1
1.2 Physicochemical Properties of Deuterium and Associated Applications	3
1.3 Metal-catalyzed Deuteration Methods	9
1.4 Summary	15
Chapter 2: Arene C-H Activated H/D Exchange	16
2.1 Background	16
2.2 Proposal	21
2.3 Synthesis of Benzene-<i>d</i>₆	23
2.3 Conclusions and Future Work	35
2.4 Experimental and Spectral Data	35
References	38
Appendices	47
Appendix 1: Analytical Methods of Benzene H/D Exchange	47
A1.1 Gas-Chromatography Mass Spectrometry	47
A1.2 Quantitative ¹H + ²H Nuclear Magnetic Resonance Spectroscopy	53
Appendix 2: Spectral Data	56

List of Figures

Figure 1-1: A fusion process forming deuterium and helium-3.....	1
Figure 1-2: Deuterated forms of water and hydrogen gas, common industrial sources of deuterium.	2
Figure 1-3: Schematic of the Girdler sulfide process. †.....	3
Figure 1-4: Isotopic effects of heterolytic bond cleavage through difference in zero-point energy. Adapted from ref. ¹³	4
Figure 1-5: KIE of morphine N-demethylation to normorphine. ¹⁴	4
Figure 1-6: Examples of deuterated drugs.	5
Figure 1-7: Deuterated analogue of green OLED host material (left) and plausible mechanism of degradation (right). ³¹	6
Figure 1-8: Impact of crystallization in deuterated solvents (left) versus non-deuterated solvent (right) post-annealing, imparting better stacking.	7
Figure 1-9: Spin states of ² H nuclei.	8
Figure 1-10: DMI images of [6,6’]- ² H ₂ -glucose uptake and metabolism over time, identifying pancreatic cancer based on increased [3,3’]- ² H ₂ -lactate production. ⁴³	9
Figure 1-11: Catalytic deuteration of acetone. ⁴⁶	10
Figure 1-12: Possible reaction kinetic profiles describing instances of inverse KIE state distinguished by the first transition state being influenced by ZPE (left) or having no influence (right). Adapted from ref. ⁷⁰	12
Figure 2-13: Examples of an OLED host material (left) and pharmaceutical drug (right) containing derivatized benzene rings with deuterated motifs.....	16
Figure 2-14: Functionalization of benzene-d ₆ allows for versatile introduction of deuterated phenyl groups for organic electronics (left) and pharmaceuticals (right).....	17
Figure 2-15: Early examples of benzene H/D exchange reactions by Horiuti and Polanyi (1), Ingold, Raisin, and Wilson (2), and Leitch (3).....	18
Figure 2-16: Schematic of circular H/D exchange industrial process incorporating the deutraMed Inc. D2X™ refining process for D ₂ O.....	23
Figure 2-17: Glass pressure vessels (left) used for preliminary reactions with heterogeneous catalyst stirred as a slurry at high temperature (right).....	24
Figure 2-18: Mass spectra of benzene products from Pd/C (left) and Pt/C (right) show that a greater abundance of benzene-d ₁ (79 m/z) product is present using Pt/C.	25
Figure 2-19: The catalyst medium is prepared by dispensing Pt/C as a slurry on filter paper under vacuum suction and dried before using (left). The filter paper is placed inside the Teflon liner on a stand	

to keep it above the liquid surface (right), folding the filter paper allows for larger filter papers to fit inside and does not impact reactivity.....	31
Figure 2-20: Teflon cup insert and disassembled stainless steel jacket of hydrothermal autoclave reactor (left) and sealed reactor (right).....	37
Figure A1-1: Compatibility of different mass spectrometry ionization methods across polarity and analyte mass.....	48
Figure A1-2: Using the standard GC conditions (80 – 200 °C) causes benzene to elute too quickly with the solvent front, leaving a blank result.	50
Figure A1-3: Isothermal GC column temperature of a 1:1 mixture of benzene and benzene-d6 elutes in ~3.75 min. Due to benzene-d6 having a slightly lower boiling point, the peak is instead a coalescence of two unresolved peaks.	51
Figure A1-4: Above 85% D, fragmentation of the benzene ring deflates the calculated %D with no way of discerning cause between fragmentation and presence of an isotopologue. Reasons for inflated %D values below 85% are unclear, accounting for ¹³ C peaks and possible [M+H] adducts contribute ~1% difference, which does not equate with the 10+% increase in values observed.....	52
Figure A1-5: A benzene-d6 standard (99.7% D) shows fragmentation peaks which would coincidentally correspond with isotopologues benzene-d2, -d4, and -d5, resulting in an inaccurate calculated value of 92% D.	53
Figure A1-6: ¹ H NMR spectrum of deuterated benzene (88.9% D, δ 7.3 ppm) with maleic acid as standard (δ 6.3 ppm).	54
Figure A1-7: Full ² H NMR spectrum of deuterated benzene (88.9% D, δ 7.3 ppm) with methanol-d4 (δ 3.24 ppm) as the internal standard (top). Zoomed to show benzene peak.	55

List of Tables

Table 1-1: Impact of Pt(II) Lewis acid on relative rate of N-methylimidazole H/D exchange.....	10
Table 2-1: Pt-catalyzed H/D exchange of substituted arenes using D ₂ O. ^{79,92}	19
Table 2-2: Effect of sterics and side reactions in reverse H/D exchange with mono-substituted benzene. ⁹⁴	20
Table 2-3: Catalyst screening results in glass pressure vessels calculated from mass spectra.....	25
Table 2-4: Benchmark reactions of a single batch of Pt/C catalyst after repeated use. The catalyst was re-used under the above conditions using fresh benzene and D ₂ O for each repetition to show that the reaction performance is reduced dramatically after as little as 3 uses. Noting that the reaction after 6 uses continues to the same detriment suggests that the catalyst has undergone a critical change.	26
Table 2-5: Results of pulse titration analysis, revealing the catalytic surface area had been reduced under the high reaction temperature.....	26
Table 2-6: Gradual increase in temperature promotes reactivity but cannot exceed 140 °C to stay within the pressure limits of the vessel.	28
Table 2-7: Time optimization and correlation of reaction time with catalyst loading.....	28
Table 2-8: Pt/C catalyst loading screening.....	29
Table 2-9: Using 6 molar equivalents of D ₂ O relative to benzene deuterates nearly the same extent as 2 cycles using 3 equivalents.....	29
Table 2-10: Screening of D ₂ O addition in autoclave reactions.	31
Table 2-11: Optimization of second cycle to attempt full H/D exchange.....	32
Table 2-12: Catalyst loading control reactions, revealing 0.2 mol% to be most efficient overall.	34
Table A1-1: Ion abundance values from GC-MS spectrum, with benzene isotopologue distribution of sample extracted from data.	49
Table A1-2: Weighed quantities of standards and sample, with representative integration values from NMR spectra.	55

List of Abbreviations

% D	Percent deuterium content
¹ H	Proton
² H	Deuterium
APCI	Atmospheric-pressure chemical ionization
APPI	Atmospheric-pressure photo-ionization
D	Deuterium
D ₂	Deuterium gas
D ₂ O	Deuterium oxide / heavy water
DMI	Deuterium Magnetic Resonance
EI	Electron Impact Ionization
GC-MS	Gas-Chromatography Mass Spectrometry
H ₂	Hydrogen gas
H ₂ S	Hydrogen sulfide
HDO	Degraded heavy water
KIE	Kinetic isotope effect
MRI	Magnetic Resonance Imaging
m/z	Mass-to-charge ratio
NMR	Nuclear Magnetic Resonance
OLED	Organic light-emitting diode
OPV	Organic photo-voltaic
OSC	Organic solar cell
PAH	Polycyclic aromatic hydrocarbon
Pd/C	Palladium on carbon
PET	Positron Emission Tomography
PK	Pharmacokinetics
Pt/C	Platinum on carbon

QE	Quantum efficiency
qNMR	Quantitative NMR
S _N Ar	Nucleophilic aromatic substitution
ZPE	Zero-point energy

List of Schemes

Scheme 1-1: Lewis-acid catalyzed deuteration of N-methylimidazole (MeIm) via Pt(II) species. ⁶²	10
Scheme 1-2: Reduction of the aldehyde intermediate affords α -deuteration in the 6-membered transition state of 2 due to H/D exchange of the hydride ligand.....	11
Scheme 1-3: Control experiments supported by energy profile calculations show that the energy barrier for hydride H/D exchange is too great in the tetrahedral Ru complex. ⁶⁹	11
Scheme 1-4: The associative mechanism of H/D exchange through heterogeneous metal catalysis. It is crucial for the chemisorption of benzene to be in proximity to a pre-chemisorbed deuterium for exchange to occur.	14
Scheme 1-5: The dissociative mechanism involves a metal-arene bond to liberate hydrogen, where deuterium can exchange on the metal surface and perform subsequent addition onto the arene ring.	15
Scheme 2-1: Reverse H/D exchange control.....	34
Scheme A1-1: Chemical ionization of benzene-d6 eliminates deuterium atom via addition-elimination with dichloromethane reagent gas.....	48

Chapter 1: Deuterium

1.1 Background

Hydrogen (H) is the most abundant element in the universe, making up approximately 75% of all matter. Naturally occurring hydrogen exists in two stable isotopes, hydrogen or sometimes referred to as protium, and deuterium (D). Protium contains one proton and one electron. Deuterium differs from hydrogen as it possesses a neutron in its nucleus. In natural waters, deuterium comprises approximately 0.0312% by weight of earth's ocean waters in the form of deuterium oxide (D₂O) or hydrogen-deuterium oxide (HDO).¹ Due to its presence in aqueous sources, deuterium can be found in virtually all naturally occurring hydrogen-containing compounds, both organic and inorganic. Deuterium is proposed to have been formed in the early universe through big bang nucleosynthesis, where lighter elements hydrogen, helium, and their respective isotopes were created.^{2,3} Deuterium is a necessary precursor in the synthesis of helium, requiring the temperature of the early universe to cool enough to allow deuterium generation to occur before initiating helium creation.^{2,3} However, as the fusion of helium took place, the universe cooled further and had insufficient heat for helium to continue fusion to make the heavier elements, with the exception of some lithium. This resulted in a consistent ratio of deuterium to hydrogen within the universe and is believed to be evidence supporting the Big Bang theory.²

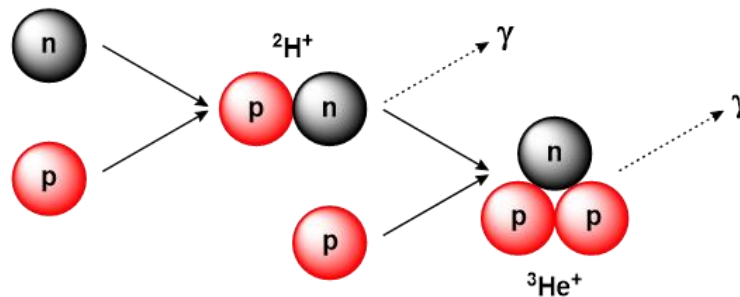


Figure 1-1: A fusion process forming deuterium and helium-3.

Deuterium's existence was first confirmed in 1931 by Harold C. Urey. In the decades prior, anomalies pertaining the mass of hydrogen and density of water emerged.⁴ Additionally, exploration into isotopes was growing in interest at this time, with the discovery of oxygen-17 and oxygen-18 by Nobel laureate William Giauque and Herrick Johnston in 1929.⁵ These events motivated Urey to investigate the presence of deuterium. Liquid hydrogen samples were concentrated through low-temperature distillation and electrolysis methods, which were examined spectroscopically via the Balmer series.⁶ For his work, Urey was awarded the Nobel prize in 1934. Hundreds of papers pertaining to deuterium were published in its wake, including the isolation of pure D₂O by Gilbert Lewis shortly after Urey's discovery.⁷ Today, D₂O and D₂ gas are applied in a variety of fields ranging from chemical manufacturing to nuclear energy production.



Figure 1-2: Deuterated forms of water and hydrogen gas, common industrial sources of deuterium.

Deuterium oxide, known colloquially as heavy water, is the most common source of deuterium on earth. Heavy water can be harvested from natural water sources, this is performed industrially through thermodynamic exchange processes using gases like hydrogen sulfide (H₂S) or ammonia (NH₃).⁸ Hydrogen sulfide is used in the eponymous Girdler sulfide / Geib-Spevack (GS) process, invented by Karl-Hermann Geib and Jerome Spevack in 1943 (**Figure 1-3**).^{8,9} Enrichment occurs by thermodynamic equilibrium between hydrogen sulfide and water. The affinity of deuterium towards H₂S or H₂O is manipulated by the temperature of two columns, a “cold” column at 30 °C, and respective “hot” column at 130 °C. Water is fed into the hot column, where deuterium has marginal affinity for hydrogen sulfide, and the opposite is true for the cold column. Deuterium enriched water can be extracted while traveling from the cold column to the hot column, reaching upwards of 20 percent deuterium content (% D) after 3 stages.⁹ Distillation is used to further enrich the heavy water to >99% D, often used for nuclear reactors and research purposes. The Girdler sulfide process is the most prevalent method used for heavy water refinement globally, with some of the largest production facilities located in India. Ammonia gas can be implemented with the GS process but is more notably used in the mono-thermal ammonia-hydrogen process.^{10,11} Here, the feedstock is an ammonia synthesis gas, a mixture of hydrogen and nitrogen. Deuterium, which is naturally present in the hydrogen feed gas, is stripped by use of a catalyst (e.g. potassium amide) and transferred to liquid

ammonia. The isotopically enriched ammonia is transferred to a cracking furnace, obtaining the HD gas. The gas can be further refined by distillation and converted to heavy water by combustion.

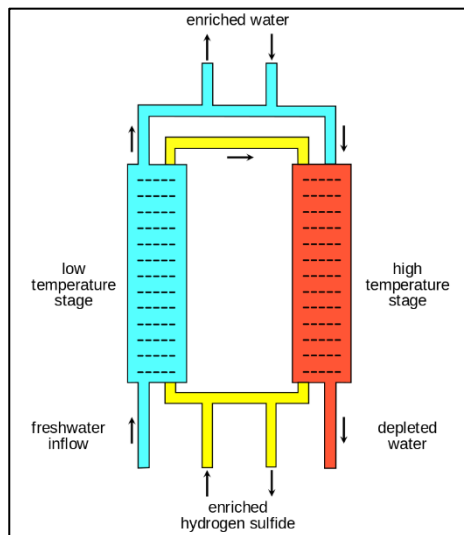


Figure 1-3: Schematic of the Girdler sulfide process. [†]

1.2 Physicochemical Properties of Deuterium and Associated Applications

Primary Kinetic Isotope Effect

Deuterium differs from protium by the addition of one neutron which increases its mass from 1.008 Daltons (Da) to 2.014 Da. While additional neutrons are a defining characteristic of isotopes generally, deuterium is unique as the mass difference is nearly double that of protium, the largest change in mass of any isotope. Organic reactions implementing isotopes are subject to the phenomenon known as the kinetic isotope effect (KIE) and is utilized in a variety of academic and industrial applications. The KIE stems from the differing zero-point energies of bonds between atoms (typically carbon) and deuterium. Zero-point energy (ZPE) can be described analogously to two masses connected by a spring, where the atoms are viewed as the masses and the spring is the bond between them. One attribute that dictates the bond strength is the vibrational energy of the bond in its lowest energy, this energy level is the ZPE.¹² Since deuterium is much heavier than protium, the zero-point energy of a bond to deuterium is lower than protium and creates a relatively stronger bond, implying that bonds to deuterium require more energy to cleave. The difference in bond energy can have a remarkable impact on the rate of a reaction due to a higher bond-breaking energy in the transition state compared to when protium is present, when this occurs it is noted as the primary KIE

[†] [Girdler sulfide process](#) © Roland Mattern, [CC by 3.0](#)

(Figure 1-4). This difference in rates is used routinely in academic research to aid in the elucidation of reaction mechanisms.^{12,13} By selectively replacing hydrogen atoms for deuterium, the changes seen in rate can reveal the bonds that are broken or formed in a reaction and which steps in a reaction contribute significantly to its progression. Exploitation of the primary KIE has been explored across a variety of applications over the years and opened new strategies for modern industrial practices.

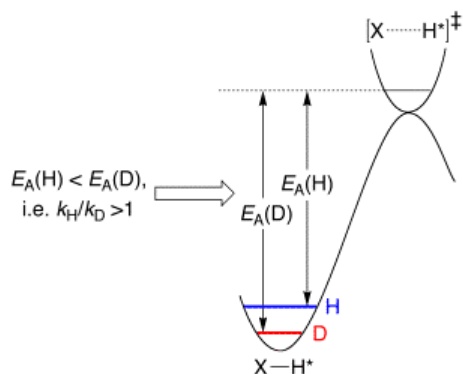


Figure 1-4: Isotopic effects of heterolytic bond cleavage through difference in zero-point energy. Adapted from ref.¹³

Deuterium kinetic isotope effects in pharmacology

Mechanistic investigations using KIEs are widely used in academic research, but also provide insight into the pharmacokinetics (PK) of drug metabolism to better understand a drug's pharmacology and improve future drug development. The first written case of KIE in metabolic study was in 1961 by Alison et al. where the potency of morphine was probed by the deuteration of the N-methyl group.¹⁴ The observed enzymatic binding and the rate of oxidative N-demethylation were reduced, causing the potency of deuteriomorphine to be less than the unlabelled drug (Figure 1-5). Over time, this work and others contribute to the study of drug metabolism by cytochromes P450 (P450), and the effect deuterium has on these reactions. This family of enzymes is involved in approximately 75% of all drug metabolism, drawing focus from the pharmaceutical industry for drug development.¹⁵

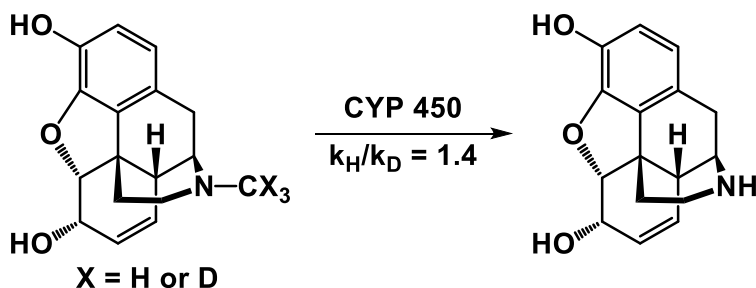


Figure 1-5: KIE of morphine N-demethylation to normorphine.¹⁴

In the past ten years, two new drugs containing deuterium have come into the market along with several potential drugs entering various phases of clinical trials. Deutetrabenazine (Austedo[®]) is a vesicular monoamine transporter 2 (VMAT2) inhibitor used in the treatment of involuntary movement disorders or dyskinesia in patients with Huntington's disease.¹⁶ Deuterium is used to extend the presence of the active metabolites by slowing the *O*-demethylation, doubling the drug's half-life, and reducing the dose frequency. Deucravacitinib (Sotyktu[™]) uses deuterium in a similar manner, utilizing deuterium on the amide-methyl moiety to slow *N*-demethylation.¹⁷ Attenuating demethylation maintains the inhibitory selectivity in addition to metabolic stability.

Slowing metabolism is not the only role deuterium plays in drug design, as chirality can also induce minor to severe side effects in biological molecules.¹⁸ The most common example is seen in the infamous thalidomide scandal, where the *R*-enantiomer provides the intended sedative effect, but the *S*-enantiomer is a teratogen. Thalidomide was provided as a racemic mixture, but even in enantiopure administration, can undergo chiral inversion to create the toxic enantiomer.¹⁹ Introducing deuterium into these chiral centers reduces isomerization and preserve the desired stereochemistry.²⁰ One example of this is PXL065, a deuterated analogue of pioglitazone (Actos[®]) which is currently in phase 2 clinical trials.^{21–23} Pioglitazone is used to treat a form of non-alcohol fatty liver disease, and is administered as a racemic mixture. While both enantiomers are effective in treatment, the *S*-enantiomer is an agonist to the peroxisome proliferator-activated receptor- γ (PPAR γ), causing off-target effects like edema, fluid retention, and loss in bone density.²² PXL065 is *R*-pioglitazone that is stereochemically retained by deuterium, changing the R:S ratio from 1:1 to 4:1. In the trial, liver fat content dropped comparably between both drug analogues and none of the adverse effects were observed from the PXL065 patients.²¹

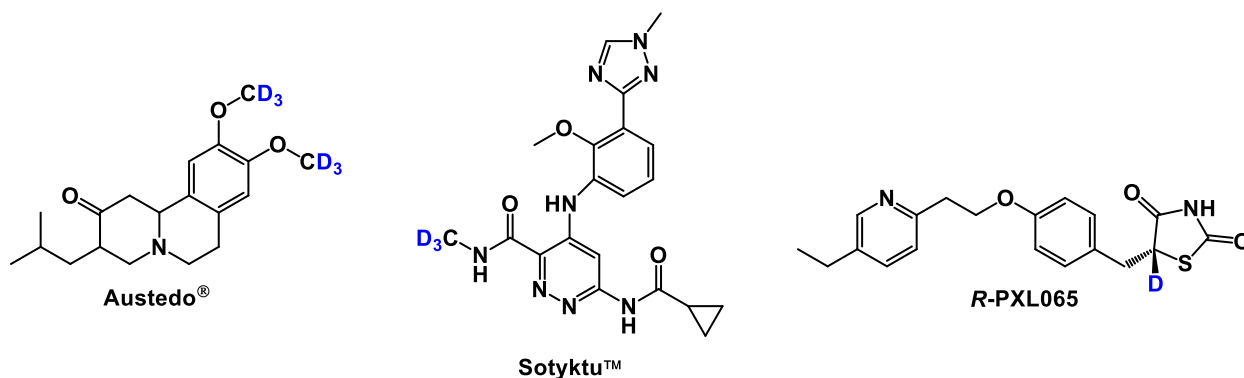
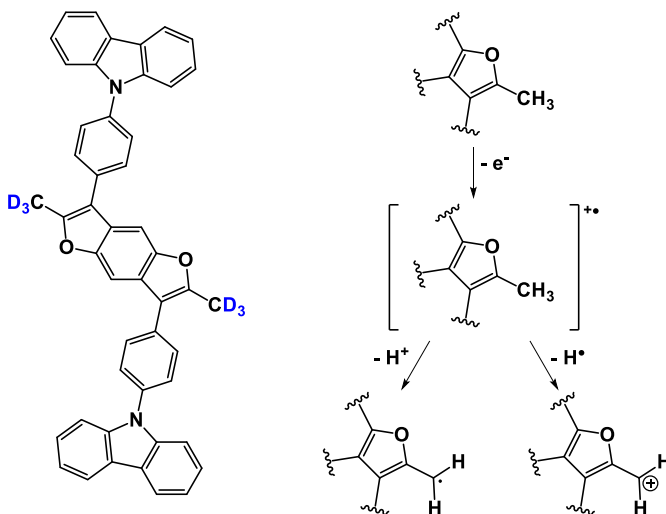


Figure 1-6: Examples of deuterated drugs.

Improvement of opto-electronic devices

The diminished ZPE of carbon-deuterium bonds is recognized to enhance the bond strength, but the change in the harmonics finds use in a wide array of electronic devices. The increase in vibrational frequency that a carbon-deuterium (C-D) bond provides will impact photoluminescent and electroluminescent properties of related organic compounds. Deuterium was noted to improve the phosphorescent lifespan of naphthalene when all hydrogen atoms were exchanged for deuterium.²⁴ More recently, the advantages and potential solutions that deuterium can bring are being explored on organic light-emitting diodes (OLEDs). OLEDs have a diverse array of technologies, being developed for commercial electronic displays as an alternative to liquid-crystal displays. Different methods of luminescence are being experimented to find the most appropriate solution like fluorescence, phosphorescence, and radical fluorescence.²⁵⁻³⁰ The adoption of OLED devices is bottlenecked by the stability of the devices at high voltage and the overall lifespan of the displays. To combat these obstacles, maximizing the quantum efficiency (QE) of the organic emitters and improving their resistance to degradation is necessary. All forms of OLED devices have seen remarkable improvement with deuterium incorporation. The host material carbazolyl benzodifuran (CZBDF) is a green phosphorescing molecule, and increased in device lifespan by a factor of 5 when the furan methyl group was replaced by a tri-deuteriomethyl group (-CD₃) (**Figure 1-7**).³¹ Increased stability is proposed to be from the minimization of oxidative degradation of the methyl group, where a cationic radical allows for the removal of hydrogen through radical heterolysis or ionic cleavage. The quantum efficiency of these devices, a key measurement of a device's performance, the ratio of charges output by the devices relative to those going in. Maximizing the QE allows for higher display brightness and contrast with minimal electricity usage. Due to the lower bond stretching frequency of deuterium, less energy is lost from non-radiative processes, which increases the QE across all types of OLEDs.

Figure 1-7: Deuterated analogue of green OLED host material (left) and plausible mechanism of degradation (right).³¹



The adoption of organic-based electronics extends further into energy conversion devices using organic solar cells (OSCs) and more broadly, organic photovoltaics (OPVs). Taking inspiration from deuterated OLED efforts, Yamamoto and co-workers tested the effect of deuterium on benzyl fullerenes.³² An improvement of solar cell efficiency was noted for one of the deuterated derivatives, when comparing performance to similar fullerenes used in commercial OSCs. Deuteration of molecules can alter their solubility due to reduced polarizability induced by the shorter C-D bond, but this is an insignificant difference in most cases.³³ Deuterium labelling of acceptor polymer side chains can improve the crystallinity and separation of acceptor and donor phases in the final cell, which is known to dramatically enhance the efficiency of solar cells through π - π stacking.³⁴⁻³⁷ These changes in morphology can be influenced by deuterium even without direct introduction into the material. Previous studies show that deuterated solvents in polymer-solvent systems can have reduced miscibility, this allows for better π - π interactions between the conjugated systems (**Figure 1-8**).³⁸ In turn, crystallization proceeds more readily, creating thin films with closer molecular stacking with greater stability, optimal for efficient charge transport. Solar cell efficiency degrades with age, and the time needed for the efficiency to drop by 20% as referred to as T_{80} .³⁹ Several solar cell materials were constructed with crystallization in deuterated and non-deuterated solvent, three of the cells were projected to have T_{80} values 8x greater when crystallized in deuterated solvent comparatively. However, adding deuterium to electron donor materials can impart deleterious attributes. One study examined the effects of site-specific deuteration on poly(3-hexylthiophene) (P3HT), affixing deuterium to either the alkyl side chain or the heterocycle.³⁶ They found deuterium could increase the occurrence of non-radiative processes, creating a drop in efficiency as large as 50% in both cases. Additionally, they found that deuteration of the thiophene lowered the absorptivity, inhibiting photon-induced charge transfer and further worsening device performance.³⁶ While the exact advantages of deuterium usage in OPVs are variable, the explanation of deuterium's impacts on OSC performance is ongoing.

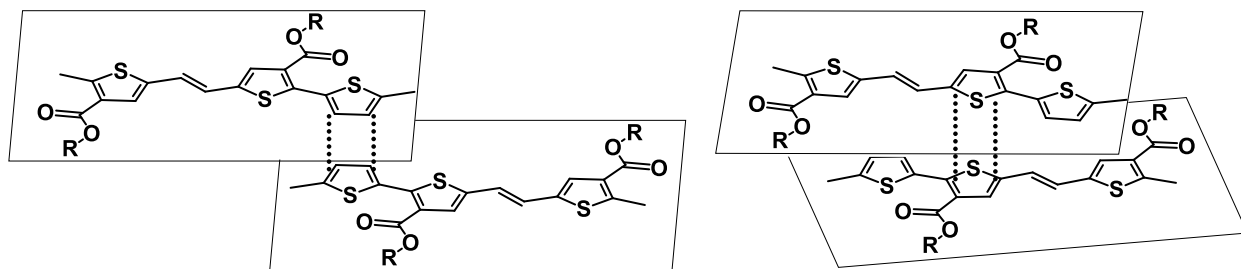


Figure 1-8: Impact of crystallization in deuterated solvents (left) versus non-deuterated solvent (right) post-annealing, imparting better stacking.

Spin properties and Nuclear Magnetic Resonance

The nucleus of a deuterium atom is referred to as a deuteron and differs from protium by the additional neutron. Neutrons, while possessing no charge do provide additional spin to nuclei. Neutrons can have spin states of either $-\frac{1}{2}$ or $\frac{1}{2}$, and therefore gives the overall spin of the deuteron either integers 1 or 0 spin (**Figure 1-9**).⁴⁰ Deuterons rarely achieve a zero-spin state, due to a remarkably high thermal energy barrier (10^{11} kJ/mol) and are considered to always be in ground state spin of 1.⁴⁰ This gives the deuteron a quadrupole magnetic moment, which can increase the resonance broadening.^{40,41} However, the quadrupole magnetic moment of deuterons are relatively small in comparison to that of larger isotopes (^6Li , ^{14}N). This factored with the compositional masses of deuterons versus protium make their gyromagnetic ratios significantly different.⁴⁰ This property dictates its usefulness in modern spectroscopic applications.

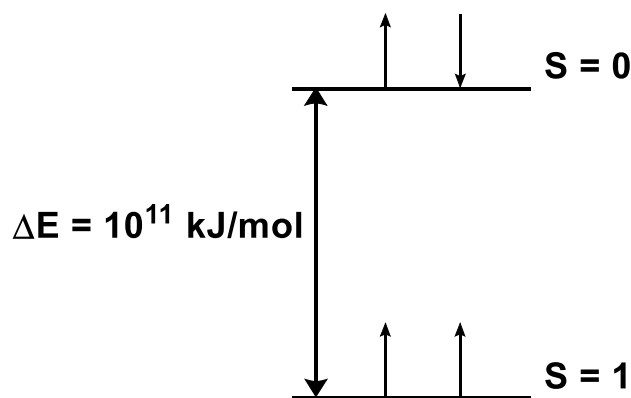


Figure 1-9: Spin states of ^2H nuclei.

Nuclear magnetic resonance (NMR) spectroscopy is a common analytical tool used in science and engineering to investigate the structure of various compounds. Deuterium is often used as a standard to minimize changes in the magnetic field of NMR instruments which cause broadening of peaks. As such, deuterium enriched solvents are often employed for preparation of NMR samples. Since the gyromagnetic ratio of deuterium is distinct from other nuclides, the signal falls under a different frequency and is not seen in acquired spectra. This is particularly important in proton (^1H) NMR, where the signal of the solvent would otherwise overpower signals from the compound of interest. Another way proton signals are modified is by a common technique known as “ D_2O shake”. This involves adding small quantities of D_2O to a sample for ^1H NMR, causing any exchangeable protons ($-\text{OH}$, $-\text{NH}$, etc.) to be swapped with deuterium where their respective signals will be lost in the spectrum. Exchanging protons for deuterium atoms imparts other artifacts in ^1H NMR. Deuterium atoms will undergo spin-spin coupling with other nuclei and have differing J value constants than proton coupling. In both ^1H and ^{13}C NMR, these values can be calculated

using common ratios between the proton and deuterium coupling constants ($6.5 \times J_{X-D}$).⁴⁰ Each of these phenomena provide powerful tools in NMR to accomplish structural analysis or mechanistic investigation.

Deuterium (^2H) NMR is also an available technique for structural analysis but is used infrequently due to the low natural abundance of deuterium in un-enriched molecules. Deuterium labelled biomolecules are employed routinely in metabolic studies in addition to proteomics. This idea is being taken further in the field of medical imaging with Deuterium Metabolic Imaging (DMI), which combines Magnetic Resonance Imaging (MRI) with ^2H NMR to deduce metabolic activity.⁴² DMI poses as an alternative to techniques like Positron Emission Tomography (PET) as the deuterium labelled tracers can be identified after metabolism. This additional capability has aided in distinguishing pancreatic cancer from pancreatitis by monitoring glucose metabolites (**Figure 1-10**).⁴³ PET methods cannot distinguish these diseases as only the uptake of glucose is observed. Consequently, inflammation can increase glucose uptake similar to pancreatic cancer, giving inconclusive diagnoses. Increased metabolism of glucose into lactate has been noted in human cases of pancreatic cancer different to pancreatitis.^{44,45} Tracking and identifying this inflated lactate production can discern the diagnosis.

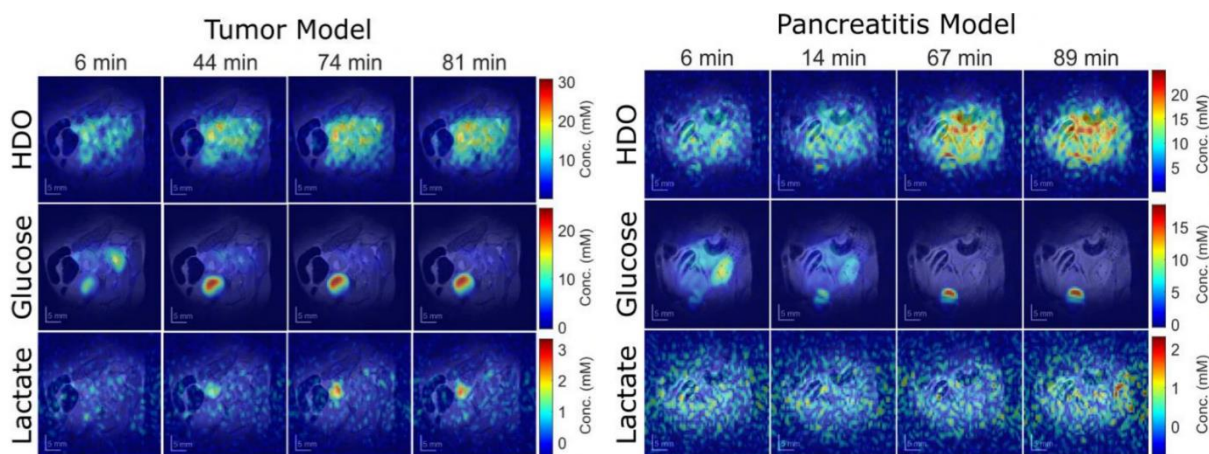


Figure 1-10: DMI images of $[6,6']\text{-}^2\text{H}_2$ -glucose uptake and metabolism over time, identifying pancreatic cancer based on increased $[3,3']\text{-}^2\text{H}_2$ -lactate production.⁴³

1.3 Metal-catalyzed Deuteration Methods

Not much time passed between deuterium's discovery and chemists' attempts to introduce deuterium into organic compounds. One of the earliest accounts of deuteration of an organic compound is by Halford et al. in 1934, where a mixture of acetone, potassium carbonate, and heavy water were combined to deuterate acetone (**Figure 1-11**).⁴⁶ Reports of metal-catalyzed deuteration also appeared at this time to deuterate gases like methane, ammonia, and ethylene.⁴⁷⁻⁵¹ Much of the work done at this time revolved around well-known

chemistry such as hydrogenations, reductions, acid-base reactions, and aromatic substitutions.⁵²⁻⁵⁶ These techniques can still be found today to insert deuterium into compounds, with newer methodology and synthetic strategies being attempted.

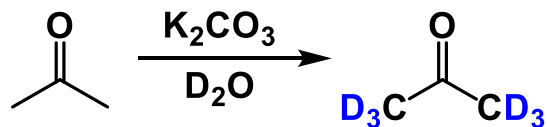
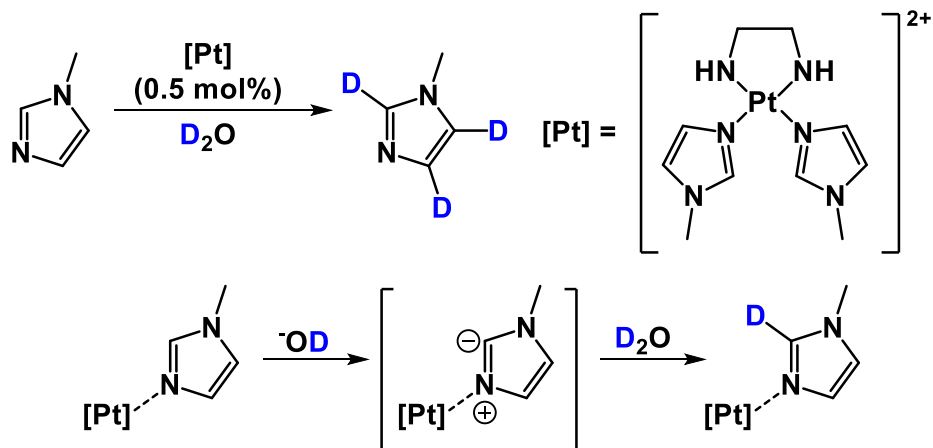


Figure 1-II: Catalytic deuteration of acetone.⁴⁶

Metals can act as Lewis acids to aid in H/D exchange on select substrates. Earlier transition metals like cobalt (Co) and chromium (Cr) are typically recognized as hard acids and can coordinate with hard bases to aid in basic hydrogen/deuterium exchange with groups like amines and carboxylic acids.^{57,58} Later transition metals like silver (Ag), mercury (Hg), and platinum (Pt) salts are soft, and can coordinate to compatible sites like unsaturated carbon and nitrogen bonds. This coordination has shown to increase the acidity of neighbouring hydrogens to permit faster exchange with deuterium in the presence of base (Scheme 1-1).⁵⁹⁻⁶³ This effect varies based on the metal-substrate bond character and can accelerate the exchange process by several orders of magnitude.

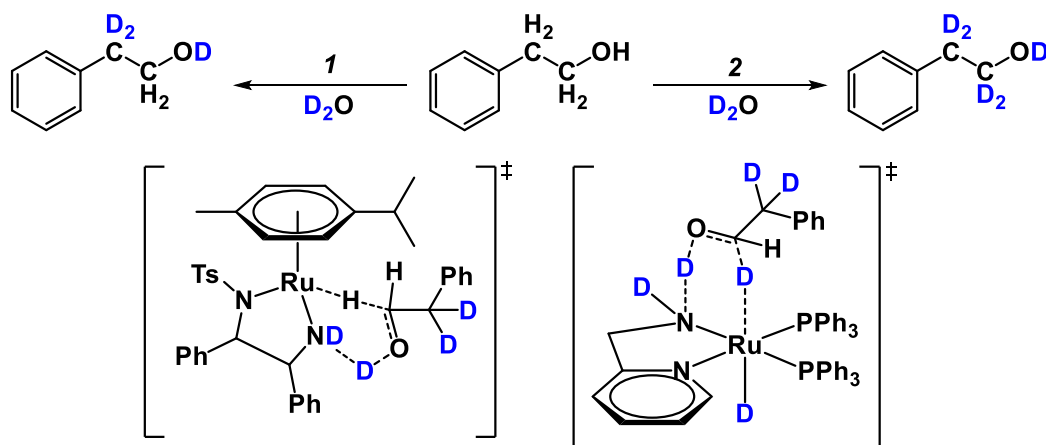


Scheme 1-1: Lewis-acid catalyzed deuteration of *N*-methylimidazole (MeIm) via Pt(II) species.⁶²

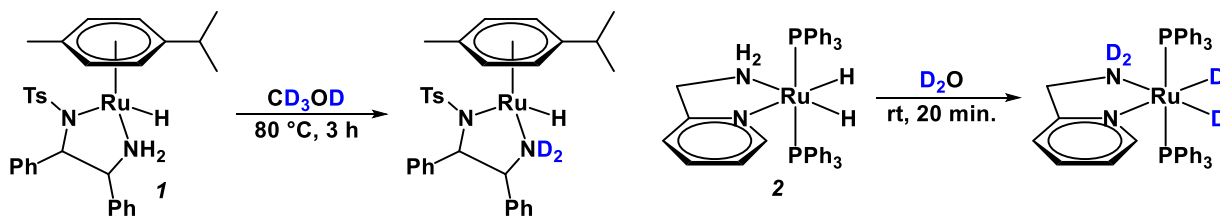
Substrate	Relative rate		
	C2-H	C4-H	C5-H
MeIm	1	1	1
<i>enPt</i> ²⁺ (MeIm) ₂	6.3 x 10 ²	4.8 x 10 ¹	4.8 x 10 ¹

Table 1-1: Impact of Pt(II) Lewis acid on relative rate of *N*-methylimidazole H/D exchange.

Metal catalysts based on the late transition metals have further utility as C-H activation catalysts, providing a direct and highly efficient method for functionalizing molecules. Metals with high d-orbital electron occupancy like those found in groups 8-10 can activate the C-H bond of saturated and unsaturated compounds.⁶⁴ The versatility that C-H activation can provide proves to be a powerful strategy, making it an attractive approach to H/D exchange reactivity. Metal complexes in homogeneous conditions can be modified extensively with different ligands, permitting mild and highly selective H/D exchange.⁶⁵⁻⁶⁸ A simple example of this change in selectivity can be seen when comparing the regioselectivity of two ruthenium (Ru) catalysts deuterating 2-phenylethyl alcohol (**Scheme 1-2**).⁶⁹ It was observed that hydrogens at the α -position to the hydroxyl group would not exchange with tetrahedral catalyst **1** but would readily exchange with the octahedral catalyst **2**. The proposed rationale behind the selectivity is due to the octahedral complex exchanging hydride ligands with deuteride ligands more readily than the tetrahedral hydride complex.⁶⁹ Because the hydride ligand of tetrahedral complex **1** does not exchange for deuterium (**Scheme 1-3**), the hydrogenation step of the aldehyde intermediate does not install a deuterium atom in the α -position. While this is one case of directing regiospecific deuteration, selective deuteration can also be achieved using directing groups on substrates akin to directed *ortho*-metalation (DoM).



Scheme 1-2: Reduction of the aldehyde intermediate affords α -deuteration in the 6-membered transition state of **2** due to H/D exchange of the hydride ligand.



Scheme 1-3: Control experiments supported by energy profile calculations show that the energy barrier for hydride H/D exchange is too great in the tetrahedral Ru complex.⁶⁹

Direct C-H activation typically proceeds through oxidative addition with the late transition metals and is assisted by agostic interactions with the C-H bond (known as a σ -complex). A σ -complex involves donation of 2 electrons to the metal center through a 3-center 2-electron (3c-2e) bond, forming a stabilized intermediate as indicated by the strong interaction (5-10 kcal/mol).^{64,70} Once formed, the C-H bond is cleaved and may partake in H/D exchange with a deuterium source before the reverse process of reductive elimination turns over the deuterated product. In most cases of C-H activation catalysis, H/D exchange has demonstrated a faster rate of exchange with deuterium over protium in alkanes, marked as an instance of inverse kinetic isotope effect.⁷⁰ Rationale for this effect is based on the discreet rates of oxidation (k_{OC}) and reduction (k_{RC}) in the first transition state, which interconvert between a σ -complex and alkyl-hydride complex. Metal-hydride/deuteride bond stretching frequencies are weaker than the bond between carbon and hydrogen/deuterium, suggesting a smaller ZPE. From this, two possible events would permit an inverse KIE (**Figure 1-12**). The first has the transition state energies of protium and deuterium to differ, causing the reduction of the alkyl-hydride complex to a σ -complex to proceed faster with deuterium, and the overall equilibrium would appear to have an inverse KIE.⁷⁰ The second scenario poses that the C-H/D bond is broken during oxidative coupling and therefore, ZPE has no role in distinguishing protium and deuterium energy levels in the transition state. This would make the oxidative coupling from a σ -complex to alkyl hydride significantly faster with protium than deuterium ($k_{OC}^H > k_{OC}^D$), thus the overall equilibrium of the forward and reverse reactions would also show apparent inverse KIE.⁷⁰ Homogeneous C-H activation can take place through other mechanisms, such as σ -bond metathesis or electrophilic activation however their exploration in H/D exchange are limited.^{71,72}

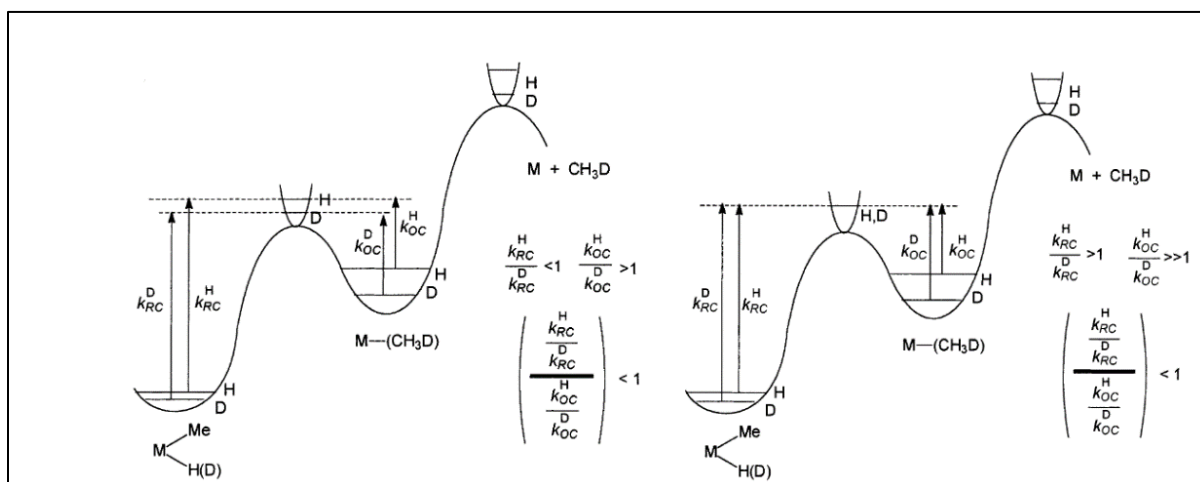
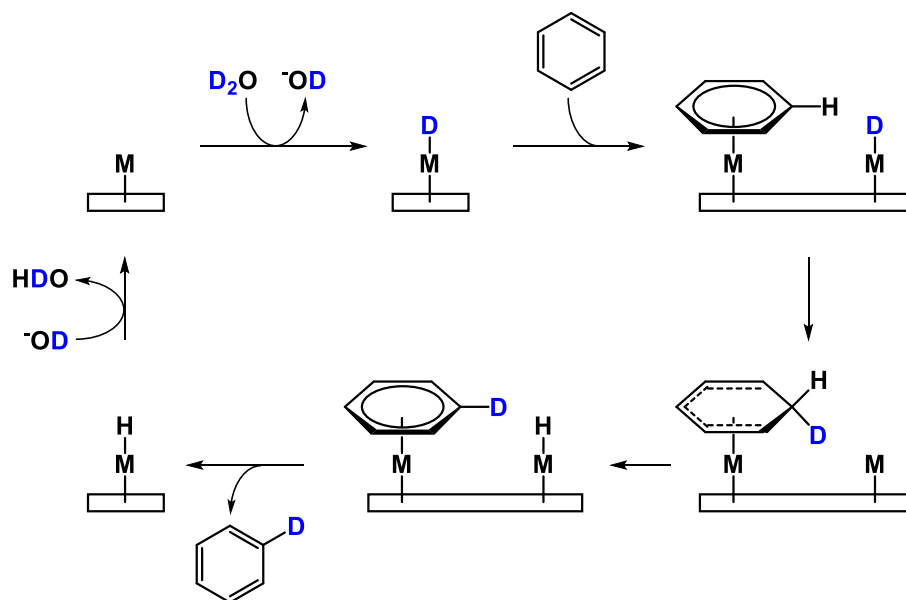


Figure 1-12: Possible reaction kinetic profiles describing instances of inverse KIE state distinguished by the first transition state being influenced by ZPE (left) or having no influence (right). Adapted from ref.⁷⁰

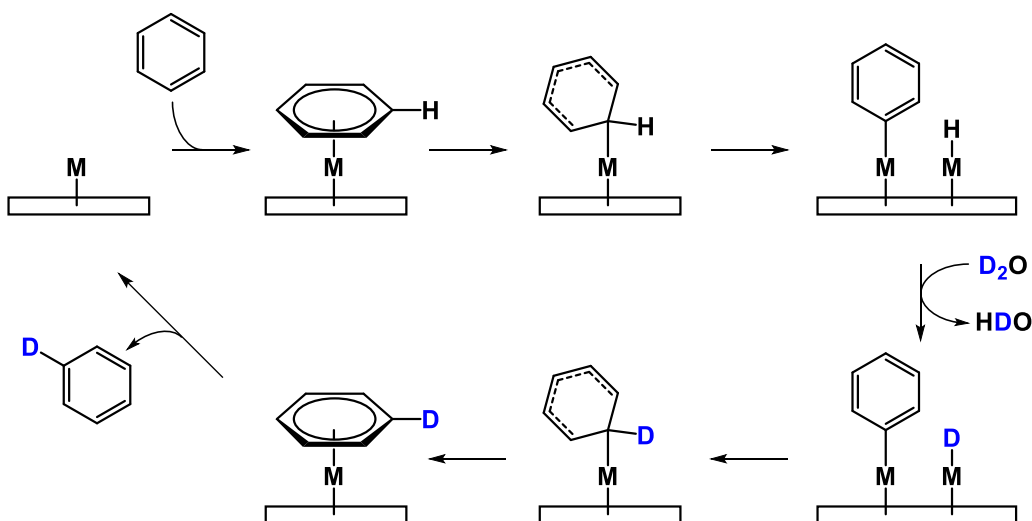
The aforementioned late transition metals, particularly the noble metals like platinum (Pt), palladium (Pd), nickel (Ni), cobalt (Co), ruthenium (Ru) and rhodium (Rh) have also been established in performing H/D exchange as heterogeneous catalysts.⁷³⁻⁷⁷ These metals are known for their robustness, resilience to oxidation, and their easy removal from reaction mixtures as heterogeneous mixtures, making them desirable catalysts. However, the advantages of tuneable selectivity and milder reaction conditions are lost when using heterogeneous catalysts. Reaction conditions are specific to each substrate and may require higher temperatures, limiting the tolerance of functional groups and stereochemistry of substrates. While these caveats pose restrictions on their synthetic utility, their ease of use and recyclability make heterogeneous catalysis a useful strategy when complete deuteration of molecules are needed. Heterogeneous catalysts are often affixed to a support media, maximizing surface area and in some cases providing additional electronic effects which enhance reactivity.⁷⁸ Activated carbon is a common support material with palladium-on-carbon (Pd/C) and platinum-on-carbon (Pt/C) being used routinely as catalysts in hydrogenation reactions.

The solid phase nature of these catalysts distinguishes their reactivity from their homogeneous counterparts, and as such their mechanisms of catalysis differ. Garnett and co-workers remarked on aromatic and unsaturated substrates being feasible for high deuterium incorporation through heterogeneous catalysis.^{77,79,80} Through their investigation, they proposed two possible pathways that H/D exchange operates. The initial conditions require substrate to form a π -complex with the metal, while deuterium atoms dissociated from the deuterium source (D_2O , D_2 , etc.) have been chemisorbed to the metal surface. From this point, exchange can take place via an associative or dissociative mechanism.⁷⁹ The associative path involves the chemisorbed deuterium to attack nearby substrate and performs H/D exchange analogous to nucleophilic aromatic substitution (S_NAr) with the charged intermediate stabilized by the substrate-metal π -complex (**Scheme 1-4**). For the dissociative mechanism, the π -complexed substrate is rotated and attacked by a metal radical to form a σ -bound C-sp² radical species where the abstracted hydrogen is chemisorbed to another metal atom (**Scheme 1-5**).⁷⁹ A chemisorbed deuterium atom may then substitute the metal that is bound to the substrate, forming the C-D bond and returning the substrate to its initial π -complex. The careful distinction between these two mechanisms hinges on the σ -bond formed in the dissociative pathway.^{79,80} Since hydrogen atoms can dissociate more easily from the substrate, this implies that deuterium atoms which are chemisorbed onto the catalytic surface may source from the deuterated substrate as well as a secondary deuterium source. The associative mechanism does not relinquish a hydrogen atom without the nearby presence of a pre-existing chemisorbed deuterium, meaning that deuterium may only come from a secondary source like heavy water or deuterium gas.⁸⁰ Therefore, the dissociative and associative mechanism can be elucidated by examining the deuterium scrambling of deuterated and non-deuterated substrate in absence of heavy water. Under these conditions, the dissociative

mechanism will pre-dominate if the catalyst is suitable. From these studies, it is recognized that within the noble metals exists some bias between the associative and dissociative pathway for each metal. Weitkamp supported this idea while examining how naphthalene reacts with each of these metals under a supply of deuterium. Products of these reactions were resultant of π -bond saturation and H/D exchange, conclusions postulated that the associative mechanism could conduct H/D exchange and hydrogenation while the dissociative pathway would tend towards deuterium exchange exclusively.⁸¹ Through this lens, platinum and iridium are classified as mainly following a dissociative mechanism, palladium tending toward the associative mechanism, leaving ruthenium and rhodium falling somewhere in between.⁸¹



Scheme 1-4: The associative mechanism of H/D exchange through heterogeneous metal catalysis. It is crucial for the chemisorption of benzene to be in proximity to a pre-chemisorbed deuterium for exchange to occur.



Scheme 1-5: The dissociative mechanism involves a metal-arene bond to liberate hydrogen, where deuterium can exchange on the metal surface and perform subsequent addition onto the arene ring.

1.4 Summary

The discovery of deuterium has been a powerful discovery in the scientific community as a natural isotope. Today, many countries worldwide partake in strenuous industrial processes to extract and purify it from natural sources, lending to its value as a precious resource chemical. The unique mass and spin properties of deuterium contribute to advanced applications across numerous industries. These advances are largely due to changing the intrinsic properties of molecules when deuterium is incorporated into them, prompting the development of a wide array of strategies over the decades to do so. Because of this, the focus of deuterium has largely shifted away from D_2O towards finding new ways of deuterating compounds to further potential applications.

Chapter 2: Arene C-H Activated H/D Exchange

2.1 Background

Benzene is a six-member carbocyclic compound and is a common isolate from petroleum. It is a clear, non-polar liquid used extensively as a solvent and is often functionalized to produce a multitude of derivatives for commercial use. Benzene and its derivatives are common motifs seen across several industrial fields, including pharmaceuticals and organic electronics (**Figure 2-1**). Incorporation of benzene rings into drug molecules can be crucial for drug binding through π - π interactions with biological compounds like tyrosine, phenylalanine, and tryptamine.⁸² Likewise, benzene and larger aromatic compounds create the backbone for organic-based electronic devices. The aromatic nature of benzene can be utilized to accomplish electrical conductivity and photoemission, giving rise to organic solar cells (OSCs) and light emitting diodes (OLEDs). In the advancement of these industries, the incorporation of deuterium has been long studied with advantageous effects because of its adoption. And while implementing deuterated benzene is already seen in some industries, seen with host materials used in OLED production, other sectors like the pharmaceutical industry have been slower to explore its potential. With benzene as a versatile building block, incorporating deuterium directly into benzene creates easy access to synthetically useful derivatives for these industries (**Figure 2-2**).^{83,84} Deuterating benzene directly simplifies this by avoiding developing methodology to accompany various functional groups that may otherwise be incompatible with current H/D exchange methods.

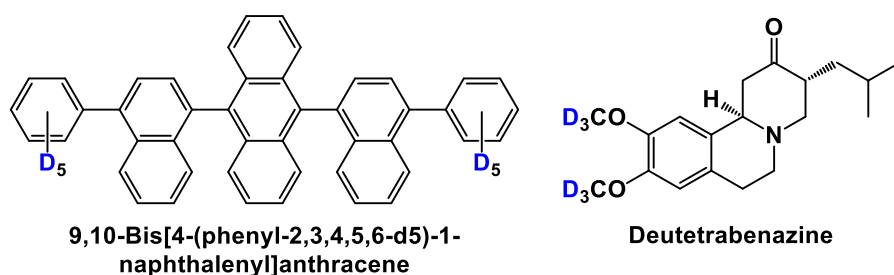


Figure 2-13: Examples of an OLED host material (left) and pharmaceutical drug (right) containing derivatized benzene rings with deuterated motifs.

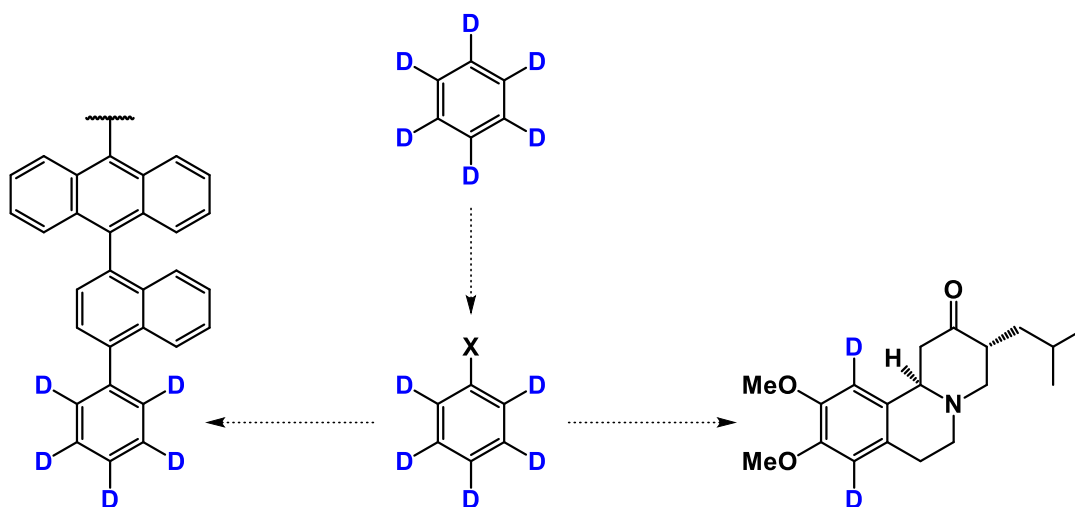


Figure 2-14: Functionalization of benzene- d_6 allows for versatile introduction of deuterated phenyl groups for organic electronics (left) and pharmaceuticals (right).

As mentioned previously, many of the early investigations of deuterium exchange were performed on simple gaseous compounds of aliphatic and unsaturated nature. Therefore, it is unsurprising that aromatic substrates would soon follow suit. Benzene, being the simplest of aromatic compounds was a prime candidate for testing reactivity of aromatic substrates. Horiuti and Polanyi, pioneers of hydrogenation chemistry, were keen to explore the behaviour of deuterium under hydrogenation conditions.⁸⁵ Using nickel and platinum catalysts they demonstrated the first report of deuterium exchange between benzene and deuterium enriched hydrogen gas (**Figure 2-3, equation 1**). This was shortly followed by an account of H/D exchange from the same authors, this time using D_2O as the deuterium source.⁸⁶ They found that a solution of water containing 3% deuterium could H/D exchange with benzene or ethylene over a nickel catalyst, achieving 1.3% deuterium incorporation into ethylene after 24 hours and 1.5% deuterium content in benzene after 2 hours.⁸⁶ These findings prompted further studies, with reports made in the years following offering different approaches and refining the initial conditions.⁸⁷⁻⁸⁹ Most notably, Ingold, Raisin, and Wilson illustrated a homogeneous process using sulfuric acid to perform H/D exchange through electrophilic aromatic substitution.⁸⁷ Exchange was found to occur readily, but at high concentration of sulfuric acid induced substitution with sulfur trioxide (generated *in situ*) to form benzene sulfonic acid as a side product. Further tuning of their conditions allowed for quantitative production of deuterated benzene with enrichment as high as 99.8% D (**Figure 2-3, equation 2**).⁹⁰ While this was the highest degree of enrichment obtained at that time, the ease of heterogeneous-catalyzed deuteration motivated the work of Leitch 20 years later.⁹¹ Re-investigating platinum-catalyzed exchange, he was able to successfully generate benzene- d_6 by repetitive hydrothermal reactions. Over 4 cycles, samples of benzene were isolated near-quantitatively, yielding a final product containing approximately 98.5% D (**Figure 2-3, equation 3**).⁹¹ This

procedure had remarkable improvement as the reaction proceeded at lower temperatures relative to the nickel-catalyzed methods, and arduous preparation of deuterated sulfuric acid was eliminated.

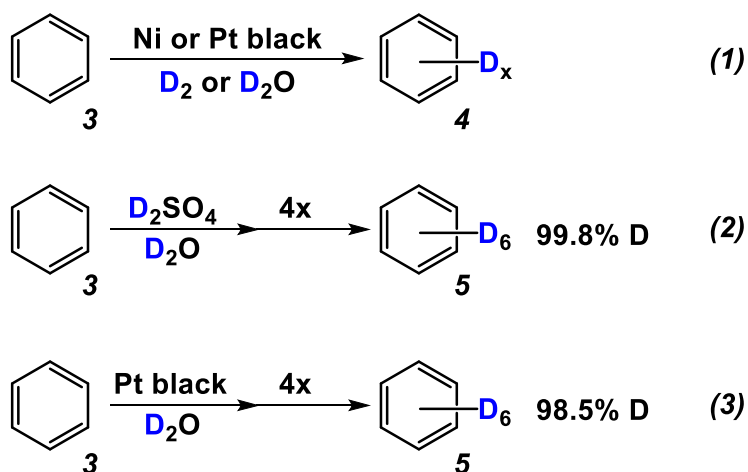


Figure 2-15: Early examples of benzene H/D exchange reactions by Horiuti and Polanyi (1), Ingold, Raisin, and Wilson (2), and Leitch (3).

In the years following Leitch's publication, further studies were conducted by Garnett and others to explore the behaviour and capabilities of the Pt-catalyzed reaction. The substrate scope was expanded beyond benzene to evaluate the impact of electronic and steric effects.^{79,92} Reactivity was tolerated across some electron-donating and withdrawing substituents (**Table 2-1**) with little to no effect on exchange. If the reaction does proceed through a radical substitution mechanism as noted in the dissociative pathway, resistance to electronic effects would be an observed feature as radical intermediates are stabilized by either electron donating or withdrawing groups.⁹³ Despite this tolerance, other substrates with electron donating or withdrawing groups did not participate in H/D exchange as expected. To explain deviations in reactivity, steric interactions and side reactions were suggested. This was supported in a later study by Fraser et al., where benzene derivatives with high deuterium content were subjected to reverse H/D exchange with protons, probing steric effects and regioselectivity of exchange (**Table 2-2**).⁹⁴ Hindrance of *ortho* and *meta* exchange were apparent across nearly all substrates, consistent with steric repulsion inhibiting adsorption with nearby carbons. Observations of high *ortho*-selectivity were seen in derivatives with heteroatoms like aniline and phenol. One possible reason for this effect could come from lone-pair interactions with the metal surface, preferentially orienting the ring such that exchange occurs with adjacent carbons. Conversely, such lone-pair interactions can be detrimental to the catalytic surface. Compounds that contain heteroatoms like sulfur, oxygen, and nitrogen can strongly interact with the metal surface, effectively shutting down the active sites from the desired exchange reaction.⁹⁵ This is known commonly as catalyst poisoning and occurs across all transition metals of group 8 through 11.⁹⁶ Other ways H/D exchange can be hindered under C-H

activation conditions is from competing side reactions such as hydrogenolysis or reductions, creating undesirable products that can potentially poison the catalyst.⁹⁴

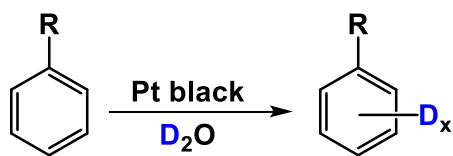


Table 2-1: Pt-catalyzed H/D exchange of substituted arenes using D₂O.^{79,92}

<i>Substituent</i>	<i>Temp. (°C)</i>	<i>Reaction time (hrs)</i>	<i>%D</i>
-COONa	130	24	91%
-COOH		12	73.1%
-NH ₂		24	78.7%
-Br		24	0%
-NO ₂		24	0%
-Me	120	4	35.1%
-Et		4	58.5%
-iPr		4	42.9%
-tBu		4	1.74%
-Me		2	16%
-CF ₃		2	14%

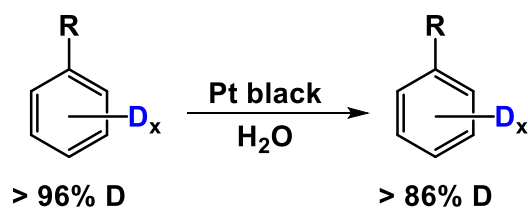


Table 2-2: Effect of sterics and side reactions in reverse H/D exchange with mono-substituted benzene.⁹⁴

<i>Substituent</i> (R)		<i>Position of H</i>			<i>%H in total</i>
		<i>ortho</i>	<i>meta</i>	<i>para</i>	
-F	A ¹	0.56	0.56	0.28	1.4
	B ²	1.99	6.27	3.14	11.4
-Cl	A	0.48	0.48	0.24	1.2
	B	0.41	7.08	4.21	11.7
-OMe	A	0.20	0.20	0.10	0.5
	B	0.20	4.05	4.05	8.3
-OEt	A	0.20	0.20	0.10	0.5
	B	0.20	5.50	6.00	11.7
-CN	A	0.48	0.48	0.24	1.2
	B	1.68	5.76	6.42	13.9
-COOMe	A	0.40	0.40	0.20	1.0
	B	0.51	1.17	1.14	2.8
-NH ₂	A	0.48	0.48	0.24	1.2
	B	10.48	0.98	0.70	12.1
-OH	A	0.20	0.20	0.10	0.5
	B	8.50	2.32	0.77	11.6
-NMe ₂	A	1.70	0.82	0.88	3.4
	B	1.87	2.50	2.94	7.3

¹ Deuterium enriched starting material. ² Product after reverse H/D exchange.

While platinum was a prime catalyst during many of these investigations, attention to the other metals within the platinum group was warranted to compare their respective utility. Work done by Sagert and coworkers gives insight to this when looking at each of these metals' activity on graphitized carbon black support exchanging deuterium from water to hydrogen gas.⁹⁷ Of the 6 noble metals, platinum had not only the fastest rate but the lowest activation energy. Incidentally, platinum also ranks highest for catalytic activity in kinetic studies with the fastest rate of H/D exchange between D₂O and benzene.⁹⁸ However, an important consideration for benzene is that hydrogens on aromatic motifs can exchange with deuterium

more readily than aliphatic protons due to π -complex formation. Empirically, the chemoselectivity of these metals is demonstrated when comparing their reactivity on different molecular motifs. Iridium and platinum exchange hydrogens more readily on sp^2 carbons than the other Pt group metals, while palladium and nickel will predominately deuterate aliphatic carbons.^{99–102} Precise rationale for these affinities has not been extensively studied, though it is argued that the nature of the π -complex between metal and substrate is key.⁹⁸ This rationale is based on Mulliken's charge-transfer theory, where the π -complex can be viewed as a transfer between the donor (substrate) and the acceptor (metal).¹⁰³ Substrates with compatible ionization potential to the electron affinity of the metal would have better tendency to form a π -complex. Additionally, the symmetries of the substrate bonding orbital and metal anti-bonding orbital impact charge-transfer, thus having an additional effect on metal-substrate π -complex ability. Therefore, the combination of these properties can give some insight to the observed chemoselectivity of benzene and other aromatic substrates with platinum group catalysts.

2.2 Proposal

Organic compounds like benzene and its higher-order polycyclic aromatic hydrocarbon (PAH) derivatives are routinely employed in well-established organic electronics industries. The aromaticity of these compounds creates large, delocalized networks of π -bonds, allowing for efficient transfer of charge and photoactive properties. These features are capitalized in organic electronic devices like organic solar cells (OSCs) and organic light emitting diodes (OLEDs). However, the widespread adoption of organic electronics is limited by the decreased lifespan and lower operating efficiency of the resulting devices that are derived from materials containing benzene and PAHs. In recent years, the incorporation of deuterium into molecules that are the foundation of such devices has proven to be a novel, highly effective approach to greatly diminishing these devices' limitations. Exchanging hydrogen with its heavier isotope deuterium utilizes KIE to impart greater stability to such compounds. In both OLED and OSC devices, incorporating deuterium greatly reduced their tendency to undergo decomposition and other unwanted processes, resulting in better device efficiency and longevity.^{26,30,31} To support these advances further and better facilitate similar new discoveries in deuterium science, new synthetic techniques must be established that efficiently and effectively incorporate deuterium into a host of diverse molecular classes.

Recently, the Murphy group involved itself in a 5-year collaboration with deutraMed Inc., an emerging Canadian retailer of deuterated small organic molecules. The goal of this collaboration is to develop chemical techniques that incorporate deuterium into company-specified molecular targets for their immediate production and commercialization. deutraMed Inc. has an exclusive license to commercialize Canada's vast deuterium gas (D_2) and D_2O resources, which forms the basis of their business plan. This

comes as a response to the emerging shift in D₂O supply worldwide. In 1997, Canada's production of heavy water had shutdown but continued to sell from its large stockpile in the years following. Despite a lack of production means to replenish this supply, the vast quantities of D₂O in inventory was sufficient to maintain the market demand until 2012 when Ontario Power Generation announced it would stop selling D₂O.¹⁰⁴ With such abundance of D₂O in the time preceding, the widespread use of deuterium in routine analysis and commercial applications made deuterium appear ubiquitous and trivial. Due to this dependency, identifying and purveying new and existing resources is needed to continue access to D₂O and the derivatives made from it. While many strategies for introducing deuterium into molecules exist, often these methods are designed with the intent of transferring as much of the deuterium from the source into the compound as possible to minimize production costs. However, deuteraMed Inc. has developed a D₂O refinery (D2X™) which enriches depleted D₂O waste streams to high deuterium content (99+ %D).^{104,105} With this refining process, it is economically most efficient when the degraded D₂O streams contain no less than 90% D. To amalgamate this novel provision of deuterium, methods must be developed to deuterate compounds which complement the capabilities of the refinery. Therefore, the processes developed in this research are centralized around the constraint of degrading D₂O by no greater than 10%. Benzene-*d*₆ was the first molecule targeted for development, as it is a versatile building block used in a multitude of industrial and commercial applications, and as such is in high demand. Furthermore, with larger arenes having important uses in the electronics industry it is important that the procedures for benzene be suitable for PAHs to accommodate this. Having a unified process to deuterate aromatics not only simplifies the production but ensures that waste streams are congruent to suit the integral refining process. In full, the result of this work herein will take high-purity D₂O to perform H/D exchange on benzene to furnish benzene-*d*₆, with waste streams collected and recycled through the refinery to create a circular economy.

This work:

- Unified arene H/D exchange procedure with <10% D₂O degradation.
- Consistent waste streams for refinement.

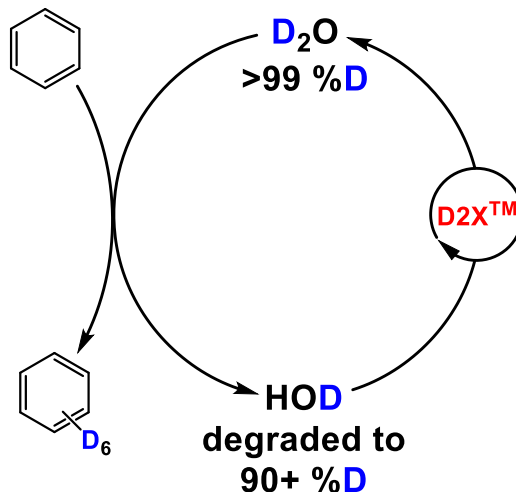


Figure 2-16: Schematic of circular H/D exchange industrial process incorporating the deuteraMed Inc. D2X™ refining process for D₂O.

2.3 Synthesis of Benzene-d₆

Beginning the development of this synthesis, it was uncertain how the chemistry would behave. Variations in reaction conditions (temperature, catalyst, time, etc.) and less obvious variables (reaction vessel, atmosphere, pressure, etc.) can affect how the reactions proceed, and adjusting these without understanding their impact can complicate the method development significantly. With this in mind, it was logical to apply pre-existing procedures to evaluate and fix initial problems as they arose. Following literature precedent, the preliminary work would be to design the process around maximal transfer of deuterium from D₂O to benzene. Since D₂O is a costly and limited reagent, designing around exhaustive depletion would require smaller quantities of D₂O to be used in each trial. With many variables to consider and test, preserving D₂O at this stage would allow for the greatest number of experiments to be performed to determine the best conditions for optimization. Once the optimal conditions are found, adjusting the amount of D₂O is the simplest way to reduce its degradation in the exchange process, and any effects that arise could be attributed to this factor alone. The starting ratios of benzene to D₂O were reasoned based on the following, for each mole of benzene will be 6 moles of hydrogen atoms belonging to said benzene, and D₂O has 2 moles of deuterium atoms per molecule. Therefore, if we use 3 molar equivalents of D₂O per 1 molar equivalent of benzene, there will be an equimolar mixture of deuterium atoms to hydrogen atoms in each reaction. With all the deuterium atoms belonging to D₂O at the start of the reaction, all deuterium atoms would be exchanged with hydrogen from the benzene ring if complete degradation of D₂O occurred. The next factor to determine is the catalyst for H/D exchange. For the choice of catalyst, existing processes cite Pd and Pt as catalysts of choice as they are known to exhibit high activity and robustness. Considering

the industrial nature of this project, it was most suitable to choose heterogeneous Pd and Pt catalysts for testing first. Heterogeneous catalysts are easily separable from the reaction mixture, which minimizes purification of benzene and the waste D₂O that would be otherwise labour intensive and costly on a large-scale industrial process. Most procedures of deuteration with heterogeneous catalysts occur at high temperatures and given the volatile nature of benzene these reactions must be performed in sealed vessels. Preliminary reactions were performed in glass pressure vessels, equipped with Teflon screw caps and chemically resistant O-rings to seal the reaction mixture (**Figure 2-5**). For catalysts, commercially available palladium-on-carbon (Pd/C) and platinum-on-carbon (Pt/C) were used as the carbon support increases catalytic surface area and requires no preparation. Screening both catalysts, the Pt/C catalyst was observed to deuterate more benzene than the Pd/C trial (**Figure 2-6**), with platinum installing deuterium six-fold greater in a four-hour span (**Table 2-3**). This was anticipated as previous reports show palladium catalysts are more proficient at aliphatic deuteration, while platinum catalysts exchange aromatic hydrogens more readily.^{100,102} With this knowledge, the Pt/C catalyst was used in all further experiments. Taking measurement of H/D exchange was performed using a developed gas chromatograph-mass spectrometry (GC-MS) method, which the distribution of isotopologues and total % D is calculated from (see **Appendix 1** for further details).



Figure 2-17: Glass pressure vessels (left) used for preliminary reactions with heterogeneous catalyst stirred as a slurry at high temperature (right).

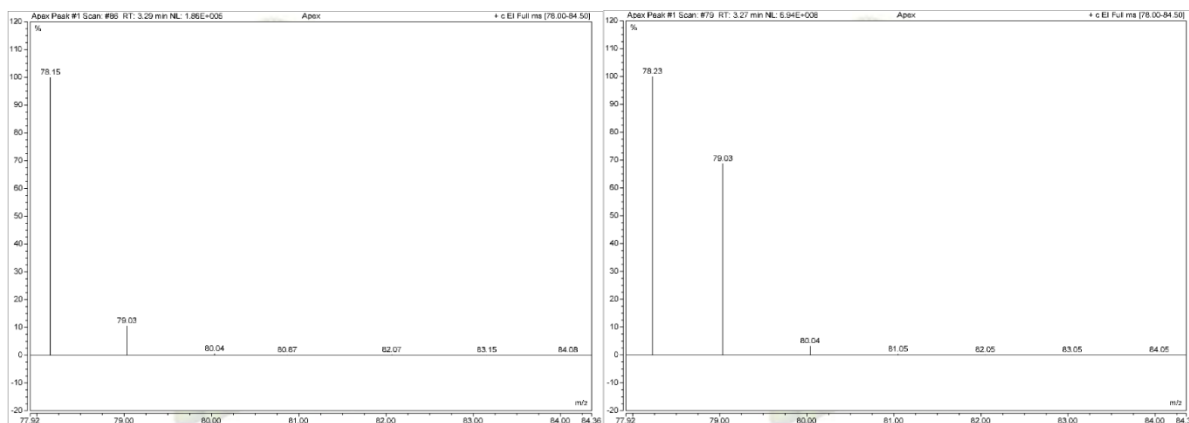


Figure 2-18: Mass spectra of benzene products from Pd/C (left) and Pt/C (right) show that a greater abundance of benzene-*d*1 (79 m/z) product is present using Pt/C.

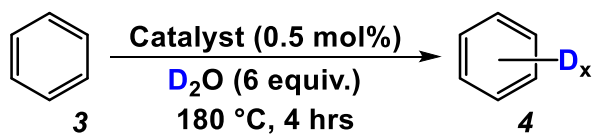


Table 2-3: Catalyst screening results in glass pressure vessels calculated from mass spectra.

Entry	Catalyst	Isotopic Distribution							Total %D
		D_0	D_1	D_2	D_3	D_4	D_5	D_6	
1	5% Pd/C	94%	6%	0%	0%	0%	0%	0%	1%
2	5% Pt/C	62%	38%	0%	0%	0%	0%	0%	6%

Having chosen the catalyst, vessel, and molar ratios, the first trials were attempted on small scale using previous patent literature as a guide.¹⁰⁶ Reactions were prepared by adding reagents to the pressure vessel stirring as a slurry with the catalyst under heat. 180 °C was tried first but would prove to be unreliable due to pressures occasionally exceeding the O-ring's ability to seal the flask. The extent of deuteration at this temperature ranged from 3-6% in a 24-hour period. Extending the reaction to three days permitted 15% deuterated product but was deemed insignificant as 25% D could be reached in less time through two successive 24-hour cycles. Besides vessel stability, performing reactions at 180 °C proved to be deleterious to the catalyst activity when recycling was employed. Several reactions would be performed with the same catalyst, where the H/D exchange performance proved to be weaker when repeating the same conditions compared to fresh catalyst (**Table 2-4**). This was believed to be sintering of the support under such high temperatures, where the catalyst support shrinks under high heat to cause reduction in surface area.^{96,107} Samples of this catalyst were sent for determining catalytic surface activity, yielding the monolayer uptake

volume. The monolayer uptake volume is a measurement of gas that is adsorbed onto the catalyst, which can be used to calculate the surface area of the total catalyst and catalyst active sites. These are used to determine the dispersion, a factor presenting the percentage of the active sites in the sample relative to the theoretical number of active sites the sample should have. The change in dispersion factor between the fresh and used catalyst showed that the number of active sites had decreased by over 93% and catalytic surface area had shrunk tremendously (**Table 2-5**). The change in catalyst morphology was visually noticeable compared to fresh catalyst, where the fresh catalyst is a fine dispersed powder whereas degraded catalyst appeared clumped despite moisture removal.

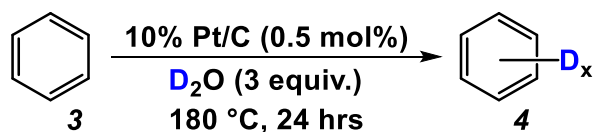


Table 2-4: Benchmark reactions of a single batch of Pt/C catalyst after repeated use. The catalyst was re-used under the above conditions using fresh benzene and D₂O for each repetition to show that the reaction performance is reduced dramatically after as little as 3 uses. Noting that the reaction after 6 uses continues to the same detriment suggests that the catalyst has undergone a critical change.

Entry	Catalyst condition	Isotopic Distribution							Total %D
		D ₀	D ₁	D ₂	D ₃	D ₄	D ₅	D ₆	
1	Fresh	8%	21%	29%	24%	14%	13%	0%	38%
2	3 Uses	70%	24%	4%	1%	0%	0%	0%	6%
3	6 Uses	74%	22%	4%	1%	0%	0%	0%	5%

Table 2-5: Results of pulse titration analysis, revealing the catalytic surface area had been reduced under the high reaction temperature.

Entry	Catalyst Trial	Monolayer			
		Uptake Volume (μmol/g)	Active Metal Surface Area (m ² /g)	Metal Surface Area (m ² /g)	Dispersion (%)
1	Fresh Catalyst	27.93	2.69	26.55	10.90
2	After 6 uses	1.77	0.17	1.70	0.69

These complications prompted inspection of the reaction temperature to determine if milder temperatures could achieve similar or improved results. Temperatures ranging from 110 – 140 °C were chosen to test as the activation barrier of Pt/C has been noted at temperatures above 100 °C, with

temperatures at 140 °C being the limit that reactions could be performed reproducibly under the pressure limits of the flasks.⁹⁷ Improved exchange was observed starting as low as 110 °C, showing progressive growth with each increase in temperature (**Table 2-6**). Of these, the best results were obtained at 140 °C with good reproducibility. To fully understand the limits of H/D exchange at this temperature, the timescale of the reaction and subsequent impact of catalyst loading were the next objectives. If the exchange was not complete within the 24-hour period, extending the reaction time would show if more deuterium could exchange with benzene per reaction cycle. To this end, a reaction time of five days dramatically raised the degree of exchange and could reach upwards of 80% D after three reaction cycles (**Table 2-7, entries 1-3**). While this was a promising result, the total time needed to achieve 80% D was 15 days under these conditions. One way for the reaction time to be reduced is by increasing the amount of catalyst used. Therefore, the catalytic loading was doubled and tripled to address this while simultaneously evaluating the rate-dependence of the catalyst (**Table 2-8**). In doing so, a first reaction cycle could deuterate benzene to 45% D, demonstrating that the same result using 0.5 mol% catalyst could be achieved in almost half the time when twice the amount of catalyst was used. The benefit of using even greater amounts of catalyst was minimal, as it had a diminishing impact on the rate. This correlation was corroborated when the time needed to synthesize 80% deuterated benzene was reduced from 15 days to 9 days over three cycles (**Table 2-7, entries 4-6**). Problems arose again going beyond this stage as the 4th cycle performs subpar, even when the ratio of water to benzene is changed, a plateau begins to appear around 85% D (**Table 2-7, entry 7**). In a final attempt to push the extent of 4th cycle exchange, one improvement was made which telescoped the reaction by doubling the quantity of D₂O. It was found that using 6 molar equivalents of D₂O in the first cycle could afford nearly the same amount of deuterobenzene as two successive cycles with 3 equivalents (**Table 2-9**). However, even with the additional supply of D₂O the progress of deuteration on benzene was little changed, as the plateau effect seemed to persevere. And further increasing the amount of D₂O to remedy this was practically difficult as the total volume of the reaction would quickly exceed the capacity of the pressure vessels. Going beyond the capacity of the vessels creates a severe safety hazard since the diminished headspace above the reaction mixture would raise the pressure generated during the reaction and perpetuate the already existing pressure limitations.

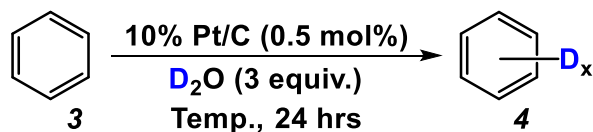


Table 2-6: Gradual increase in temperature promotes reactivity but cannot exceed 140 °C to stay within the pressure limits of the vessel.

Entry	Temp. (°C)	Isotopic Distribution								Total %D
		D ₀	D ₁	D ₂	D ₃	D ₄	D ₅	D ₆		
1	110	75%	15%	4%	3%	1.5%	1.5%	0%	8%	
2	120	72%	16%	6%	3%	1%	1%	1%	9%	
3	130	68%	20%	5%	3%	2%	1%	1%	10%	
4	140	60%	24%	8%	4%	2.5%	1%	0.5%	12%	

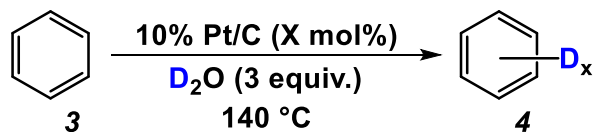


Table 2-7: Time optimization and correlation of reaction time with catalyst loading.

Entry	Cat. Loading (mol%)	Cycle Time (days)	Cycle #	Isotopic Distribution							Total %D
				D ₀	D ₁	D ₂	D ₃	D ₄	D ₅	D ₆	
1	0.5%	5	1	4%	14%	25%	30%	20%	6%	1%	45%
2			1%	3%	8%	18%	28%	30%	12%	68%	
3			0%	2%	4%	8%	21%	33%	32%	79%	
4	1%	3	1	4%	13%	25%	31%	21%	6%	1%	45%
5			1%	3%	8%	18%	28%	30%	12%	68%	
6			0%	2%	4%	8%	21%	33%	32%	79%	
7			0%	0%	4%	5%	16%	29%	46%	85%	

Table 2-8: Pt/C catalyst loading screening.

Entry	Cat.		Isotopic Distribution							Total %D
	Loading (mol%)	Time (days)	D ₀	D ₁	D ₂	D ₃	D ₄	D ₅	D ₆	
1	0.5%	3	7%	23%	30%	25%	12%	3%	0%	37%
2		5	4%	14%	25%	30%	20%	6%	1%	45%
3	1%	3	3%	12%	24%	30%	23%	8%	1%	47%
4	1.5%	1	19%	38%	25%	15%	3%	1%	0%	24%

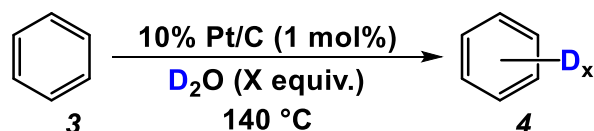


Table 2-9: Using 6 molar equivalents of D₂O relative to benzene deuterates nearly the same extent as 2 cycles using 3 equivalents.

Entry	D ₂ O (equiv.)	Time (days)	Cycle #	Isotopic Distribution							Total %D
				D ₀	D ₁	D ₂	D ₃	D ₄	D ₅	D ₆	
1	3	3	2	1%	3%	8%	18%	28%	30%	12%	68%
2	6	6	1	1%	4%	8%	22%	33%	24%	8%	64%

At this point, the scope of modifications that could be made was limited primarily due to the pressure vessel. Serendipitously, a recommendation was made by colleagues in the department to implement hydrothermal autoclave reactors to solve some of these problems. These reactors are made of stainless steel designed for high-temperature synthesis and can withstand pressures orders of magnitude higher than the glass pressure vessels (**Figure 2-7**). Additionally, the reactor jackets are equipped with Teflon containers making the entire vessel hydrophobic. With the new reactors, a different approach to introduce the catalyst was imagined. Since both reagents were volatilized under the reaction conditions if the catalyst was suspended above the liquid phase the reaction may still be able to proceed in the vapour phase. Separation of the catalyst from the reaction mixture would be advantageous both in laboratory practice and in the industrial process as it would remove a separation step during workup, further simplifying the production. To test this, the Pt/C catalyst was affixed to commercial filter paper and was

raised above the reaction liquid using a Teflon stand. Initial trials proved very successful, with many of the trends previously seen in the pressure vessels mimicked. And when the amount of catalyst was reduced back to 0.5 mol%, it was possible to achieve 60% D in a single reaction in half the time that would be needed in the glass pressure vessels (**Table 2-10, entry 1**). Considering the improvement in catalytic activity when vapour phase exchange was used instead of the catalyst slurry medium, indicated that the changes in catalyst-reagent interactions were crucial for the efficiency of the exchange process. This could be linked to the changes in diffusion of benzene and D₂O in the vapour phase and subsequently affect how the active catalyst is populated by each component. Similarly, when the catalyst loadings were increased in the pressure vessel reactions, a tapering effect occurred where exchange rate would not increase significantly, despite faster exchange seen in the steel reactors under like conditions. If volatilization of benzene and water is important to exchange, one could reason that exchange in the catalyst slurry would be optimal with catalyst exposed on the surface of the liquid. As such, the amount of catalyst loaded into the reaction would be beneficial until the surface area of the liquid phase was maximally occupied with catalyst, and any additional catalyst would be submerged under the liquid surface. Furthermore, the hydrophilicity of the pressure vessels' glass walls allows the heavy water vapour to condense and cling to the flask surface more readily, hindering the concentration of D₂O in the vapour phase. A combination of these factors could contribute to the observed loss in reaction performance in the pressure vessels, each one being remedied with vapour phase exchange in full Teflon containment. The next step was to continue modifying the ratios of D₂O to benzene as some improvement was seen in prior tests but had still been largely unexplored. Scaling the molar quantities of D₂O had markedly improved the performance of the first cycle, obtaining as high as 80% deuterium content by mass spectrometry (**Table 2-10**). Interestingly, the rate of exchange was seemingly unchanged by the increase in D₂O, as the timescale of these reactions scaled proportionally with insignificant benefit to prolonging the reaction time (**Table 2-10, entries 3-4**). Conveniently, this correlation indicated that the number of days needed for the reaction to complete would be half the molar equivalents of D₂O used in said reaction (i.e. A reaction using 18 molar equivalents of D₂O would need no more than 9 days to complete). From this, it was observed that the same degree of H/D exchange could be met using both 18 equivalents and 24 equivalents of D₂O with their respective reaction times. While it may seem obvious that the former of these two conditions would be best as it is all around the most efficient, one must keep in mind that degradation of the D₂O is a consideration of equal importance. Beginning each reaction with 99.9% enriched D₂O, the final D₂O deuterium content after the reactions can be calculated as 87% and 90% D respectively. Therefore, the conditions using 24 equivalents should be used. Alternatively, since such a high enrichment is made in the first cycle, the extent of D₂O degradation in further cycles will be significantly less. If the waste streams from the first and second cycle were combined, the isotopic purity

of the waste would fit within the 90% margin. Considering this alternative and the conservation of D₂O consumption throughout testing, it was opted to continue using 18 equivalents.



Figure 2-19: The catalyst medium is prepared by dispensing Pt/C as a slurry on filter paper under vacuum suction and dried before using (left). The filter paper is placed inside the Teflon liner on a stand to keep it above the liquid surface (right), folding the filter paper allows for larger filter papers to fit inside and does not impact reactivity.

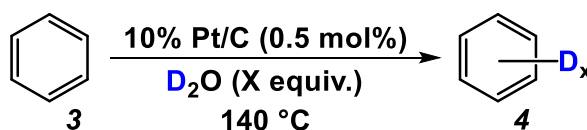


Table 2-10: Screening of D₂O addition in autoclave reactions.

Entry	Reaction		Isotopic Distribution							Total %D [†]
	D ₂ O (equiv.)	Time (days)	D ₀	D ₁	D ₂	D ₃	D ₄	D ₅	D ₆	
1	6	3	1%	8%	12%	23%	30%	21%	6%	60%
2	12	6	1%	3%	6%	15%	28%	32%	15%	71%
3	18	9	0%	1%	4%	9%	22%	36%	29%	79%
4	18	12	0%	1%	4%	9%	21%	36%	30%	80%
5	24	12	0%	1%	4%	8%	20%	34%	33%	64%

[†] Deuterium content measured by GC-MS.

It was around this time that the method of analyzing the deuterium content of benzene had shifted. Up to this stage, the measurement of deuterium incorporated into benzene was measured exclusively using (GC-MS). From here on in, the measurement of deuterium in benzene is performed by quantitative NMR (qNMR). The reason for this change is discussed in **Appendix 1**. With this new method, it was revealed that the results of the first cycle using 18 equivalents were inaccurate, enriching benzene to a deuterium

content of 72-75% D rather than the previously reported 80% D. Despite this new information, the conclusions regarding D₂O degradation and the similarities between using 24 and 18 equivalents of D₂O were largely unaltered. Seeing that one cycle acquires such high deuteration, it would seem possible that one could accomplish full deuterium exchange of benzene within 2 cycles. Hence, a second cycle under identical conditions was performed. Curiously, the reaction only increased the amount of deuterium by 20-23% (**Table 2-11, entries 2-4**). In attempts to push this further, all variables were increased independently including temperature, D₂O, and time. Of these, only increasing the quantity of D₂O in the second reaction permitted greater H/D exchange. Using 24 equivalents provided an additional 5% D versus an 18-equivalent cycle, but the benefit was deleterious beyond this as 30 equivalents gave a similar level of incorporation (**Table 2-11, entries 5-7**). Having reached this point, discussions with the industrial partner communicated that on a laboratory scale the efficacy of this process would be viable to proceed to an industrial scale where the finality of the conditions would be determined. This redirected attention to the refinement of the current procedure and running control experiments to ensure that the foundational work was indeed complete.

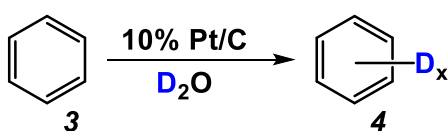


Table 2-11: Optimization of second cycle to attempt full H/D exchange.

<i>Entry</i>	<i>Cat. Loading</i> (mol%)	<i>D₂O</i> (equiv.)	<i>Reaction</i>			
			<i>Temp.</i> (°C)	<i>Time</i> (days)	<i>Cycle #</i>	<i>Total %D[†]</i>
1	0.5%	18	140	7	1	73%
2				7	2	93%
3				10	2	93%
4				14	2	96%
5	0.5%	24	140	7	2	98%
6				14	2	98%
7				7	2	98%
8	0.5%	18	160	7	1	75%
9				7	2	91% [‡]
10	1%	18	160	5	3	95%

[†] Measured by qNMR; [‡] Measured by GC-MS.

Finalizing this investigation, two main questions were identified that should be answered. First was whether the catalytic loading in the reactions was at its minimum efficiency. Secondly, is the plateauing

effect of H/D exchange a result of some energetic barrier? Exploring the first inquiry, reactions were set up at lower catalyst loadings with incremental changes (**Table 2-12**). Surprisingly, charging the reaction with as little as 0.2 mol% exceeded all prior tests in both deuteration and efficiency. Repeating these conditions for a second cycle proceed readily but suffered the same plateau to yield deuterobenzene at 95% D. Rationale for this behaviour could be explained through the dissociative mechanism of exchange. As it's been stated, a chemisorbed deuterium atom must be in proximity to the phenyl ring to exchange. By decreasing the catalytic loading, the corresponding catalytic surface shrinks with it. With fewer active sites, there is a higher probability of deuterium neighbouring a chemisorbed phenyl ring. The observation of exchange decreasing linearly with catalyst loadings below 0.2 mol% supports that this could be the threshold of its optimal catalytic surface area. This reason alone does not explain why the same efficiency is seen when catalyst is used between 0.2 – 0.4 mol%, but for the intentions of this research is not of priority. To shine some light on the plateau of exchange regularly seen in these experiments, a sample of 99.5% D benzene was acquired and subjected to the reaction conditions for 7 days (**Scheme 2-1**). If the exchange of deuterium with benzene has an energy barrier increasing with isotopic purity, one should expect very little to no exchange during this period. If the energy barrier of H/D exchange is degenerate across all isotopologues of benzene, one should see further deuteration occur in the sample. After this period, the benzene sample was analyzed and measured to be 99% D. One possible conclusion from this result is the concentration of deuterium on benzene creates a shift in equilibrium, driving deuterium to any present HDO in the system. Alternatively, with such highly deuterated benzene, any small changes in the composition of its isotopologues can change the overall deuterium content dramatically. In other words, if the relative amount of benzene-*d5* present in the sample increased during the reaction, the result observed could also occur. This change could be caused by loss of the benzene-*d6* isotopologue through evaporation. Elucidating the exact cause of this event requires more scrutinous experiments in a highly controlled setting. Ultimately the change in deuterated benzene is very small over a long period and is inconclusive that the observed plateau effect is precluded by energetics. A simpler cause of this plateau with higher deuterium-enriched benzene could be from exchange probability, where the likelihood of a protium-to-deuterium exchange event becomes less probable as fewer benzene molecules exist with protium attached. Under these circumstances, exhaustive reaction times would afford higher isotopic purity.

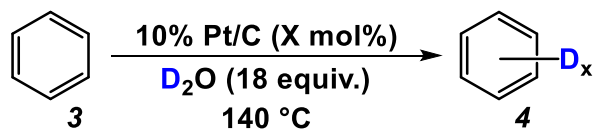
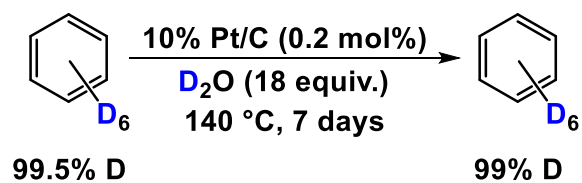


Table 2-12: Catalyst loading control reactions, revealing 0.2 mol% to be most efficient overall.

Entry	Reaction			
	Cat. Loading (mol%)	Time (days)	Cycle #	Total %D
1	0.05%	3	1	18%
2	0.1%	3	1	40%
3	0.2%	1	1	13%
4		3.5	1	86%
5		3.5	2	95%
6		7	1	84%
7		3.5	1	84%
8	0.3%	7	1	84%
9	0.4%	3.5	1	81%
10		7	1	82%



Scheme 2-1: Reverse H/D exchange control.

2.3 Conclusions and Future Work

Because the product of this work is intended for commercialization, many aspects of the investigations undergone are directed by the goals and objectives of the industrial collaborator. The efforts of this work were concentrated on the target molecule benzene-*d*6, with an initial laboratory scale process to be developed under D₂O-conservative criteria. In summary, it has been demonstrated that benzene-*d*6 can be acquired using hydrothermal conditions with a 96% isotopic purity of deuterium through 2 successive cycles using D₂O as the isotope source provided by the industrial partner. With a limit of D₂O degradation being no greater than 10%, this is accomplished through means of excess use per cycle or consolidation of waste streams from the 2 reaction cycles. The resulting procedure can be used by the industrial partner in the further process development of benzene-*d*6 synthesis on large scale.

The efforts of this work can be expanded further in the scope of this collaboration. Firstly, the methods described to perform H/D exchange on benzene can be tested on other substrates of interest, such as PAHs, heterocyclic compounds, and other substituted aromatics. Identifying the strengths and pitfalls of this methodology on these substrates would provide insight into the versatility of the finished process, and from this understanding would contribute to the design of the finished reactor to maximize its utility. Additionally, the Smith group of the Chemistry department has joined the collaboration with deutraMed Inc. to develop novel catalysts with one of the intentions being the development of catalyst(s) that will perform H/D exchange on target molecules assigned to our lab. The implementation of these catalysts will become pertinent to the research described here in addition to any future projects.

2.4 Experimental and Spectral Data

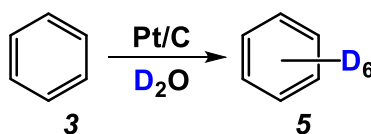
General Experimental Details

Reactions were carried out in sealed vessels as described in General Procedure A and B. All reagents were purchased from Sigma-Aldrich and used without any further purification. Transfer of D₂O was performed inside a glovebag under dry N₂ atmosphere via syringe. All NMR spectra are reported in chemical shifts (δ) in parts per million (ppm) relative to reference compounds and/or residual solvent peaks. The following abbreviations were used to explain the multiplicities: s = singlet, d = doublet, t = triplet, q = quartet, br. s = broad singlet. Proton NMR spectra (¹H NMR) were recorded at 300 MHz and are reported relative to the residual methanol-*d*4 (3.31 ppm) peak reported.

Important Safety Note

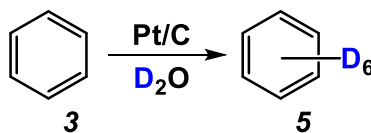
Benzene is recognized as a known carcinogen.¹⁰⁸ All handling of benzene and its isotopically labelled forms must always be performed in a fume hood with good ventilation. Platinum is also a known oxidant in the presence of alcohols, generating explosive hydrogen gas. Keeping alcohols and other susceptible materials away from platinum is important when handling. Gloves must be worn at all times when handling all materials. The reactions described are performed under closed systems under elevated temperature, creating high pressure environments that pose an explosion risk. All reaction vessels used in this work were equipped with pressure relief measures and surrounded by blast shields to mitigate this risk. Careful consideration must be used before engaging in these reactions including but not limited to the volatility and vapour pressures of chemicals used and the total volume and pressure limits of the reaction vessel.

General Procedure A: Glass pressure vessel synthesis of benzene-*d*₆



To a dry, heavy-walled glass pressure vessel with a magnetic stir bar was added benzene (1.0 equiv.), Pt/C (5-10% metal by weight, 0.5-1 mol%, 0.549-1.09 g), and D₂O (3-6 equiv.). The vessel was secured tightly by Teflon screw cap and placed in an oil bath set to 140 °C and left to stir. Once complete, the reaction is removed from the oil bath and left to cool. Once cooled, the Teflon screw cap is replaced by a ground glass joint adaptor and the liquid products are isolated by short path distillation at 150 °C. The organic phase is separated and is subjected to GC-MS analysis, where deuterium incorporation is measured by isotopic abundance.

General Procedure B: Steel autoclave reactor synthesis of benzene-*d*6



To a dry, Teflon cup insert was added benzene (1.0 equiv.), D₂O (18 equiv.), and Pt/C (10% metal by weight, 0.5 mol%, 0.55 grams) which is dispersed on Whatman #1 filter paper. The Teflon cup is closed and sealed inside the stainless-steel jacket (**Figure 2-8**). The reactor is placed inside an oven set to 140 °C and left for the duration of the reaction. The reactor is then removed from the oven and left to cool before opening. Once cooled, the reactor jacket and Teflon cup are opened, and the catalyst is removed before transferring the contents to a separatory funnel. The organic phase is collected and is subjected to GC-MS analysis along with ¹H and ²H NMR analysis using maleic acid and methanol-*d*₄ as the ¹H and ²H internal standards, respectively.

¹H NMR (300 MHz, CD₃OD): δ 7.34 (s)



Figure 2-20: Teflon cup insert and disassembled stainless steel jacket of hydrothermal autoclave reactor (left) and sealed reactor (right).

References

- (1) Hagemann, R.; Nief, G.; Roth, E. Absolute Isotopic Scale for Deuterium Analysis of Natural Waters. Absolute D/H Ratio for SMOW1. *Tellus A: Dynamic Meteorology and Oceanography* **1970**, *22* (6), 712. <https://doi.org/10.3402/tellusa.v22i6.10278>.
- (2) Cyburt, R. H.; Fields, B. D.; Olive, K. A.; Yeh, T.-H. Big Bang Nucleosynthesis: Present Status. **2016**. <https://doi.org/10.1103/RevModPhys.88.015004>.
- (3) Hoyle, F.; Margaret, E.; Burbidge, G.; Fowler, W.; AGW Cameron, independently; Peebles, P.; Wagoner, R. Big-Bang Nucleosynthesis: Linking Inner Space and Outer Space. **1999**.
- (4) Lamb, A. B.; Lee, R. E. The Densities of Certain Dilute Aqueous Solutions by a New and Precise Method. *J Am Chem Soc* **1913**, *35* (11), 1666–1693. <https://doi.org/10.1021/ja02200a003>.
- (5) Giauque, W. F.; Johnston, H. L. An Isotope of Oxygen of Mass 17 in the Earth's Atmosphere. *Nature* *1929* *123:3109* **1929**, *123* (3109), 831–831. <https://doi.org/10.1038/123831a0>.
- (6) Brickwedde, F. G. Harold Urey and the Discovery of Deuterium. *Phys Today* **1982**, *35* (9), 34–39. <https://doi.org/10.1063/1.2915259>.
- (7) Lewis, G. N.; Macdonald, R. T. Concentration of H₂ Isotope. *J Chem Phys* **1933**, *1* (6), 341–344. <https://doi.org/10.1063/1.1749300>.
- (8) Galley, M. R. Future Trends in Heavy Water Production. *Atomic Energy of Canada Limited, AECL (Report)* **1983**.
- (9) Andreev, B. M. Separation of Hydrogen Isotopes in H₂O-H₂S System. *Sep Sci Technol* **2001**, *36* (8–9), 1949–1989. <https://doi.org/10.1081/ss-100104764>.
- (10) Sawant, M. R.; Patwardhan, A. W.; Gaikar, V. G.; Bhaskaran, M. Simulation of the Mono-Thermal Ammonia Hydrogen Chemical Exchange Tower as a Reactive Absorption System. *Ind Eng Chem Res* **2006**, *45* (20), 6745–6757. <https://doi.org/10.1021/ie060039y>.
- (11) Rae, H. K. *Selecting Heavy Water Processes*; 1978. <https://doi.org/10.1021/bk-1978-0068.ch001>.
- (12) Westaway, K. C. Using Kinetic Isotope Effects to Determine the Structure of the Transition States of S_N2 Reactions. *Adv Phys Org Chem* **2006**, *41*, 217–273. [https://doi.org/10.1016/S0065-3160\(06\)41004-2](https://doi.org/10.1016/S0065-3160(06)41004-2).
- (13) Parkin, G. Applications of Deuterium Isotope Effects for Probing Aspects of Reactions Involving Oxidative Addition and Reductive Elimination of H-H and C-H Bonds. *J Labelled Comp Radiopharm* **2007**, *50* (11–12), 1088–1114. <https://doi.org/10.1002/jlcr.1435>.
- (14) Elison, C.; Rapoport, H.; Laursen, R.; Elliott, H. W. Effect of Deuteration of N-CH₃ Group on Potency and Enzymatic N-Demethylation of Morphine. *Science (1979)* **1961**, *134* (3485), 1078–1079. <https://doi.org/10.1126/science.134.3485.1078>.
- (15) Atzrodt, J.; Derdau, V.; Kerr, W. J.; Reid, M. Deuterium- and Tritium-Labelled Compounds: Applications in the Life Sciences. *Angewandte Chemie - International Edition* **2018**, *57* (7), 1758–1784. <https://doi.org/10.1002/anie.201704146>.

- (16) Dean, M.; Sung, V. W. Review of Deutetrabenazine: A Novel Treatment for Chorea Associated with Huntington's Disease. *Drug Des Devel Ther* **2018**, *12*, 313–319. <https://doi.org/10.2147/DDDT.S138828>.
- (17) Roskoski, R. Deucravacitinib Is an Allosteric TYK2 Protein Kinase Inhibitor FDA-Approved for the Treatment of Psoriasis. *Pharmacol Res* **2023**, *189*, 106642. <https://doi.org/10.1016/j.phrs.2022.106642>.
- (18) DeWitt, S.; Czarnik, A. W.; Jacques, V. Deuterium-Enabled Chiral Switching (DECS) Yields Chirally Pure Drugs from Chemically Interconverting Racemates. *ACS Med Chem Lett* **2020**, *11* (10), 1789–1792. <https://doi.org/10.1021/acsmchemlett.0c00052>.
- (19) Di Martino, R. M. C.; Maxwell, B. D.; Pirali, T. Deuterium in Drug Discovery: Progress, Opportunities and Challenges. *Nat Rev Drug Discov* **2023**, *22* (7), 562–584. <https://doi.org/10.1038/s41573-023-00703-8>.
- (20) Maltais, F.; Jung, Y. C.; Chen, M.; Tanoury, J.; Perni, R. B.; Mani, N.; Laitinen, L.; Huang, H.; Liao, S.; Gao, H.; Tsao, H.; Block, E.; Ma, C.; Shawgo, R. S.; Town, C.; Brummel, C. L.; Howe, D.; Pazhanisamy, S.; Raybuck, S.; Namchuk, M.; Bennani, Y. L. In Vitro and in Vivo Isotope Effects with Hepatitis C Protease Inhibitors: Enhanced Plasma Exposure of Deuterated Telaprevir versus Telaprevir in Rats. *J Med Chem* **2009**, *52* (24), 7993–8001. <https://doi.org/10.1021/jm901023f>.
- (21) Harrison, S. A.; Thang, C.; Bolze, S.; Dewitt, S.; Hallakou-Bozec, S.; Dubourg, J.; Bedossa, P.; Cusi, K.; Ratziu, V.; Grouin, J. M.; Moller, D. E.; Fouqueray, P. Evaluation of PXL065 – Deuterium-Stabilized (R)-Pioglitazone in Patients with NASH: A Phase II Randomized Placebo-Controlled Trial (DESTINY-1). *J Hepatol* **2023**, *78* (5), 914–925. <https://doi.org/10.1016/j.jhep.2023.02.004>.
- (22) Jacques, V.; Bolze, S.; Hallakou-Bozec, S.; Czarnik, A. W.; Divakaruni, A. S.; Fouqueray, P.; Murphy, A. N.; Van der Ploeg, L. H. T.; DeWitt, S. Deuterium-Stabilized (R)-Pioglitazone (PXL065) Is Responsible for Pioglitazone Efficacy in NASH yet Exhibits Little to No PPAR γ Activity. *Hepatol Commun* **2021**, *5* (8), 1412–1425. <https://doi.org/10.1002/hep4.1723>.
- (23) Monternier, P. A.; Singh, J.; Parasar, P.; Theurey, P.; DeWitt, S.; Jacques, V.; Klett, E.; Kaur, N.; Nagaraja, T. N.; Moller, D. E.; Hallakou-Bozec, S. Therapeutic Potential of Deuterium-Stabilized (R)-Pioglitazone—PXL065—for X-Linked Adrenoleukodystrophy. *J Inherit Metab Dis* **2022**, *45* (4), 832–847. <https://doi.org/10.1002/jimd.12510>.
- (24) Hutchison, C. A.; Mangum, B. W. Effect of Deuterium Substitution on the Lifetime of the Phosphorescent Triplet State of Naphthalene [2]. *J Chem Phys* **1960**, *32* (4), 1261–1262. <https://doi.org/10.1063/1.1730887>.
- (25) Qin, Y.; Xie, X.; Pang, Z.; Liu, G.; Dong, X.; Shen, S.; Zhang, Y.; Lee, C. S.; Yi, Y.; Wang, P.; Wang, Y. Deuterium Renders Fast Risc and Low Non-Radiation Decays of TADF Emitters. *Adv Opt Mater* **2023**, *11* (23), 2300981. <https://doi.org/10.1002/adom.202300981>.
- (26) Liu, X.; Chan, C. Y.; Mathevet, F.; Mamada, M.; Tsuchiya, Y.; Lee, Y. T.; Nakanotani, H.; Kobayashi, S.; Shiochi, M.; Adachi, C. Isotope Effect of Host Material on Device Stability of Thermally Activated Delayed Fluorescence Organic Light-Emitting Diodes. *Small Science* **2021**, *1* (4), 2000057. <https://doi.org/10.1002/smssc.202000057>.
- (27) He, C.; Li, Z.; Lei, Y.; Zou, W.; Suo, B. Unraveling the Emission Mechanism of Radical-Based Organic Light-Emitting Diodes. *Journal of Physical Chemistry Letters* **2019**, *10* (3), 574–580. <https://doi.org/10.1021/acs.jpclett.8b03864>.

- (28) Cho, H. H.; Gorgon, S.; Hung, H. C.; Huang, J. Y.; Wu, Y. R.; Li, F.; Greenham, N. C.; Evans, E. W.; Friend, R. H. Efficient and Bright Organic Radical Light-Emitting Diodes with Low Efficiency Roll-Off. *Advanced Materials* **2023**, *35* (45), 2303666. <https://doi.org/10.1002/adma.202303666>.
- (29) Ai, X.; Evans, E. W.; Dong, S.; Gillett, A. J.; Guo, H.; Chen, Y.; Hele, T. J. H.; Friend, R. H.; Li, F. Efficient Radical-Based Light-Emitting Diodes with Doublet Emission. *Nature* **2018**, *563* (7732), 536–540. <https://doi.org/10.1038/s41586-018-0695-9>.
- (30) Chun, C. T.; Kuo, C. H. Enhancement of OLED Efficiencies and High-Voltage Stabilities of Light-Emitting Materials by Deuteration. *Journal of Physical Chemistry C* **2007**, *111* (8), 3490–3494. <https://doi.org/10.1021/jp066116k>.
- (31) Tsuji, H.; Mitsui, C.; Nakamura, E. The Hydrogen/Deuterium Isotope Effect of the Host Material on the Lifetime of Organic Light-Emitting Diodes. *Chemical Communications* **2014**, *50* (94), 14870–14872. <https://doi.org/10.1039/c4cc05108d>.
- (32) Lu, S.; Jin, T.; Yasuda, T.; Si, W.; Oniwa, K.; Alamry, K. A.; Kosa, S. A.; Asiri, A. M.; Han, L.; Yamamoto, Y. Deuterium Isotope Effect on Bulk Heterojunction Solar Cells. Enhancement of Organic Photovoltaic Performances Using Monobenzyl Substituted Deuteriofullerene Acceptors. *Org Lett* **2013**, *15* (22), 5674–5677. <https://doi.org/10.1021/ol4026606>.
- (33) Scher, C.; Ravid, B.; Halevi, E. A. Deuterium Isotope Effects on the Dipole Moment and Polarizability of HCl and NH₃. *Journal of Physical Chemistry* **1982**, *86* (5), 654–658. <https://doi.org/10.1021/j100394a013>.
- (34) Qiu, D.; Adil, M. A.; Lu, K.; Wei, Z. The Crystallinity Control of Polymer Donor Materials for High-Performance Organic Solar Cells. *Front Chem* **2020**, *8*, 603134. <https://doi.org/10.3389/fchem.2020.603134>.
- (35) Li, L.; Jakowski, J.; Do, C.; Hong, K. Deuteration and Polymers: Rich History with Great Potential. *Macromolecules* **2021**, *54* (8), 3555–3584. <https://doi.org/10.1021/acs.macromol.0c02284>.
- (36) Shao, M.; Keum, J.; Chen, J.; He, Y.; Chen, W.; Browning, J. F.; Jakowski, J.; Sumpter, B. G.; Ivanov, I. N.; Ma, Y. Z.; Rouleau, C. M.; Smith, S. C.; Geohegan, D. B.; Hong, K.; Xiao, K. The Isotopic Effects of Deuteration on Optoelectronic Properties of Conducting Polymers. *Nat Commun* **2014**, *5* (1), 1–11. <https://doi.org/10.1038/ncomms4180>.
- (37) Zeng, L.; Zhang, M.; Gao, M.; Xue, L.; Wang, H.; Zhang, Z. G.; Ye, L. Impact of Side-Chain Deuteration on the Molecular Stacking and Photovoltaic Performance of Non-Fullerene Acceptors. *J Mater Chem A Mater* **2023**, *11* (44), 24184–24191. <https://doi.org/10.1039/d3ta04761j>.
- (38) Gao, M.; Zhang, K.; He, C.; Jiang, H.; Li, X.; Qi, Q.; Zhou, K.; Chen, Y.; Zhao, W.; Ye, L. A Generic Approach Yields Organic Solar Cells with Enhanced Efficiency and Thermal Stability. *Aggregate* **2023**, *4* (2), e289. <https://doi.org/10.1002/agt2.289>.
- (39) Zhang, Y.; Yi, H.; Iraqi, A.; Kingsley, J.; Buckley, A.; Wang, T.; Lidzey, D. G. Comparative Indoor and Outdoor Stability Measurements of Polymer Based Solar Cells. *Sci Rep* **2017**, *7* (1), 1–9. <https://doi.org/10.1038/s41598-017-01505-w>.
- (40) Levitt, M. H. *Spin Dynamics: Basics of Nuclear Magnetic Resonance*; Wiley, 2001.

- (41) Laszlo, P. *NMR of Newly Accessible Nuclei: Chemically and Biochemically Important Elements*; NMR of Newly Accessible Nuclei; Academic Press, 1983.
- (42) De Feyter, H. M.; Behar, K. L.; Corbin, Z. A.; Fulbright, R. K.; Brown, P. B.; McIntyre, S.; Nixon, T. W.; Rothman, D. L.; De Graaf, R. A. Deuterium Metabolic Imaging (DMI) for MRI-Based 3D Mapping of Metabolism in Vivo. *Sci Adv* **2018**, *4* (8), 7314–7336. <https://doi.org/10.1126/sciadv.aat7314>.
- (43) Montrazi, E. T.; Sasson, K.; Agemy, L.; Peters, D. C.; Brenner, O.; Scherz, A.; Frydman, L. High-Sensitivity Deuterium Metabolic MRI Differentiates Acute Pancreatitis from Pancreatic Cancers in Murine Models. *Sci Rep* **2023**, *13* (1), 1–10. <https://doi.org/10.1038/s41598-023-47301-7>.
- (44) Serrao, E. M.; Kettunen, M. I.; Rodrigues, T. B.; Dzien, P.; Wright, A. J.; Gopinathan, A.; Gallagher, F. A.; Lewis, D. Y.; Frese, K. K.; Almeida, J.; Howat, W. J.; Tuveson, D. A.; Brindle, K. M. MRI with Hyperpolarised [1-¹³C]Pyruvate Detects Advanced Pancreatic Preneoplasia Prior to Invasive Disease in a Mouse Model. *Gut* **2016**, *65* (3), 465–475. <https://doi.org/10.1136/gutjnl-2015-310114>.
- (45) Martinho, R. P.; Bao, Q.; Markovic, S.; Preise, D.; Sasson, K.; Agemy, L.; Scherz, A.; Frydman, L. Identification of Variable Stages in Murine Pancreatic Tumors by a Multiparametric Approach Employing Hyperpolarized ¹³C MRSI, ¹H Diffusivity and ¹H T₁ MRI. *NMR Biomed* **2021**, *34* (2). <https://doi.org/10.1002/nbm.4446>.
- (46) Halford, J. O.; Anderson, L. C.; Bates, J. R. The Introduction of Deuterium Atoms into Acetone. *J Am Chem Soc* **1934**, *56* (2), 491–492. <https://doi.org/10.1021/ja01317a509>.
- (47) Tucholski, T.; Rideal, E. K. The Reaction of Hydrogen and Deuterium with Ethylene at a Nickel Surface. *Journal of the Chemical Society (Resumed)* **1935**, No. 0, 1701–1704. <https://doi.org/10.1039/jr9350001701>.
- (48) Morikawa, K.; Benedict, W. S.; Taylor, H. S. Catalytic Exchange of Deuterium and Methane. *J Am Chem Soc* **1935**, *57* (3), 592–593. <https://doi.org/10.1021/ja01306a509>.
- (49) Taylor, H. S.; Jungers, J. C. Exchange between Ammonia and Deuterium on Catalytic Iron Surfaces. *J Am Chem Soc* **1935**, *57* (4), 660–661. <https://doi.org/10.1021/ja01307a018>.
- (50) Experiments on Heavy Hydrogen IV—The Hydrogenation and Exchange Reaction of Ethylene with Heavy Hydrogen. *Proceedings of the Royal Society of London. Series A, Containing Papers of a Mathematical and Physical Character* **1934**, *146* (858), 630–639. <https://doi.org/10.1098/rspa.1934.0177>.
- (51) Farkas, A.; Farkas, L.; Rideal, E. K. Experiments on Heavy Hydrogen IV—The Hydrogenation and Exchange Reaction of Ethylene with Heavy Hydrogen. *Proceedings of the Royal Society of London. Series A, Containing Papers of a Mathematical and Physical Character* **1934**, *146* (858), 630–639. <https://doi.org/10.1098/rspa.1934.0177>.
- (52) Wynne-Jones, W. F. K. Acid-Base Reactions Involving Deuterium. *J Chem Phys* **1934**, *2* (7), 381–385. <https://doi.org/10.1063/1.1749492>.
- (53) Horiuti, J.; Ogden, G.; Polanyi, M. Catalytic Replacement of Haplogen by Diplogen in Benzene. *Transactions of the Faraday Society* **1934**, *30* (0), 663–665. <https://doi.org/10.1039/TF9343000663>.
- (54) Halford, J. O.; Anderson, L. C. Organic Deuterium Compounds. Acetic, Malonic and Succinic Acids. *J Am Chem Soc* **1936**, *58* (5), 736–740. <https://doi.org/10.1021/ja01296a011>.

- (55) Wilson, C. L. The Preparation of Organic Compounds Containing Deuterium. Dideuteromalonic Deuteracid and Trideuteracetic Deuteracid. *Journal of the Chemical Society (Resumed)* **1935**, No. 0, 492–494. <https://doi.org/10.1039/jr9350000492>.
- (56) Ingold, C. K.; Raisin, C. G.; Wilson, C. L. Direct Introduction of Deuterium into Aliphatic Systems. Part I. Hydrogen Exchange between Sulphuric Acid and Paraffinoid Hydrocarbons. *Journal of the Chemical Society (Resumed)* **1936**, No. 0, 1643–1645. <https://doi.org/10.1039/jr9360001643>.
- (57) Legg, J. I.; Steele, J. A Study of Model Complexes of Products Expected from N-Terminal Hydrolysis of Polypeptides Containing Trifunctional Amino Acids. Tetraminecobalt(III) Complexes of Glutamic and Aspartic Acids. *Inorg Chem* **1971**, *10* (10), 2177–2182. <https://doi.org/10.1021/ic50104a017>.
- (58) Buckingham, D. A.; Marzilli, L. G.; Sargeson, A. M. Proton Exchange and Mutarotation of Chelated Amino Acids via Carbanion Intermediates. *J Am Chem Soc* **1967**, *89* (20), 5133–5138. <https://doi.org/10.1021/ja00996a009>.
- (59) Aresta, M.; Ciminale, F. Ring Opening in a Non-Basic Medium of 2-Methyl-6-Nitrobenzothiazole and H-D Exchange at the 2-Methyl Promoted by Silver(I). *Journal of the Chemical Society, Dalton Transactions* **1981**, No. 7, 1520–1523. <https://doi.org/10.1039/DT9810001520>.
- (60) Jones, J. R.; Taylor, S. E. Isotopic Hydrogen Exchange in Purines - Mechanisms and Applications. *Chem Soc Rev* **1981**, *10* (3), 329–344. <https://doi.org/10.1039/CS9811000329>.
- (61) Lewandos, G. S.; Maki, J. W.; Ginnebaugh, J. P. Kinetics of Terminal Alkyne Sp Carbon-Hydrogen Bond Activation Catalyzed by Silver(I). *Organometallics* **1982**, *1* (12), 1700–1705. <https://doi.org/10.1021/om00072a028>.
- (62) Clement, O.; Roszak, A. W.; Buncl, E. Hydrogen-Deuterium Exchange Studies in Platinum(II) Complexes of 1-Methylimidazole. *J Am Chem Soc* **1996**, *118* (3), 612–620. <https://doi.org/10.1021/ja951615c>.
- (63) Branch, C. S.; Barron, A. R. Arene-Mercury Complexes Stabilized by Gallium Chloride: Relative Rates of H/D and Arene Exchange. *J Am Chem Soc* **2002**, *124* (47), 14156–14161. <https://doi.org/10.1021/ja0206590>.
- (64) Labinger, J. A.; Bercaw, J. E. Understanding and Exploiting C–H Bond Activation. *Nature* **2002**, *417*:6888 **2002**, *417* (6888), 507–514. <https://doi.org/10.1038/417507a>.
- (65) Rhinehart, J. L.; Manbeck, K. A.; Buzak, S. K.; Lippa, G. M.; Brennessel, W. W.; Goldberg, K. I.; Jones, W. D. Catalytic Arene H/D Exchange with Novel Rhodium and Iridium Complexes. *Organometallics* **2012**, *31* (5), 1943–1952. <https://doi.org/10.1021/om2012419>.
- (66) Corpas, J.; Viereck, P.; Chirik, P. J. C(Sp²)-H Activation with Pyridine Dicarbene Iron Dialkyl Complexes: Hydrogen Isotope Exchange of Arenes Using Benzene- D₆ as a Deuterium Source. *ACS Catal* **2020**, *10* (15), 8640–8647. <https://doi.org/10.1021/acscatal.0c01714>.
- (67) Roque, J. B.; Pabst, T. P.; Chirik, P. J. C(Sp²)-H Activation with Bis(Silylene)Pyridine Cobalt(III) Complexes: Catalytic Hydrogen Isotope Exchange of Sterically Hindered C-H Bonds. *ACS Catal* **2022**, *12* (15), 8877–8885. <https://doi.org/10.1021/acscatal.2c02429>.

- (68) Zhao, L. L.; Liu, W.; Zhang, Z.; Zhao, H.; Wang, Q.; Yan, X. Ruthenium-Catalyzed Ortho- And Meta-H/D Exchange of Arenes. *Org Lett* **2019**, *21* (24), 10023–10027. <https://doi.org/10.1021/acs.orglett.9b03955>.
- (69) Bai, W.; Lee, K. H.; Tse, S. K. S.; Chan, K. W.; Lin, Z.; Jia, G. Ruthenium-Catalyzed Deuteration of Alcohols with Deuterium Oxide. *Organometallics* **2015**, *34* (15), 3686–3698. <https://doi.org/10.1021/acs.organomet.5b00134>.
- (70) Jones, W. D. Isotope Effects in C-H Bond Activation Reactions by Transition Metals. *Acc Chem Res* **2003**, *36* (2), 140–146. <https://doi.org/10.1021/ar020148i>.
- (71) Thompson, M. E.; Baxter, S. M.; Bulls, A. R.; Burger, B. J.; Schaefer, W. P.; Bercaw, J. E.; Nolan, M. C.; Santarsiero, B. D. “ σ Bond Metathesis” For C-H Bonds of Hydrocarbons And Sc-r (r = H, Alkyl, Aryl) Bonds of Permethylscandocene Derivatives: Evidence For Noninvolvement of The π System In Electrophilic Activation of Aromatic And Vinylic C-h Bonds. *J Am Chem Soc* **1987**, *109* (1), 203–219. <https://doi.org/10.1021/ja00235a031>.
- (72) Di Giuseppe, A.; Castarlenas, R.; Oro, L. A. Mechanistic Considerations on Catalytic H/D Exchange Mediated by Organometallic Transition Metal Complexes. *Comptes Rendus Chimie* **2015**, *18* (7), 713–741. <https://doi.org/10.1016/J.CRCI.2015.02.006>.
- (73) Tsukinoki, T.; Ishimoto, K.; Mukumoto, M.; Suzuki, M.; Kawaji, T.; Nagano, Y.; Tsuzuki, H.; Mataka, S.; Tashiro, M. Raney Co-Al Alloy, an Efficient Catalyst for the Selective Incorporation of Deuterium Atoms at the Benzylic Position of Aromatic Compounds. *Journal of Chemical Research - Part S* **1996**, *27* (1), 66–67. <https://doi.org/10.1002/CHIN.199628083>.
- (74) Dinnocenzo, J. P.; Banach, T. E. The Quinuclidine Dimer Cation Radical. *J Am Chem Soc* **1988**, *110* (3), 971–973. <https://doi.org/10.1021/ja00211a050>.
- (75) Maegawa, T.; Fujiwara, Y.; Inagaki, Y.; Esaki, H.; Monguchi, Y.; Sajiki, H. Mild and Efficient H/D Exchange of Alkanes Based on C-H Activation Catalyzed by Rhodium on Charcoal. *Angewandte Chemie - International Edition* **2008**, *47* (29), 5394–5397. <https://doi.org/10.1002/anie.200800941>.
- (76) Matsubara, S.; Ishibashi, K.; Maung, G. Y. T.; Morota, Y.; Umemura, T.; Kato, Y. H/D Exchange Using Hot Heavy Water. *Chimia (Aarau)* **2018**, *72* (12), 853–858. <https://doi.org/10.2533/chimia.2018.853>.
- (77) Brown, W. G.; Garnett, J. L. Platinum-Catalyzed Exchange of Aromatic Compounds with Deuterium Oxide. *J Am Chem Soc* **1958**, *80* (19), 5272–5274. <https://doi.org/10.1021/ja01552a064>.
- (78) Sattler, A.; Paccagnini, M.; Lanci, M. P.; Miseo, S.; Kliewer, C. E. Platinum Catalyzed C-H Activation and the Effect of Metal-Support Interactions. *ACS Catal* **2020**, *10* (1), 710–720. <https://doi.org/10.1021/acscatal.9b03807>.
- (79) Garnett, J. L.; Sollich, W. A. A π -Complex Mechanism for Catalytic Exchange Reactions. *J Catal* **1963**, *2* (4), 350–353. [https://doi.org/10.1016/0021-9517\(63\)90078-2](https://doi.org/10.1016/0021-9517(63)90078-2).
- (80) Garnett, J. L.; Sollich-Baumgartner, W. A. Catalytic Deuterium Exchange Reactions with Organics. XIV. Distinction between Associative and Dissociative π -Complex Substitution Mechanisms. *Journal of Physical Chemistry* **1964**, *68* (11), 3177–3183. <https://doi.org/10.1021/j100793a016>.
- (81) Weitkamp, A. W. Deuteration and Deutrogenation of Naphthalene and Two Octalins. *J Catal* **1966**, *6* (3), 431–457. [https://doi.org/10.1016/0021-9517\(66\)90169-2](https://doi.org/10.1016/0021-9517(66)90169-2).

- (82) Lanzarotti, E.; Defelipe, L. A.; Marti, M. A.; Turjanski, A. G. Aromatic Clusters in Protein-Protein and Protein-Drug Complexes. *J Cheminform* **2020**, *12* (1). <https://doi.org/10.1186/s13321-020-00437-4>.
- (83) Jung, S.; Cheung, W. L.; Li, S. jie; Wang, M.; Li, W.; Wang, C.; Song, X.; Wei, G.; Song, Q.; Chen, S. S.; Cai, W.; Ng, M.; Tang, W. K.; Tang, M. C. Enhancing Operational Stability of OLEDs Based on Subatomic Modified Thermally Activated Delayed Fluorescence Compounds. *Nat Commun* **2023**, *14* (1), 1–12. <https://doi.org/10.1038/s41467-023-42019-6>.
- (84) Fang, C.; Yang, W.; Yang, C.; Wang, H.; Sun, K.; Luo, Y. Synthesis of Isotopically Labelled 2-Isopropylthioxanthone from 2,2'-Dithiosalicylic Acid and Deuterium Cumene. *J Labelled Comp Radiopharm* **2016**, 313–316. <https://doi.org/10.1002/jlcr.3400>.
- (85) Horiuti, J.; Ogden, G.; Polanyi, M. Catalytic Replacement of Haplogen by Diplogen in Benzene. *Transactions of the Faraday Society* **1934**, *30* (0), 663–665. <https://doi.org/10.1039/tf9343000663>.
- (86) Horiuti, J.; Polanyi, M. Catalytic Interchange of Hydrogen between Water and Ethylene and between Water and Benzene [2]. *Nature* **1934**, *134* (3384), 377–378. <https://doi.org/10.1038/134377b0>.
- (87) Ingold, C. K.; Raisin, C. G.; Wilson, C. L. Direct Introduction of Deuterium into Benzene without Heterogeneous Catalysis [1]. *Nature* **1934**, *134* (3393), 734. <https://doi.org/10.1038/134734a0>.
- (88) Horiuti, J.; Koyano, T. The Direct Introduction of Deuterium into Benzene by High Frequency Current. *Bull Chem Soc Jpn* **1935**, *10* (12), 601–601. <https://doi.org/10.1246/bcsj.10.601>.
- (89) Clemo, G. R.; McQuillen, A. Experiments on Hexadeuterobenzene. Part I. *Journal of the Chemical Society (Resumed)* **1935**, No. 0, 851–855. <https://doi.org/10.1039/jr9350000851>.
- (90) Ingold, C. K.; Raisin, C. G.; Wilson, C. L. Structure of Benzene. Part II. Direct Introduction of Deuterium into Benzene and the Physical Properties of Hexadeuterobenzene. *Journal of the Chemical Society (Resumed)* **1936**, No. 0, 915–925. <https://doi.org/10.1039/jr9360000915>.
- (91) Leitch, L. C. Organic Deuterium Compounds: XII. Benzene-d₆. *Can J Chem* **1954**, *32* (8), 813–814. <https://doi.org/10.1139/v54-103>.
- (92) Brown, W. G.; Garnett, J. L. Platinum-Catalyzed Exchange of Aromatic Compounds with Deuterium Oxide. *J Am Chem Soc* **1958**, *80* (19), 5272–5274. <https://doi.org/10.1021/ja01552a064>.
- (93) Garnett, J. L.; Sollich-Baumgartner, W. A. Catalytic Deuterium Exchange Reactions with Organics. XIV. Distinction between Associative and Dissociative π -Complex Substitution Mechanisms. *Journal of Physical Chemistry* **1964**, *68* (11), 3177–3183. <https://doi.org/10.1021/j100793a016>.
- (94) Fraser, R. R.; Renaud, R. N. The Steric Effect in the Platinum-Catalyzed Exchange Reaction between Aromatic Ring Protons and Deuterium Oxide. *J Am Chem Soc* **1966**, *88* (19), 4365–4370. <https://doi.org/10.1021/ja00971a011>.
- (95) Brown, W. G.; Calf, G. E.; Garnett, J. L. Thiophen and Furan as Metal Catalyst Poisons. Novel Methods for the Specific and General Labelling of These Compounds with Isotopic Hydrogen. *Chemical Communications (London)* **1967**, No. 20, 1066–1067. <https://doi.org/10.1039/C19670001066>.
- (96) Forzatti, P.; Lietti, L. Catalyst Deactivation. *Catal Today* **1999**, *52* (2–3), 165–181. [https://doi.org/10.1016/S0920-5861\(99\)00074-7](https://doi.org/10.1016/S0920-5861(99)00074-7).

- (97) Sagert, N. H.; Pouteau, R. M. L. Hydrogen–Water Deuterium Exchange over Unsupported Group VIII Noble Metals. *Can J Chem* **1974**, *52* (16), 2960–2967. <https://doi.org/10.1139/v74-433>.
- (98) Garnett, J. L.; Sollich, W. A. Catalytic Deuterium Exchange Reactions with Organics. XIII. Characteristic Reactions of the Group VIII Transition Metals. *Aust J Chem* **1965**, *18* (7), 1003–1008. <https://doi.org/10.1071/CH9651003>.
- (99) Garnett, J. L.; Sollich-Baumgartner, W. A. Catalytic Deuterium-Exchange Reactions with Organics. XIX. π -Complex Adsorption in the Exchange of the Alkylbenzenes. *Journal of Physical Chemistry* **1965**, *69* (6), 1850–1858. https://doi.org/10.1021/j100890a011/asset/j100890a011.fp.png_v03.
- (100) Sajiki, H.; Ito, N.; Esaki, H.; Maesawa, T.; Maegawa, T.; Hirota, K. Aromatic Ring Favorable and Efficient H-D Exchange Reaction Catalyzed by Pt/C. *Tetrahedron Lett* **2005**, *46* (41), 6995–6998. <https://doi.org/10.1016/j.tetlet.2005.08.067>.
- (101) Sawama, Y.; Nakano, A.; Matsuda, T.; Kawajiri, T.; Yamada, T.; Sajiki, H. H-D Exchange Deuteration of Arenes at Room Temperature. *Org Process Res Dev* **2019**, *23* (4), 648–653. <https://doi.org/10.1021/acs.oprd.8b00383>.
- (102) Modutlwa, N.; Maegawa, T.; Monguchi, Y.; Sajiki, H. Synthesis of Deuterium-Labelled Drugs by Hydrogen-Deuterium (H-D) Exchange Using Heterogeneous Catalysis. *J Labelled Comp Radiopharm* **2010**, *53* (11–12), 686–692. <https://doi.org/10.1002/jlcr.1848>.
- (103) Mulliken, R. S. Molecular Compounds and Their Spectra. III. The Interaction of Electron Donors and Acceptors. *Journal of Physical Chemistry* **1952**, *56* (7), 801–822. <https://doi.org/10.1021/j150499a001>.
- (104) McCoy, M. Heavy Problems for Heavy Water: Exit of a Major Supplier Has Lab Chemical Makers Scrambling. *Chemical and Engineering News* **2012**, *90* (22), 30–32. <https://doi.org/10.1021/cen-09022-bus2>.
- (105) Michael McCoy. Isowater Claims Heavy Water Advance. *C&EN Global Enterprise* **2023**, *101* (5), 12–12. <https://doi.org/10.1021/cen-10105-buscon11>.
- (106) Zhen, W.; Guangjun, F.; Hanjiang, H. E.; Leilei, C. U. I.; Yi, W.; Jianing, Z.; Hui, S.; Xiaowei, W. Safe, Environment-Friendly and Cheap Method and Device for Producing Deuterated Aromatic Ring Compound. No. CN 111099955 A.
- (107) Bartholomew, C. H. Mechanisms of Catalyst Deactivation. *Appl Catal A Gen* **2001**, *212* (1–2), 17–60. [https://doi.org/10.1016/S0926-860X\(00\)00843-7](https://doi.org/10.1016/S0926-860X(00)00843-7).
- (108) Mehlman, M. A. Benzene, a Multi-Organ Carcinogen. *European Journal of Oncology and Environmental Health* **2008**, *13* (1), 7–20.
- (109) Campobasso, N.; Huddler, D. Hydrogen Deuterium Mass Spectrometry in Drug Discovery. *Bioorg Med Chem Lett* **2015**, *25* (18), 3771–3776. <https://doi.org/10.1016/j.bmcl.2015.07.007>.
- (110) Engen, J. R.; Botzanowski, T.; Peterle, D.; Georgescauld, F.; Wales, T. E. Developments in Hydrogen/Deuterium Exchange Mass Spectrometry. *Anal Chem* **2021**, *93* (1), 567–582. <https://doi.org/10.1021/acs.analchem.0c04281>.
- (111) Li, H.; Feng, L. An Improved Sealed Quartz-Tube Method for the Determination of Hydrogen Isotopes in Water. *Journal of Mass Spectrometry* **2020**, *55* (10), e4612. <https://doi.org/10.1002/jms.4612>.

- (112) Banerjee, S. Empowering Clinical Diagnostics with Mass Spectrometry. *ACS Omega* **2020**, 5 (5), 2041–2048. <https://doi.org/10.1021/acsomega.9b03764>.
- (113) Takáts, Z.; Vékey, K. Electrospray and Atmospheric Pressure Chemical Ionisation of Aromatic Compounds in Dichloromethane Solvent. *European Journal of Mass Spectrometry* **1998**, 4 (5), 365–370. <https://doi.org/10.1255/ejms.234>.
- (114) Xie, L.; Zhao, Y.; Sheng, L.; Feng, S.; Shen, A.; Chen, Y.; Zhao, C.; Song, M.; Hu, Y.; Lei, W. Determination of Isotope Abundance for Deuterium-Labeled Compounds by Quantitative ^1H NMR + ^2H NMR. *J Labelled Comp Radiopharm* **2022**, 65 (9), 234–243. <https://doi.org/10.1002/jlcr.3990>.

Appendices

Appendix 1: Analytical Methods of Benzene H/D Exchange

A1.1 Gas-Chromatography Mass Spectrometry

The analysis of deuterium had a wide array of strategies and methods can vary based on the intention and molecular properties of the analyte. The goals of analysis can pertain to isotope tracking, used commonly in proteomics for structure elucidation and mechanistic/kinetic investigation,^{15,109,110} or isotopic quantitation, important for characterization in geochemistry and medicinal chemistry.^{15,111} The latter is of interest to this research. Naturally, the measure of deuterium in molecules is the most direct way of assessing the efficacy of H/D exchange reactions. Utilizing the differences in properties between protium and deuterium is key to achieving a robust analytical procedure. The most obvious property to exploit is the difference in mass between the isotopes, and it is no surprise that mass spectrometry is used routinely for quantifying H/D exchange processes. However, with numerous types of mass spectrometry it is necessary to understand the strengths and weaknesses of each. Considering benzene and its isotopologues as the analyte of interest, mass spectrometry techniques compatible with low mass, volatile, non-polar compounds are required. Of the current methods, electron impact (EI), atmospheric-pressure chemical ionization (APCI), and photo-ionization (APPI) fit these criteria (**Figure A1-1**).¹¹² Based on the facilities available in the chemistry department, GC-MS and APCI were the best candidates. The solvent dichloromethane is known to have the best ionization efficiency with benzene, but in the ionization process an adduct forms upon the addition of a chloromethyl cation. The adduct undergoes an elimination reaction to produce the more stable tropylium ion and releasing hydrochloric acid as a by-product. During this elimination deuterium atoms can be removed from the benzene ring to form deuterium chloride, resulting in an inaccurate measurement of deuterium incorporated from the H/D exchange reaction (**Scheme A1-1**).¹¹³ Because of this, GC-MS coupled with EI was more suitable for benzene analysis. Having selected the instrument, the instrument method was next to be established.

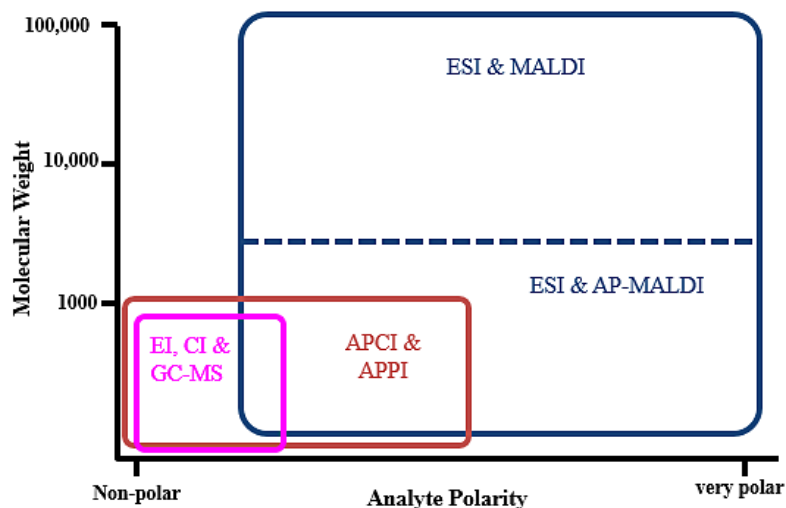
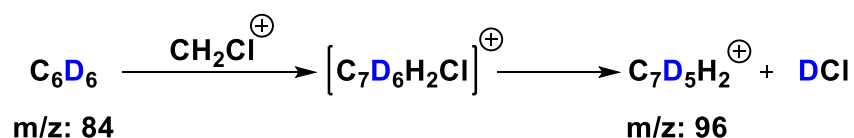


Figure A1-1: Compatibility of different mass spectrometry ionization methods across polarity and analyte mass.



Scheme A1-1: Chemical ionization of benzene-d6 eliminates deuterium atom via addition-elimination with dichloromethane reagent gas.

While benzene is a prime analyte for GC-MS as a volatile compound, its low mass and boiling point must be carefully considered for sample preparation and method development. Standard methods involve fast temperature ramps to high temperatures which would cause the analyte to elute with solvent (**Figure A1-2**). An isothermal process solves this, holding a constant oven temperature of 35°C allows benzene and its deuterated forms to elute slowly enough for solvent to precede. For this to be true, the solvent needed to dissolve benzene, have a boiling point lower than benzene, and possess no ions within the mass range of benzene and its isotopologues (78 - 84 m/z). Of the compatible solvents, ethanol and acetone were found to be suitable for this analysis. Benzene and benzene-d6 elute at ~3-4 minutes (**Figure A1-3**). With benzene and deuterated product being observable, measurement of deuterium content could be obtained from the resulting mass spectrum. Since mass spectra present ion peaks as a histogram, one must deconvolute the spectrum to acquire the true abundances. From the spectral data, the distribution of isotopologues could be determined by the following equation:

$$\%D_n = \frac{e^- \text{ count of isotopologue 'n'}}{\text{Total } e^- \text{ count}}$$

Knowing the quantities of each isotopologue generated (%D_n), the total deuterium content can be calculated using the following formula:

$$\sum_{n=1}^6 \%D_n \cdot \frac{n}{6} = \%D \text{ total}$$

Example calculation of %D from the following reaction product:

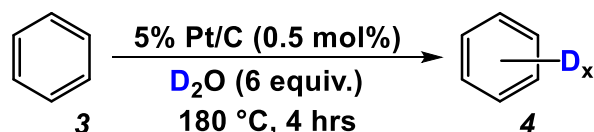


Table A1-1: Ion abundance values from GC-MS spectrum, with benzene isotopologue distribution of sample extracted from data.

		Mass-to-charge ratio (m/z)							
		78 (D ₀)	79 (D ₁)	80 (D ₂)	81 (D ₃)	82 (D ₄)	83 (D ₅)	84 (D ₆)	Total
e ⁻		6.936	4.770	2.229	2.411	8.250	4.261	2.689	1.197
count		x 10 ⁸	x 10 ⁸	x 10 ⁷	x 10 ⁶	x 10 ⁵	x 10 ⁵	x 10 ⁵	x 10 ⁹
%D _n		58%	40%	2%	0%	0%	0%	0%	100%

$$\%D_1 = \frac{639612416}{1196855821} = 58\%$$

$$\sum_{n=1}^6 \%D_n \cdot \frac{n}{6} = 0.58 \cdot \frac{0}{6} + 0.40 \cdot \frac{1}{6} + 0.02 \cdot \frac{2}{6} = 6\% \text{ total } D$$

The abundance of each isotopologue contain ‘n’ number of deuterium atoms of its 6 total hydrogens. The amount of deuterium in each isotopologue is then determined by the amount of that isotopologue multiplied by the ratio of deuterium to hydrogen in that isotopologue. The sum of all 6 isotopologues deuterium contribution yields the total deuterium content in the sample. Using GC-MS as the analytical tool worked well for most of this project. However, it would be later revealed that the accuracy of mass spectrometry is flawed as benzene becomes more isotopically enriched. As referenced in Chapter 2, the analysis of deuterated benzene shifted from GC-MS to a qNMR process. It was discovered through the qNMR method that the calculated values of deuterium incorporation were incongruent with the GC-MS method and would skew above or below the qNMR determined value throughout the progression of deuterium introduced into benzene (**Figure A1-4**). The was discovered when optimization of the second reaction repeatedly produced

a plateau, comparison of the GC-MS value and the qNMR value revealed a discrepancy in the measured value. To assess the breadth of this, several previously made samples were subjected to the same evaluation. In the most extreme case, a GC-MS value measured benzene to be 49% D but would correspond to 34% D by qNMR, a difference of 15%. A trend was observed where the GC-MS would produce a deuterium measurement greater than the qNMR measurement, until approximately 85% D where the GC-MS value would fall below that of the qNMR. To confirm the accuracy of both methods, a standard of benzene-*d*6 (99.7% D) was analyzed using both methods. From this, the deuterium content was measured at 99.6% ± 0.2 D via qNMR while the GC-MS reported 92% D. The divergence in values at high isotopic purity is determined to be from fragmentation of the parent ion, obscuring the true abundance of lower isotopologues (**Figure A1-5**). With this knowledge, all further analysis was performed exclusively by qNMR.

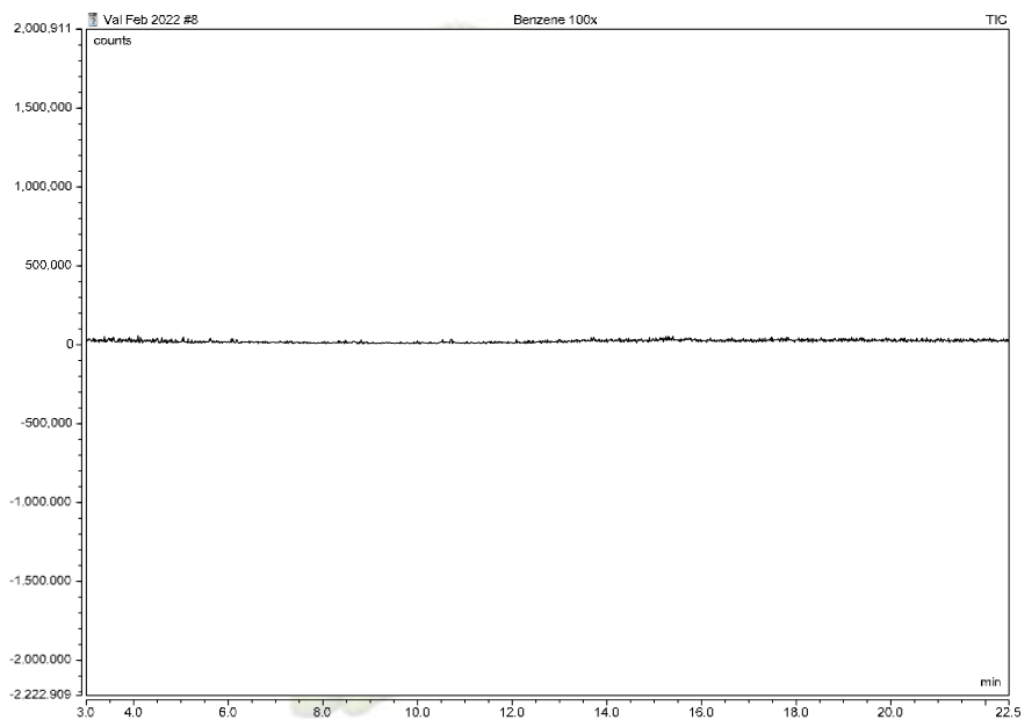


Figure A1-2: Using the standard GC conditions (80 – 200 °C) causes benzene to elute too quickly with the solvent front, leaving a blank result.

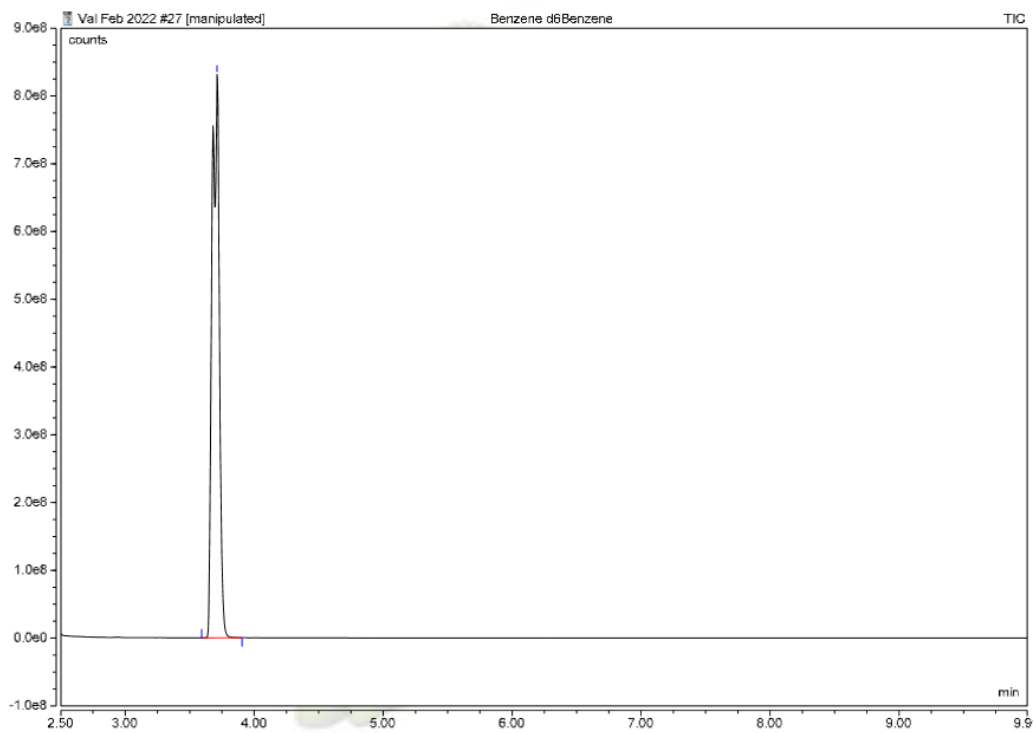


Figure A1-3: Isothermal GC column temperature of a 1:1 mixture of benzene and benzene-*d6* elutes in ~3.75 min. Due to benzene-*d6* having a slightly lower boiling point, the peak is instead a coalescence of two unresolved peaks.

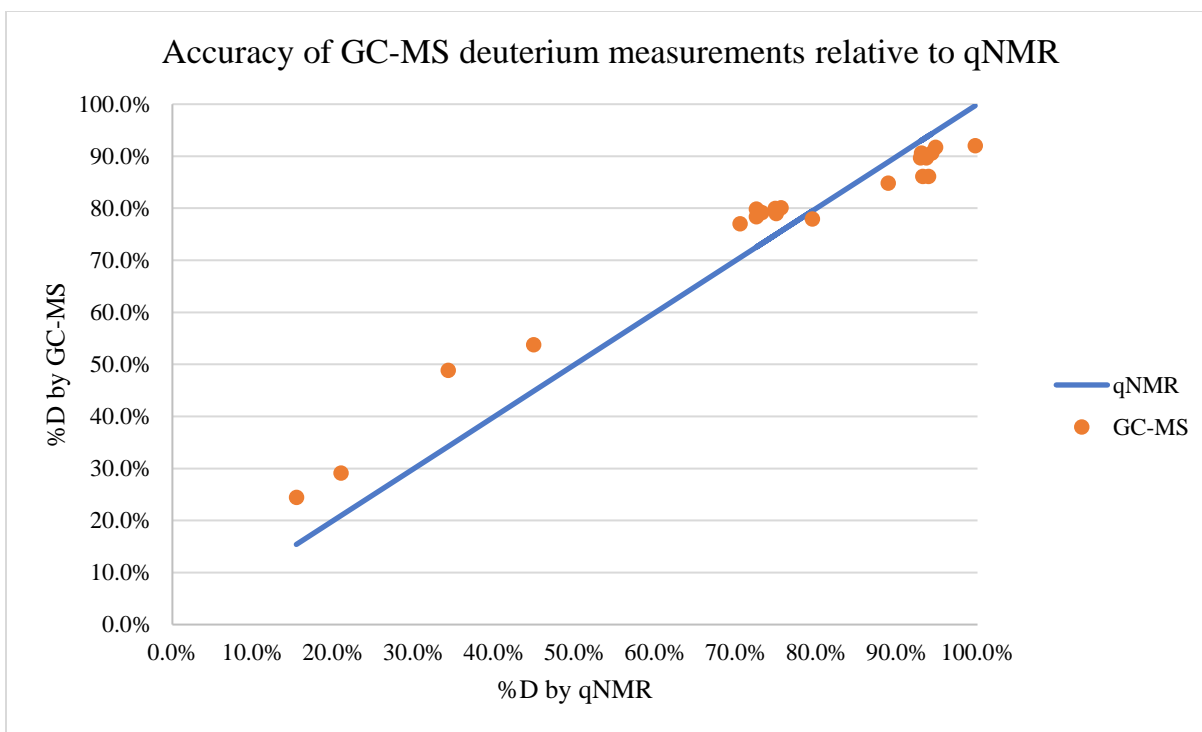


Figure A1-4: Above 85% D, fragmentation of the benzene ring deflates the calculated %D with no way of discerning cause between fragmentation and presence of an isotopologue. Reasons for inflated %D values below 85% are unclear, accounting for ^{13}C peaks and possible $[\text{M}+\text{H}]$ adducts contribute $\sim 1\%$ difference, which does not equate with the 10% increase in values observed.

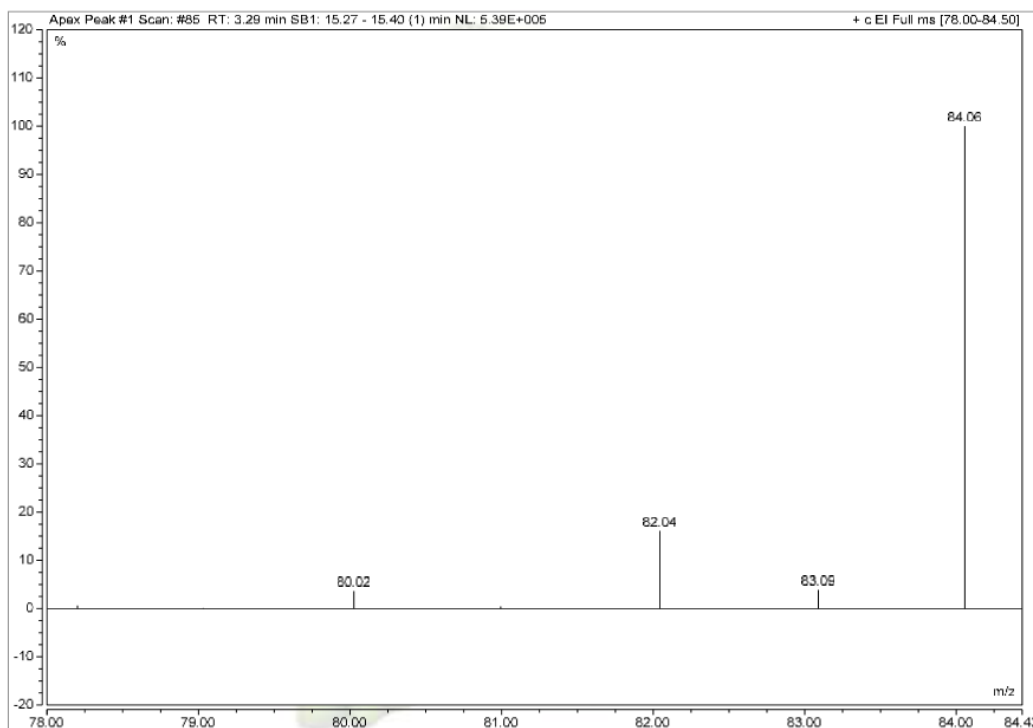


Figure A1-5: A benzene-d6 standard (99.7% D) shows fragmentation peaks which would coincidentally correspond with isotopologues benzene-d2, -d4, and -d5, resulting in an inaccurate calculated value of 92% D.

A1.2 Quantitative ^1H + ^2H Nuclear Magnetic Resonance Spectroscopy

During the course of this project, a publication was released demonstrating a qNMR method which determines the deuterium content of compounds with high accuracy and reproducibility.¹¹⁴ The method involves preparation of the deuterated sample with an appropriate proton internal standard and deuterated solvent. The sample is then run for ^1H NMR using the proton internal standard as reference (**Figure A1-6**), then ^2H NMR is followed where the deuterated solvent serves as the deuterated internal standard (**Figure A1-7**). By using the deuterated solvent as a second internal standard, both NMR spectra can be obtained from the same sample and removes the need to prepare samples for each NMR analysis. Consolidation of the samples prevents additional error through sample preparation, ensuring that both NMR spectra are correlative to the same quantities of sample and standard. For the analysis of benzene, maleic acid was chosen as the proton standard as both compounds possess sp^2 hydrogens. Despite similar hybridization, T1 relaxation times can still vary due to the differences in electronic effects between benzene aromaticity and carboxylic acids on a non-cyclic alkene. This issue was addressed in the paper as well, increasing the relaxation delay to 50 seconds encompasses many common standards and reagents used in qNMR.¹¹⁴ Methanol-*d*4 was chosen as the solvent due to its compatibility with benzene and is readily accessible from

the industrial partner. Once the spectra are obtained, the deuterium abundance can be calculated by the following equation:

$$\frac{C_D}{C_D + C_H} \cdot 100 = \% D \text{ total}$$

Where C_D and C_H are the isotopic purity of deuterium and protium, respectively. These values are calculated by the general formula below:

$$C_A = \frac{m_s \cdot N_s \cdot MW_A \cdot I_A}{m_A \cdot N_A \cdot MW_s \cdot I_s} \cdot P_s$$

$$= \frac{\frac{\text{Integral of analyte}}{\# \text{ moles of analyte protons}}}{\frac{\text{Integral of standard}}{\# \text{ moles of standard protons}}} \cdot \text{Purity of standard}$$

Where m , N , MW , and I are the mass, molar mass, number of protons, and integration of the standard (s) and analyte (A) with P_s representing the purity of the standard.

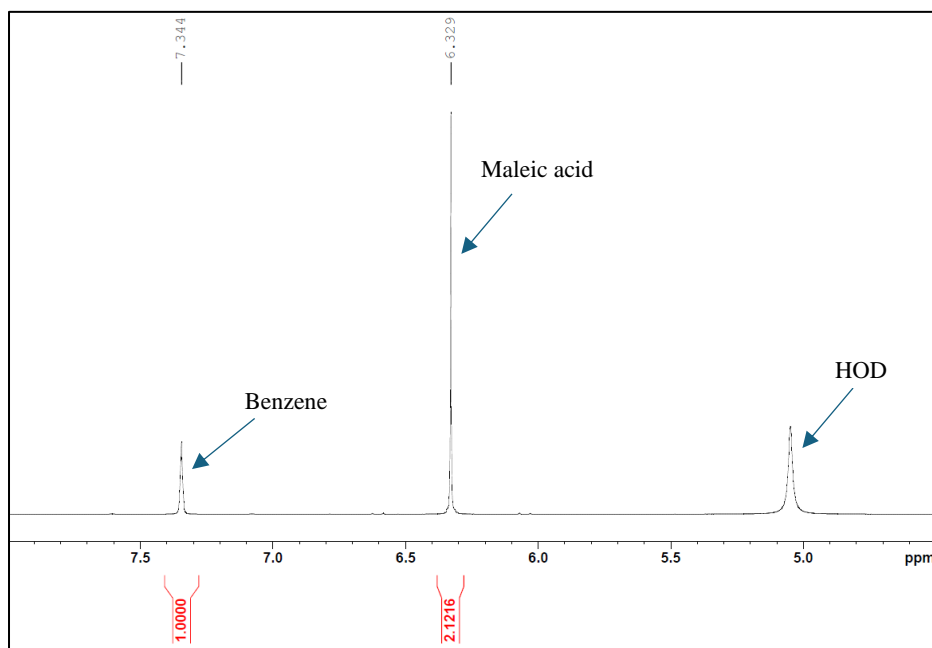


Figure A1-6: ^1H NMR spectrum of deuterated benzene (88.9% D, δ 7.3 ppm) with maleic acid as standard (δ 6.3 ppm).

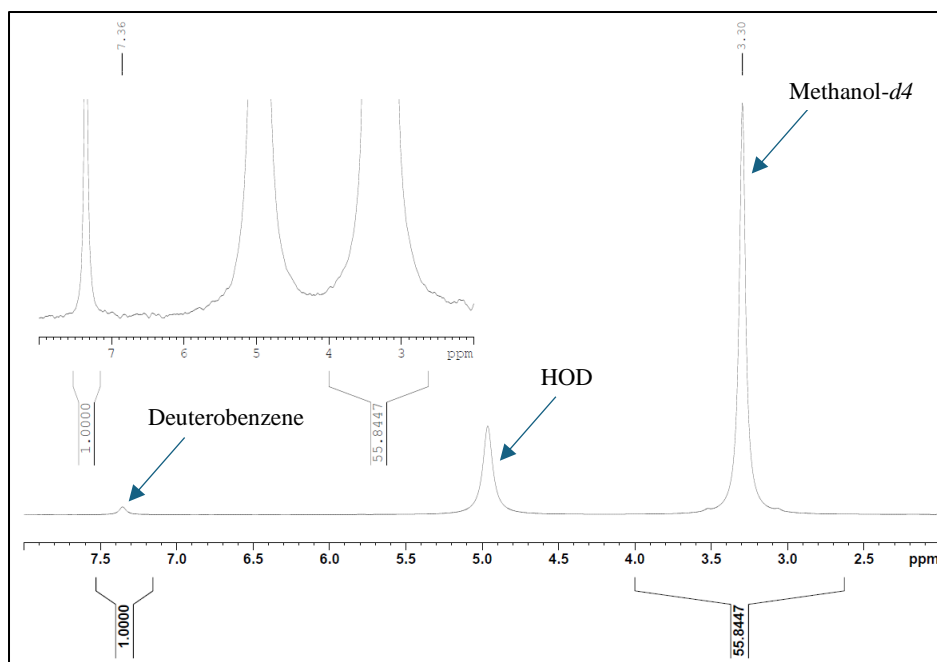


Figure A1-7: Full ^2H NMR spectrum of deuterated benzene (88.9% D, δ 7.3 ppm) with methanol- d_4 (δ 3.24 ppm) as the internal standard (top). Zoomed to show benzene peak.

Sample calculation using data from above spectra:

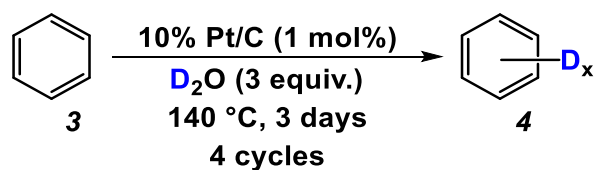


Table A1-2: Weighed quantities of standards and sample, with representative integration values from NMR spectra.

<i>Mass maleic acid (mg)</i>	<i>mmol maleic acid</i>	<i>Mass methanol-d_4 (mg)</i>	<i>mmol methanol-d_4</i>	<i>Mass benzene (mg)</i>	<i>Int. benzene</i>	<i>Int. deuterobenzene</i>	<i>Int. maleic acid</i>	<i>Int. methanol-d_4</i>
14.5	0.125	588.4	16.31	18	1.000	1.000	2.1216	55.8447

$$C_H = \frac{m_s \cdot N_s \cdot MW_A \cdot I_A}{m_A \cdot N_A \cdot MW_s \cdot I_s} \cdot P_s = \frac{0.125 \cdot 2 \cdot 78.11 \cdot 1}{18 \cdot 6 \cdot 116.072 \cdot 2.1216} \cdot 99\% = 0.08432$$

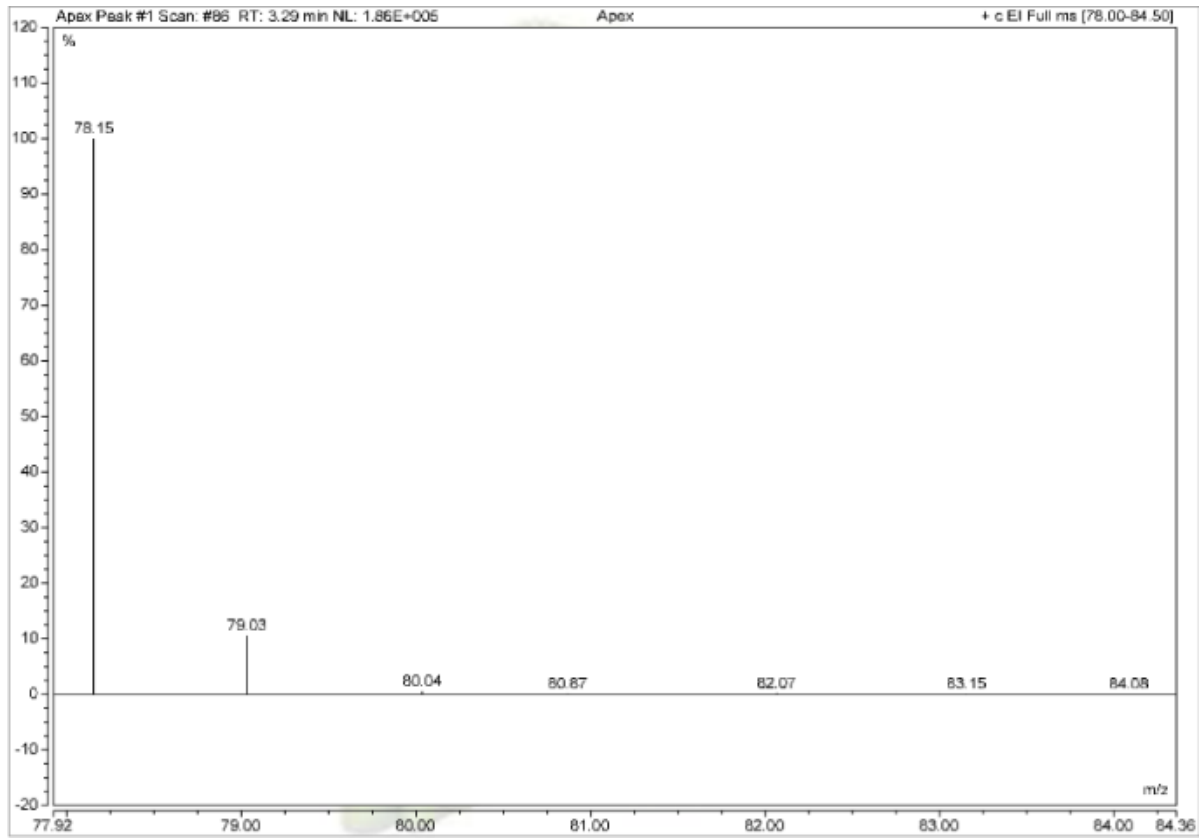
$$C_D = \frac{m_s \cdot N_s \cdot MW_A \cdot I_A}{m_A \cdot N_A \cdot MW_s \cdot I_s} \cdot P_s = \frac{16.31 \cdot 3 \cdot 84.15 \cdot 1}{18 \cdot 6 \cdot 36.066 \cdot 55.8447} \cdot 99\% = 0.6760$$

$$\frac{C_D}{C_D + C_H} \cdot 100 = \frac{0.6760}{0.6760 + 0.08432} \cdot 100 = 88.9\% \text{ D total}$$

Appendix 2: Spectral Data

Table 2-3

Entry 1



Entry 2

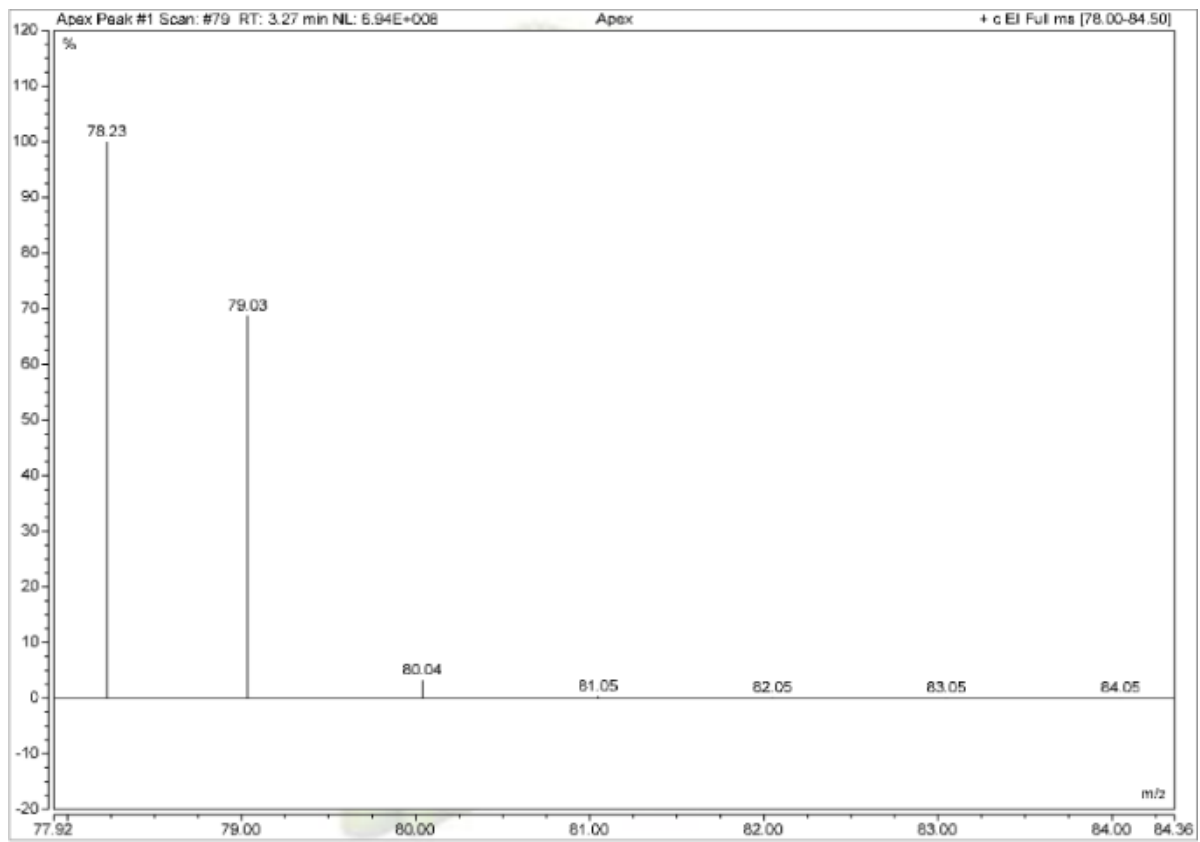
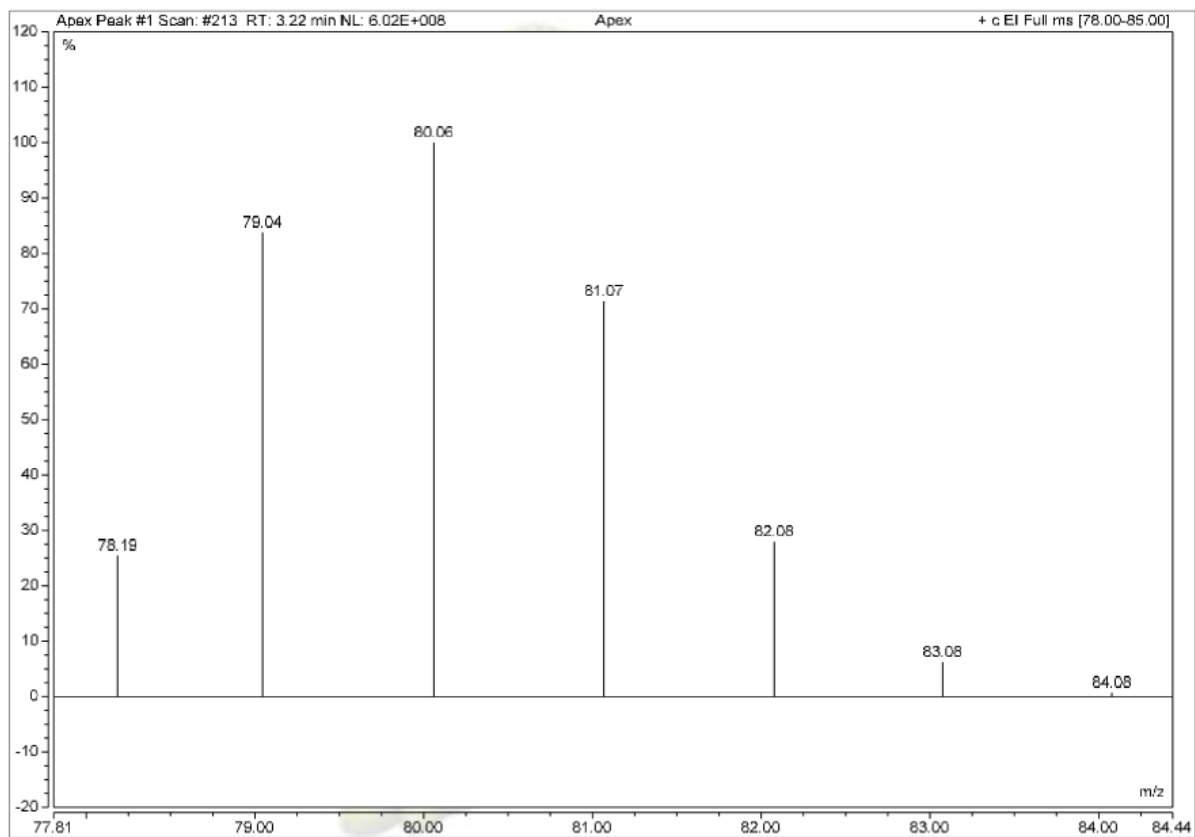
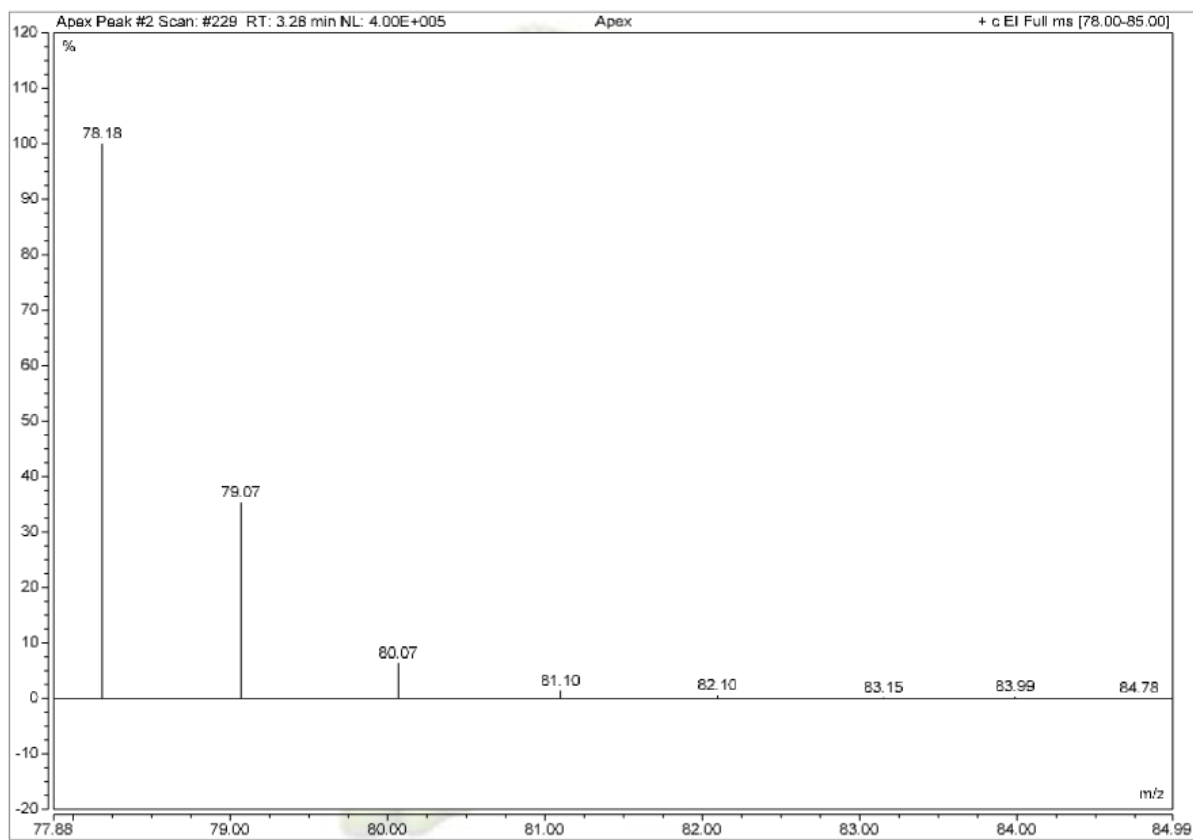


Table 2-4

Entry 1



Entry 2



Entry 3

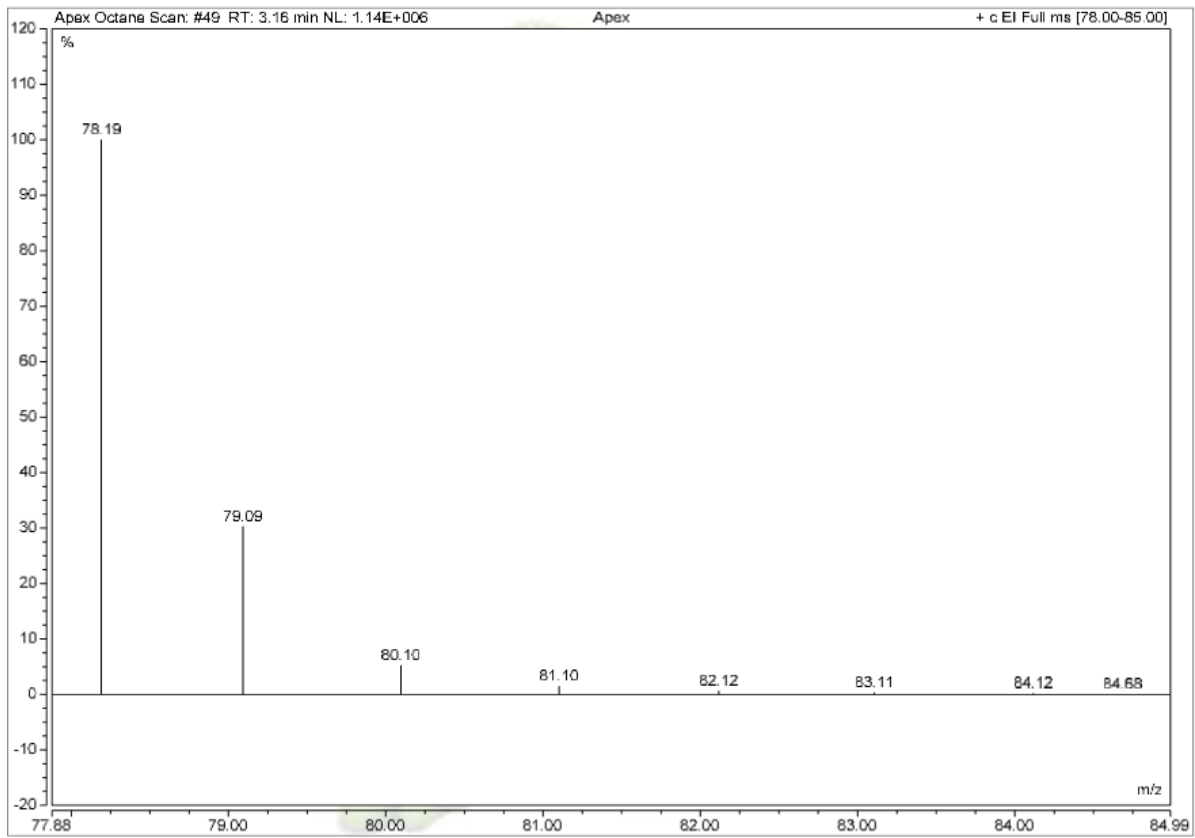
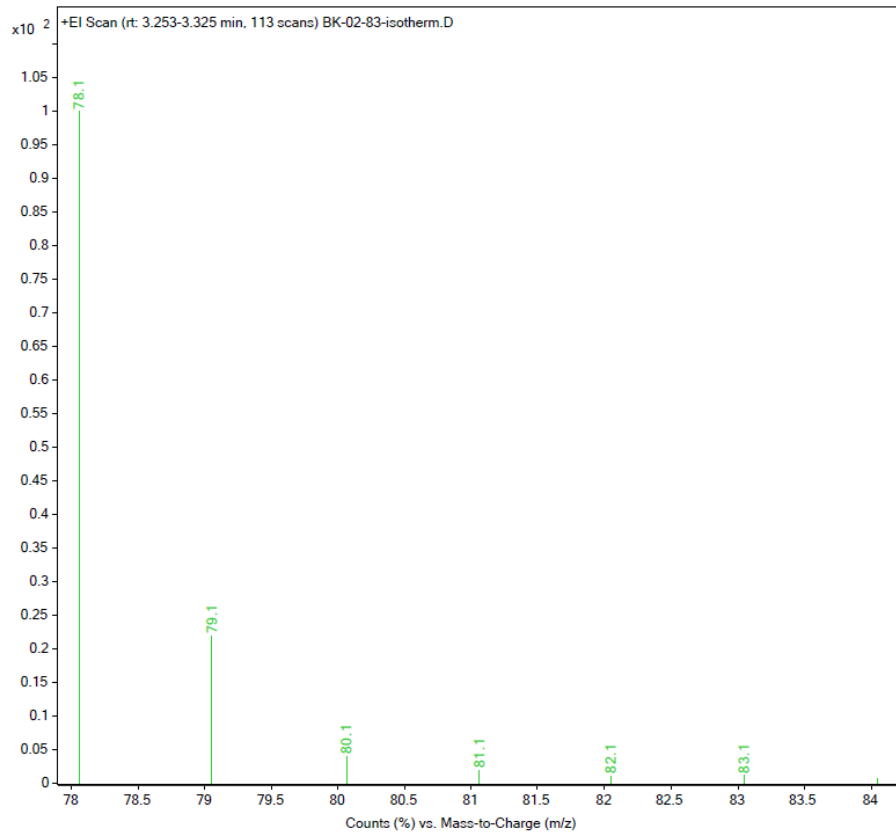
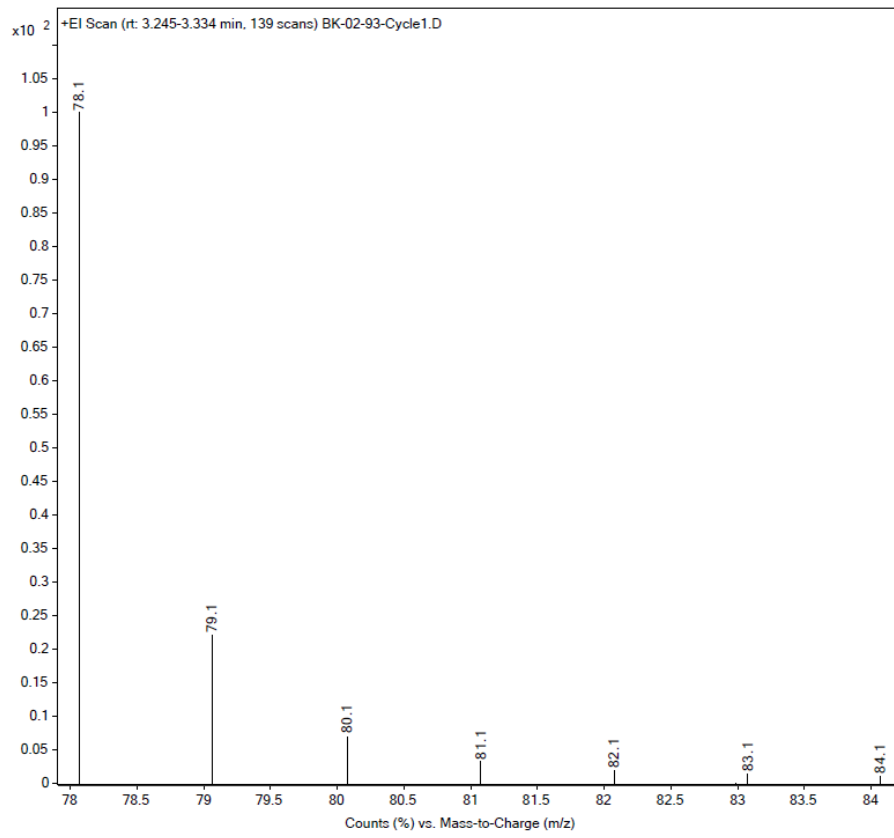


Table 2-6

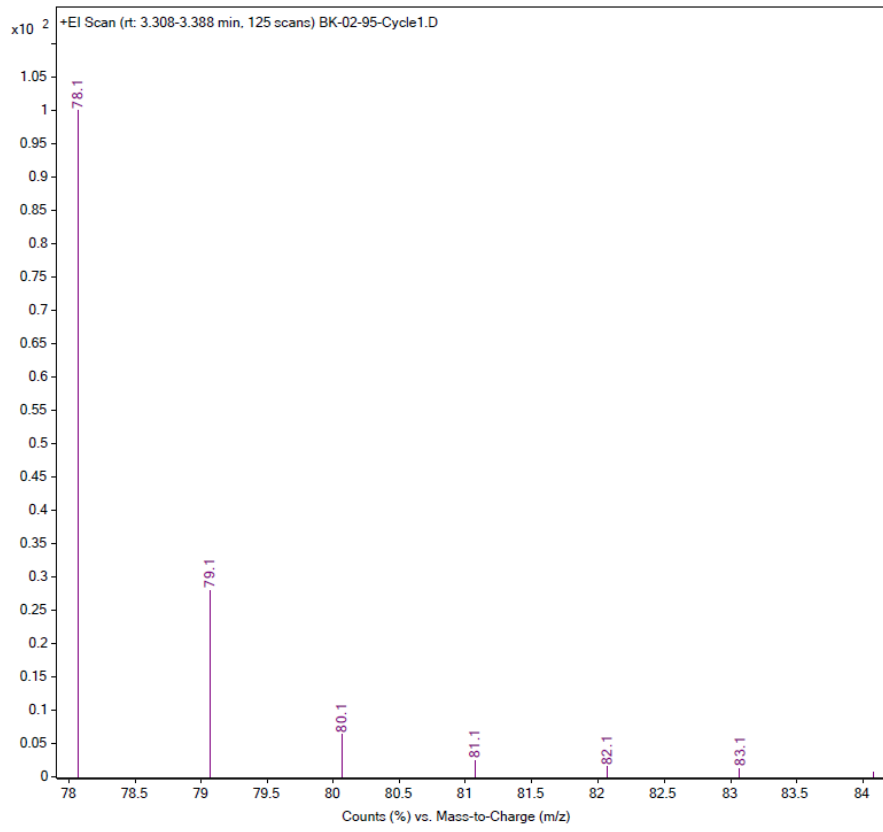
Entry 1



Entry 2



Entry 3



Entry 4

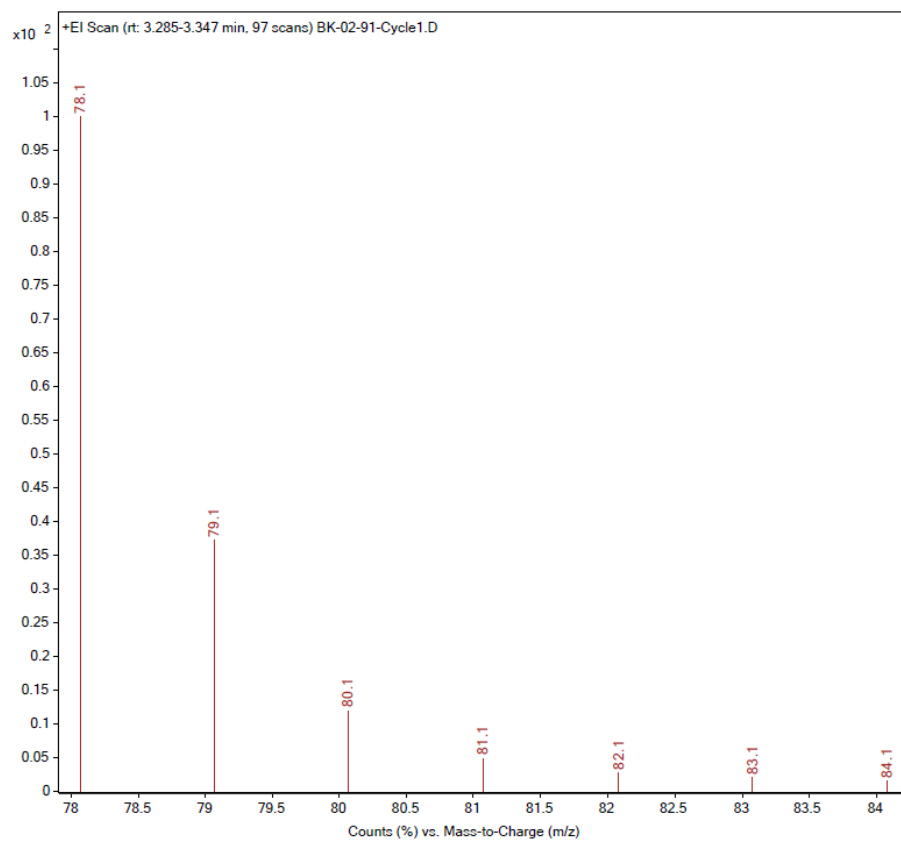
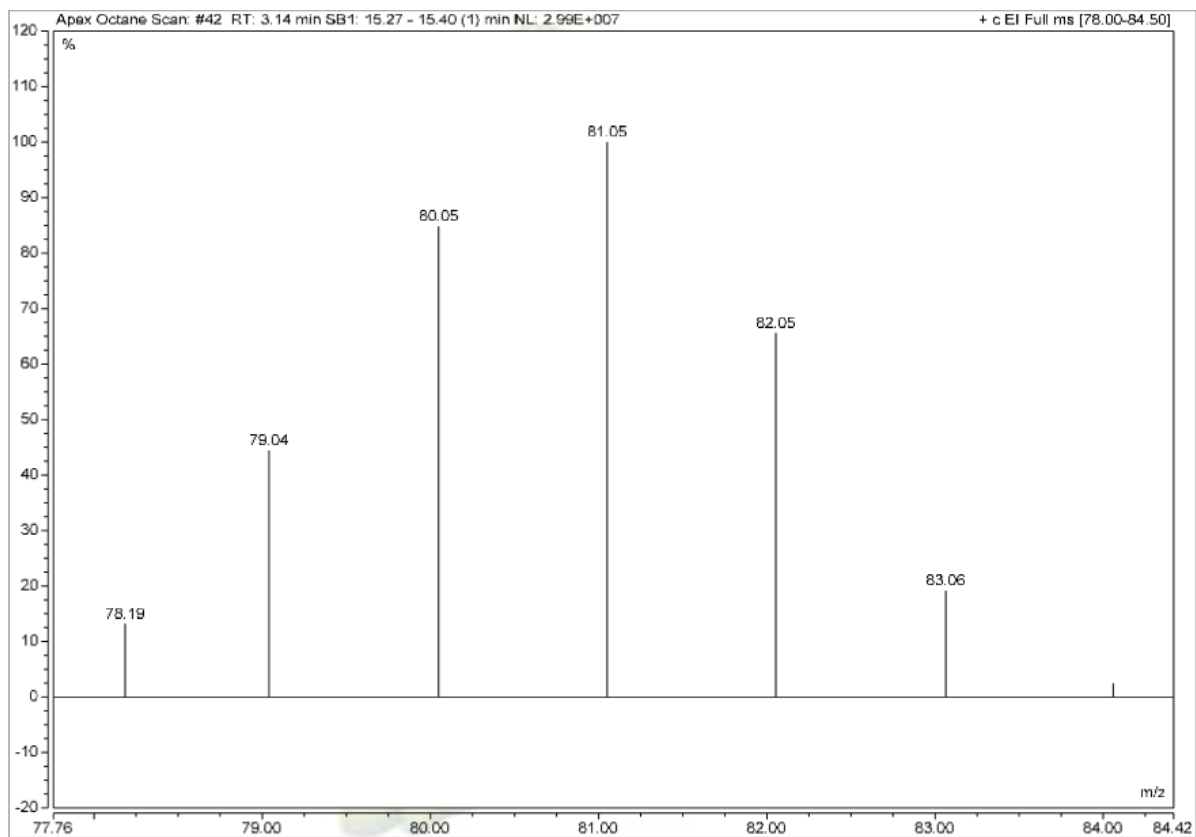
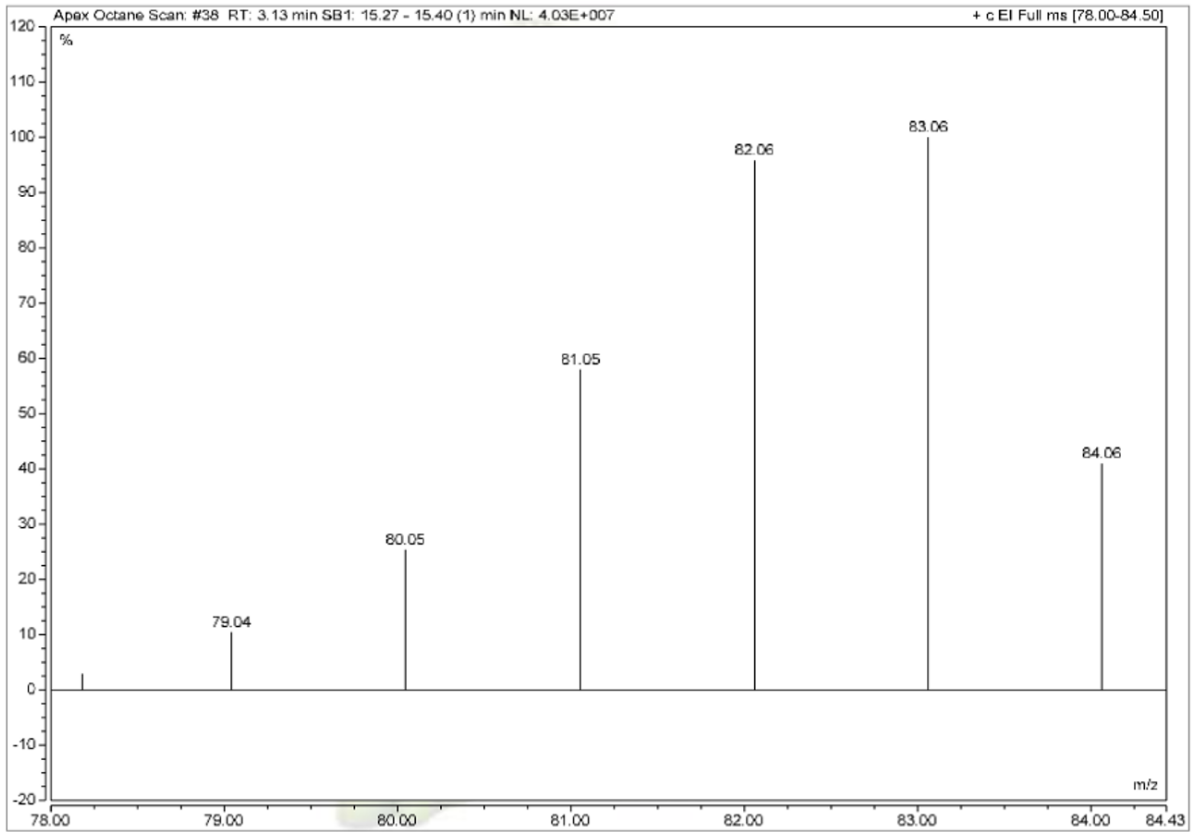


Table 2-7

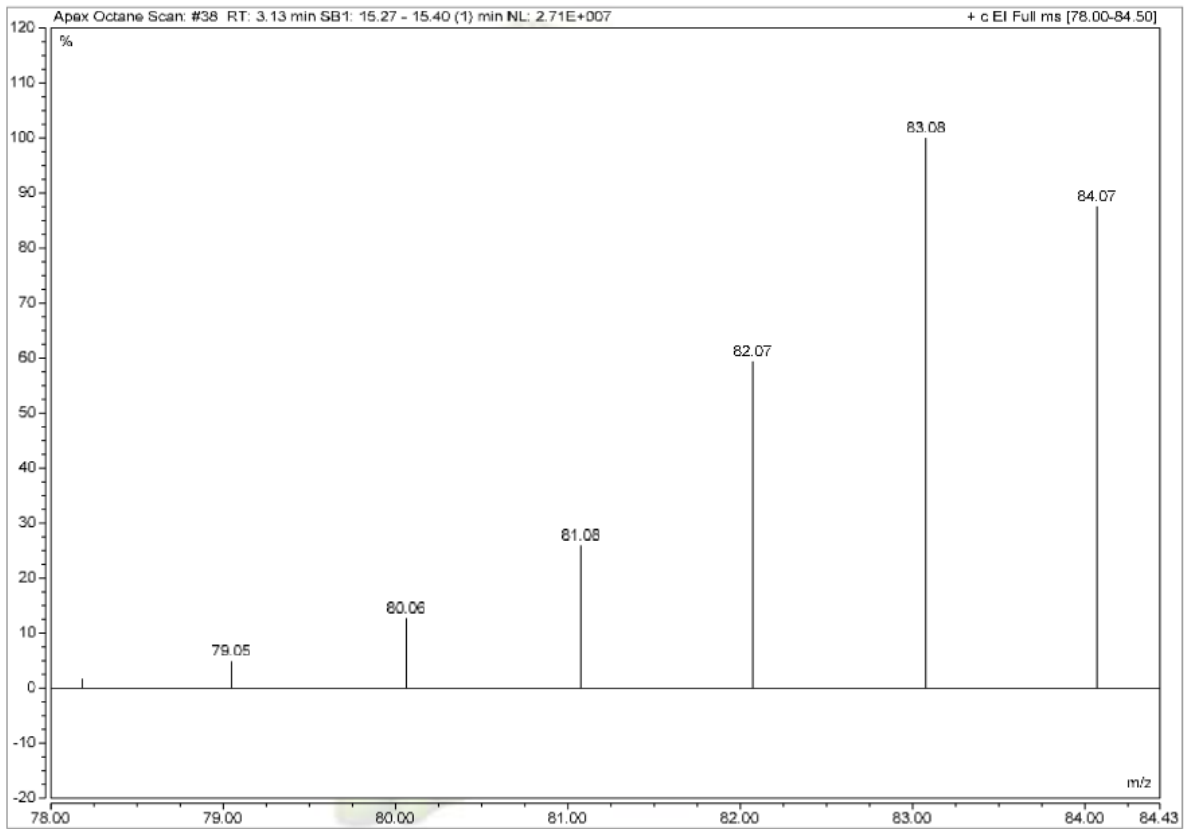
Entry 1



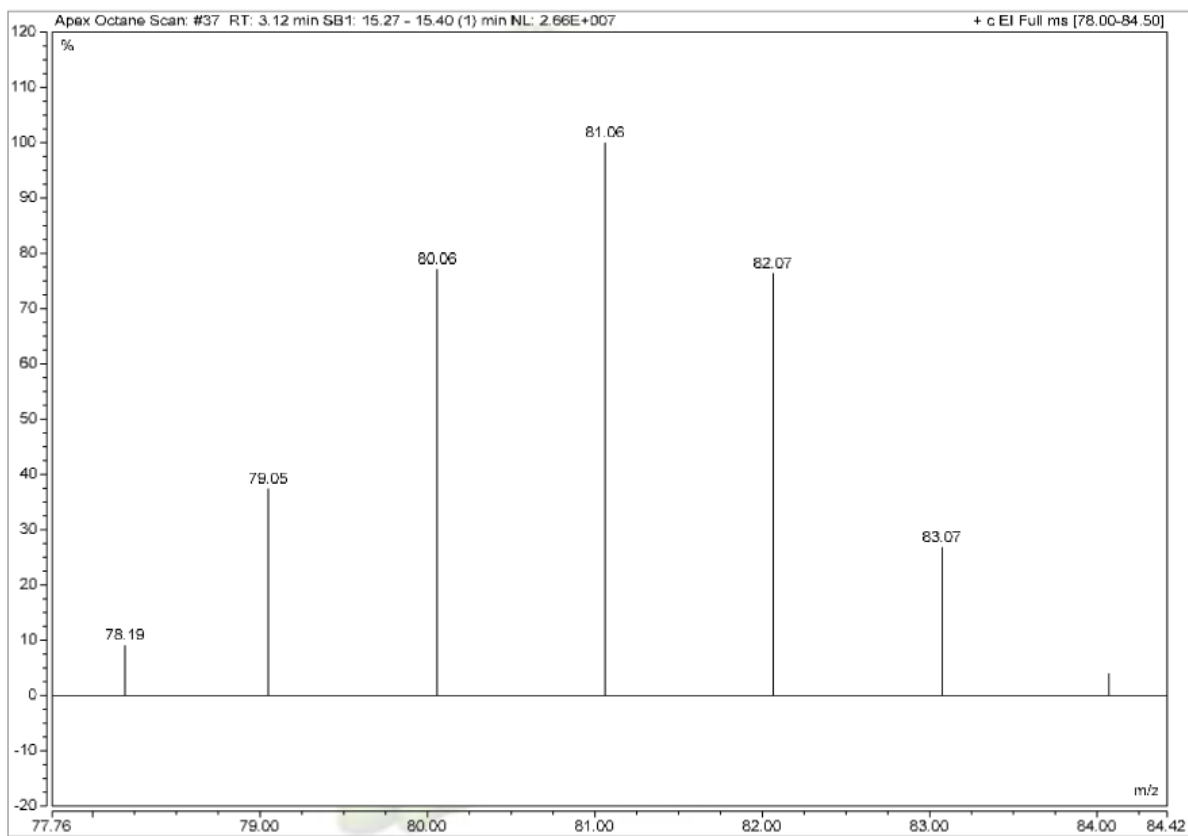
Entry 2



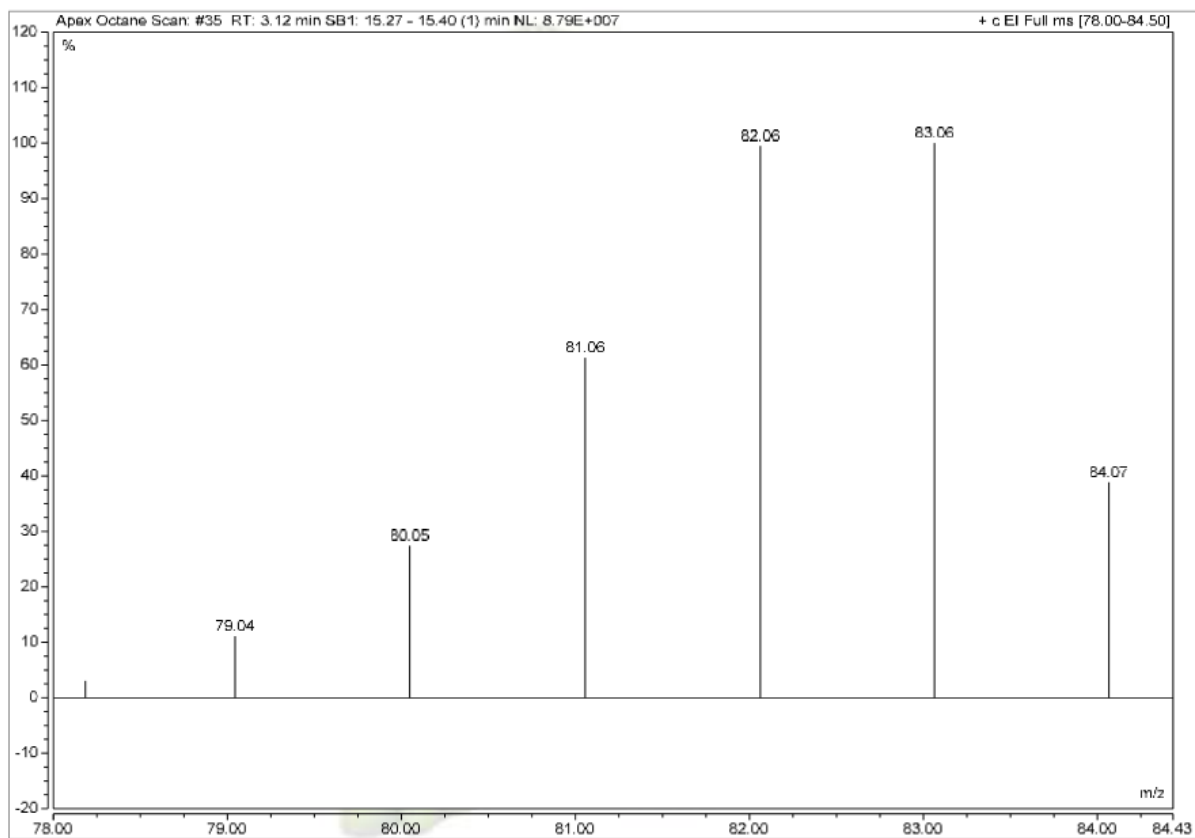
Entry 3



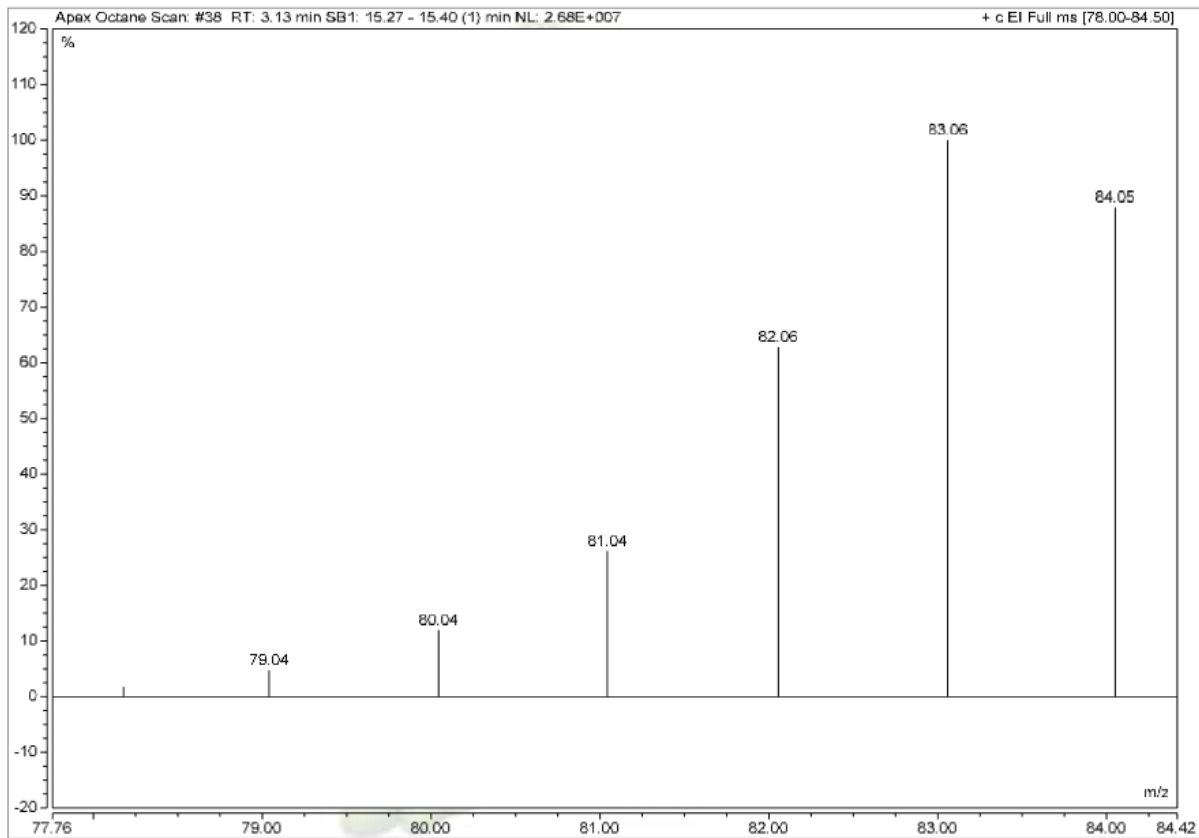
Entry 4



Entry 5



Entry 6



Entry 7

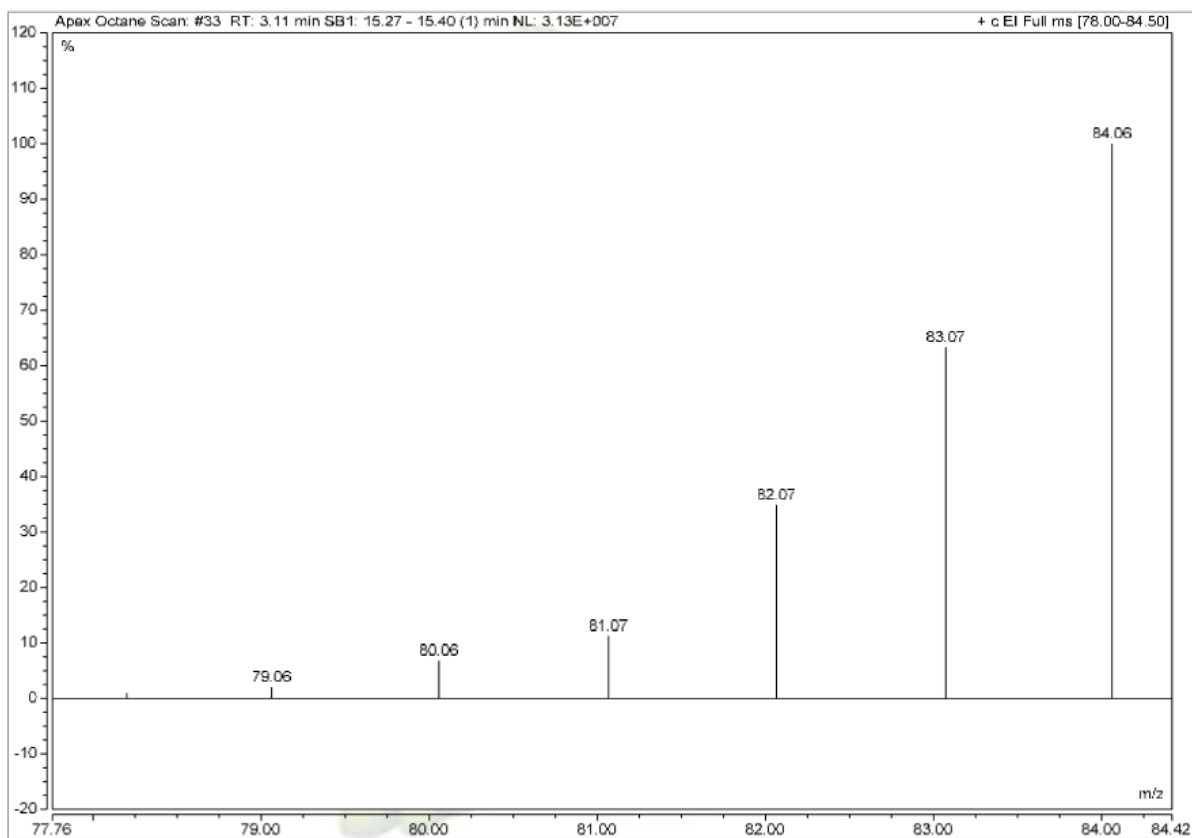
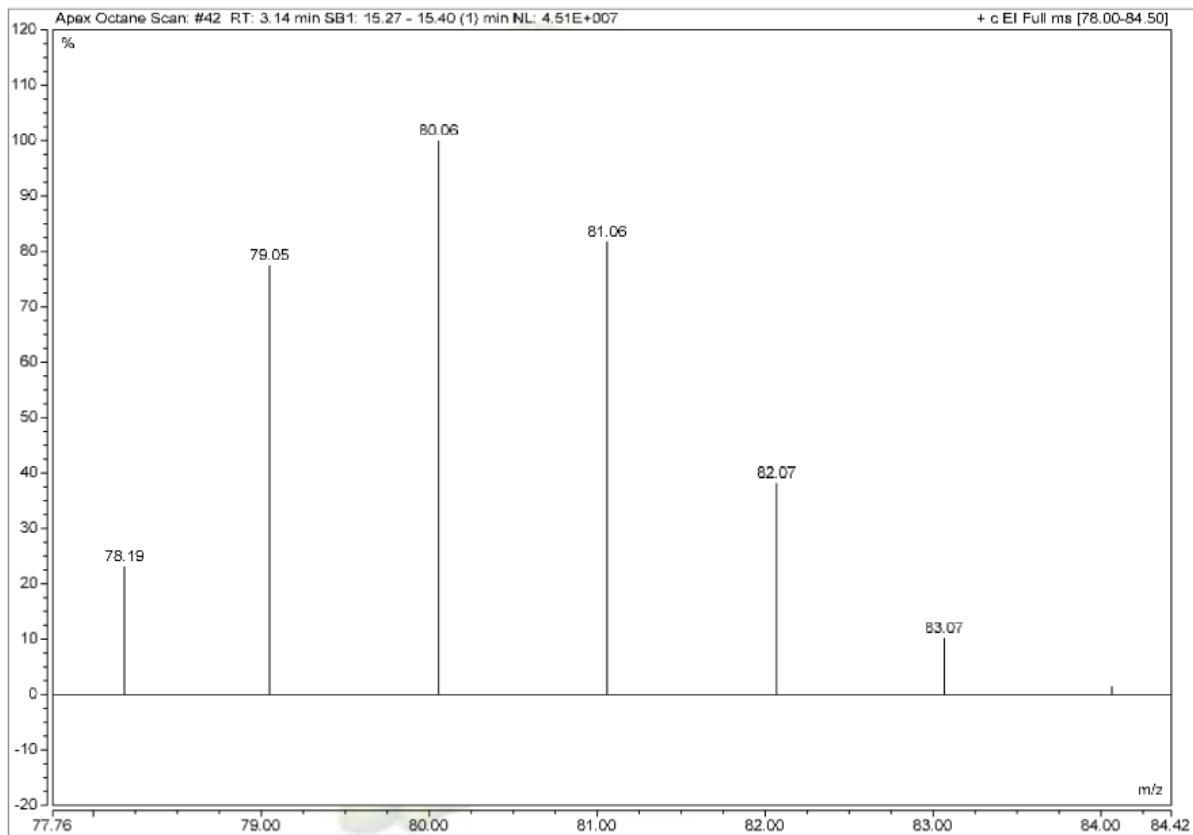
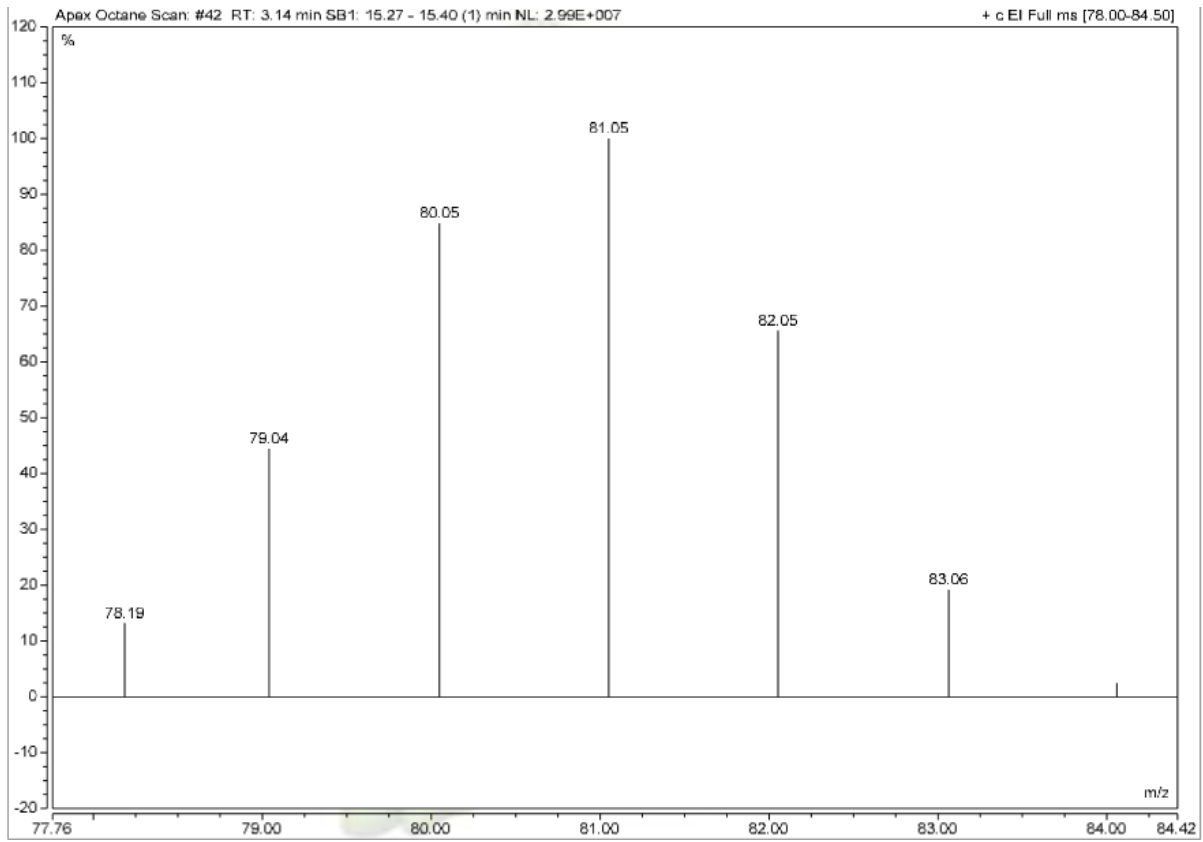


Table 2-8

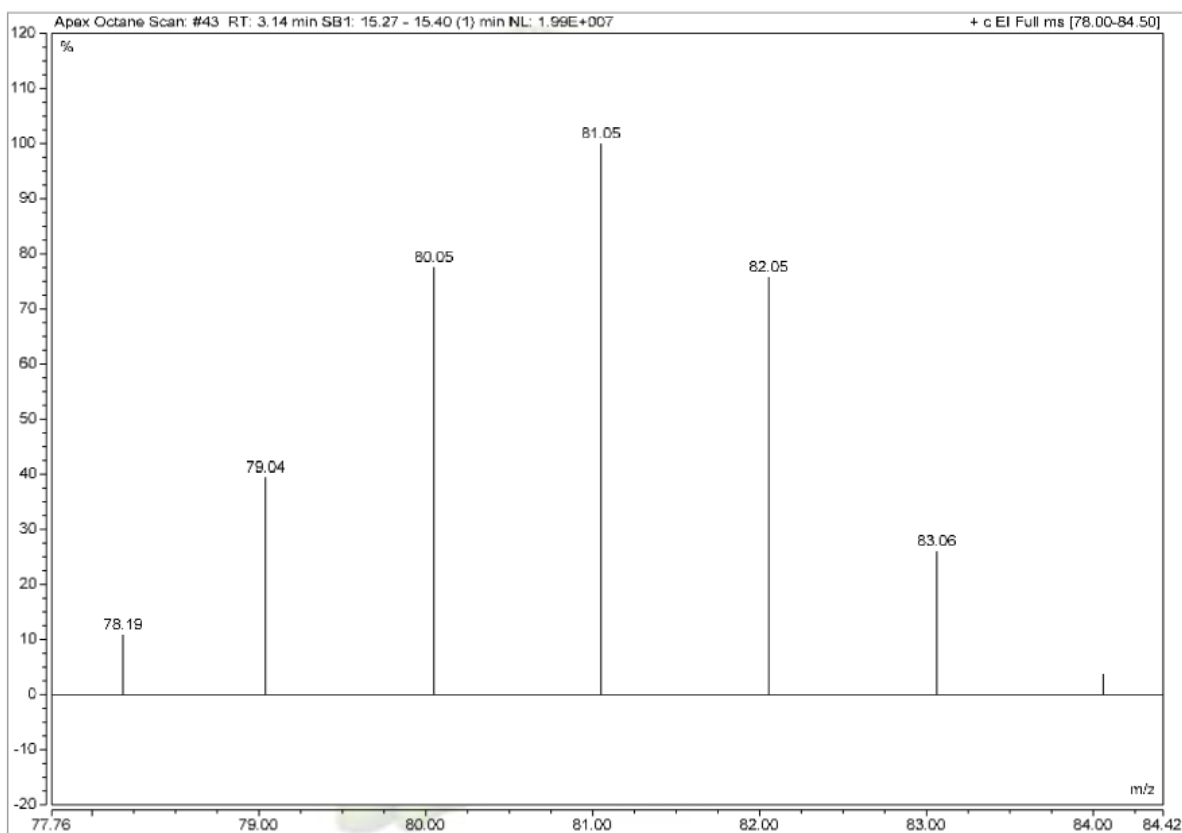
Entry 1



Entry 2



Entry 3



Entry 4

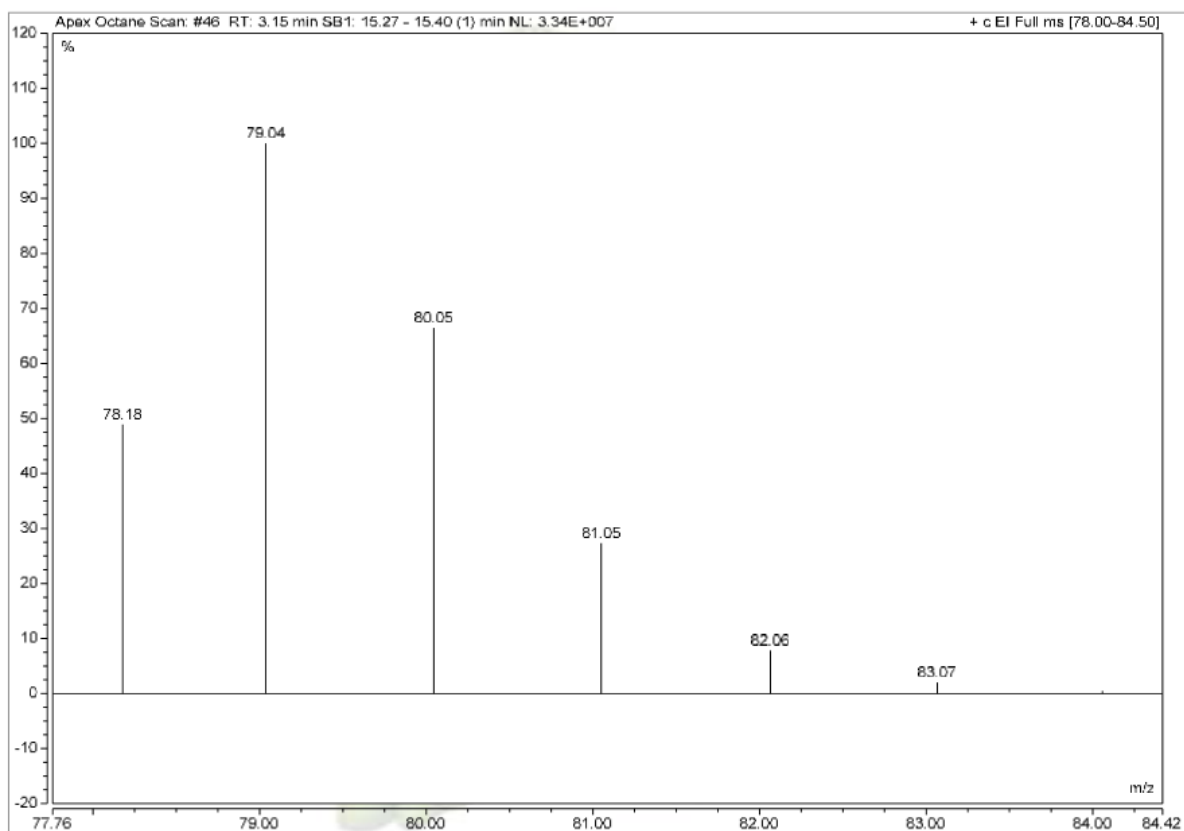
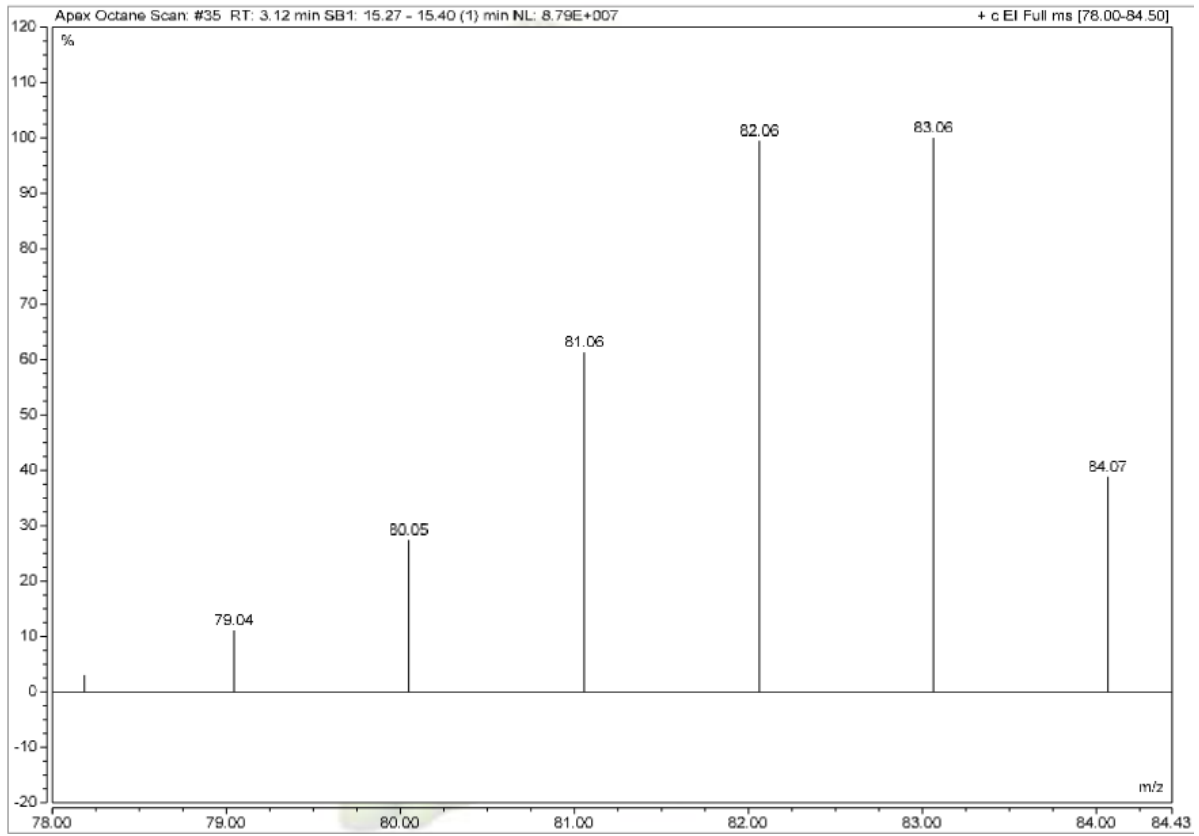


Table 2-9

Entry 1



Entry 2

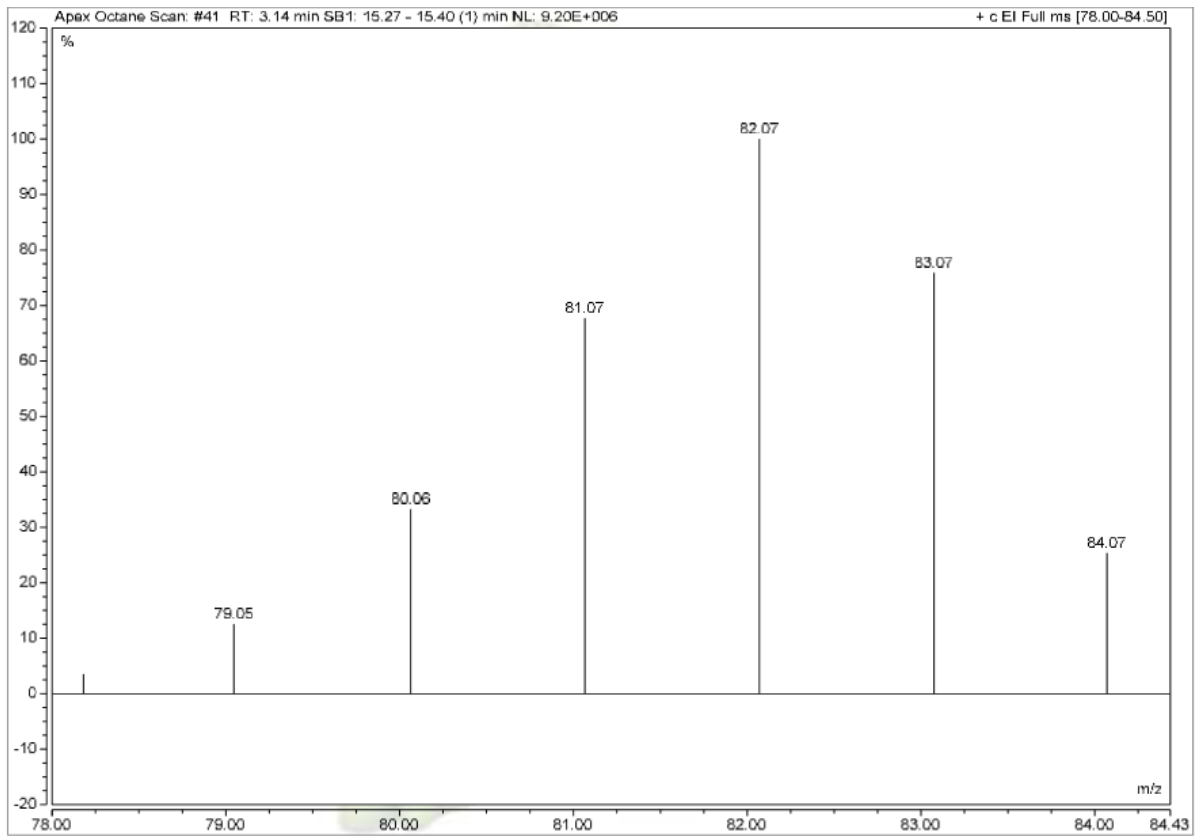
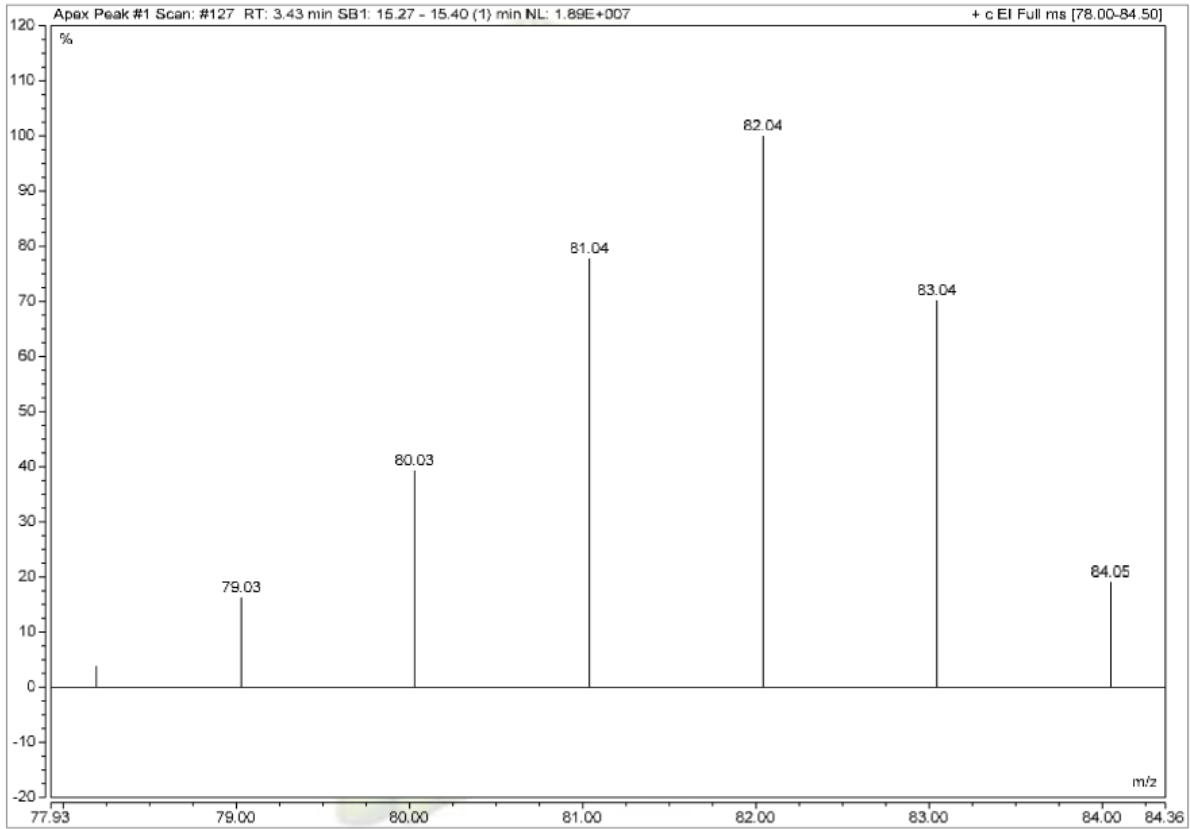
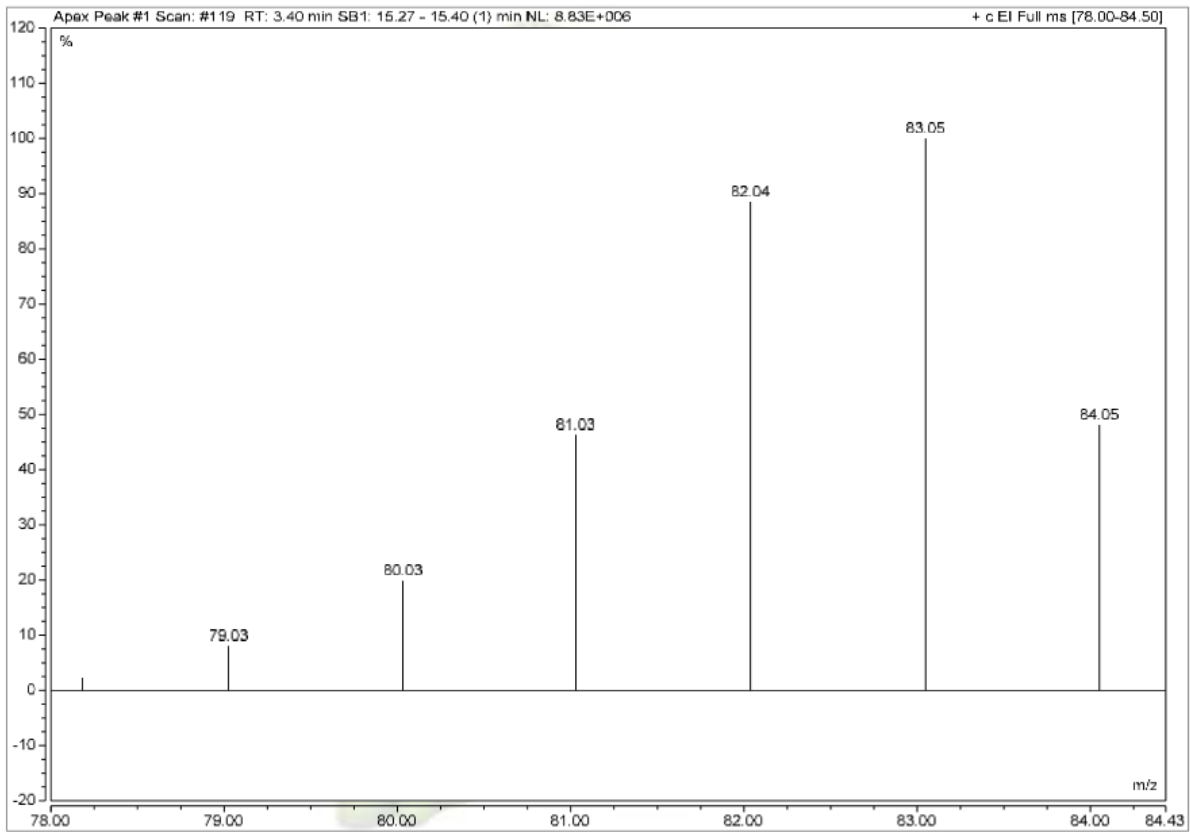


Table 2-10

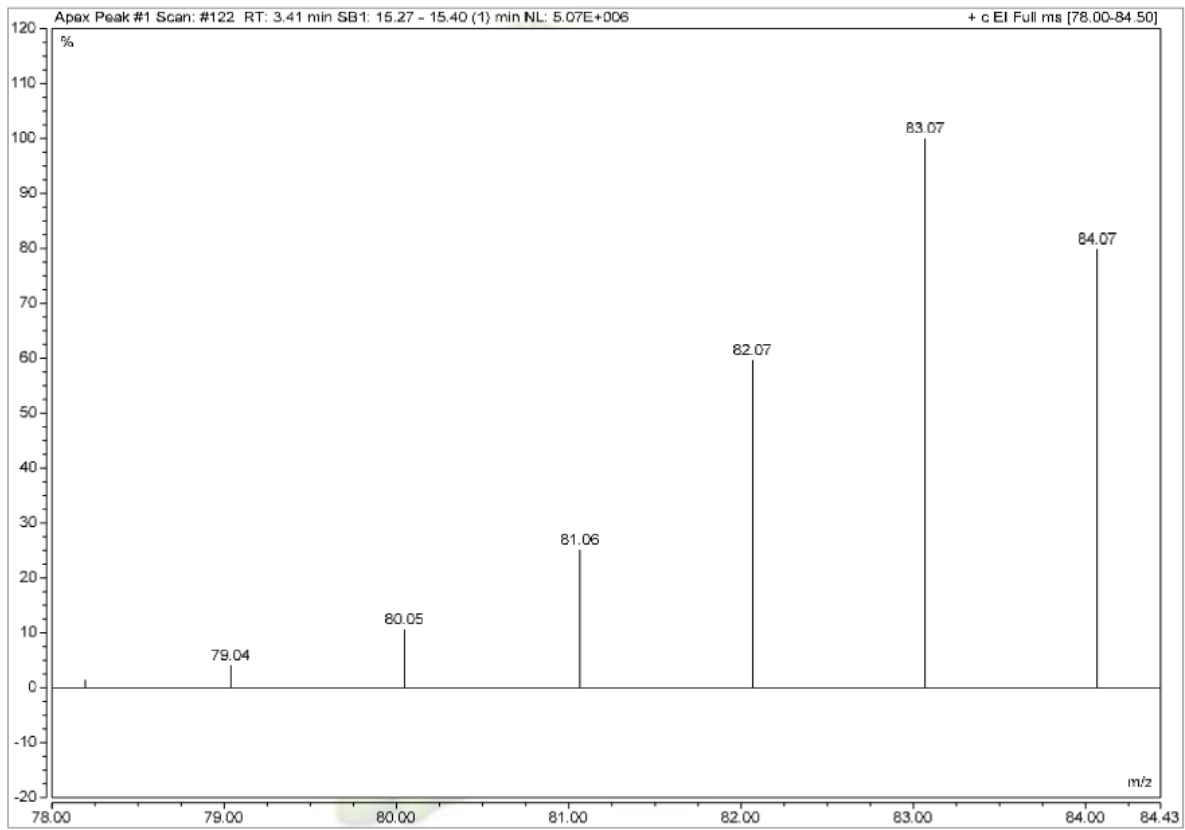
Entry 1



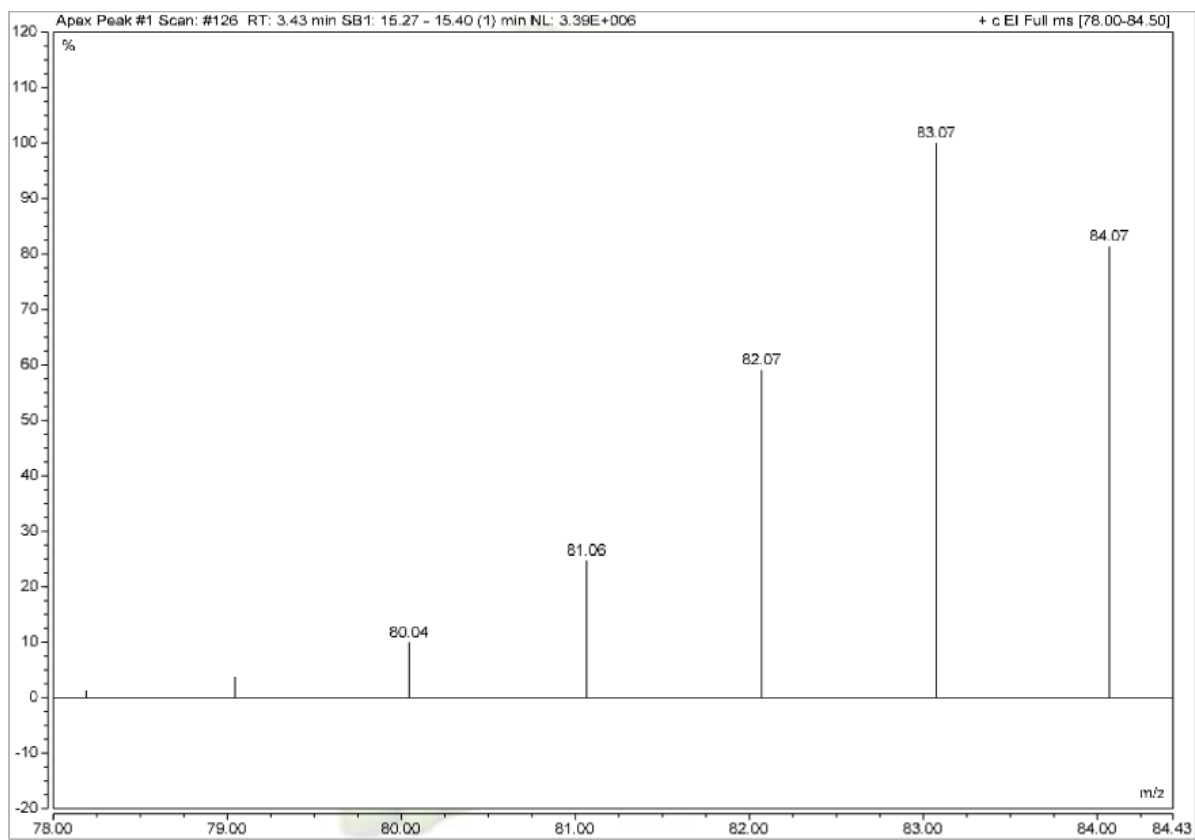
Entry 2



Entry 3



Entry 4



Entry 5

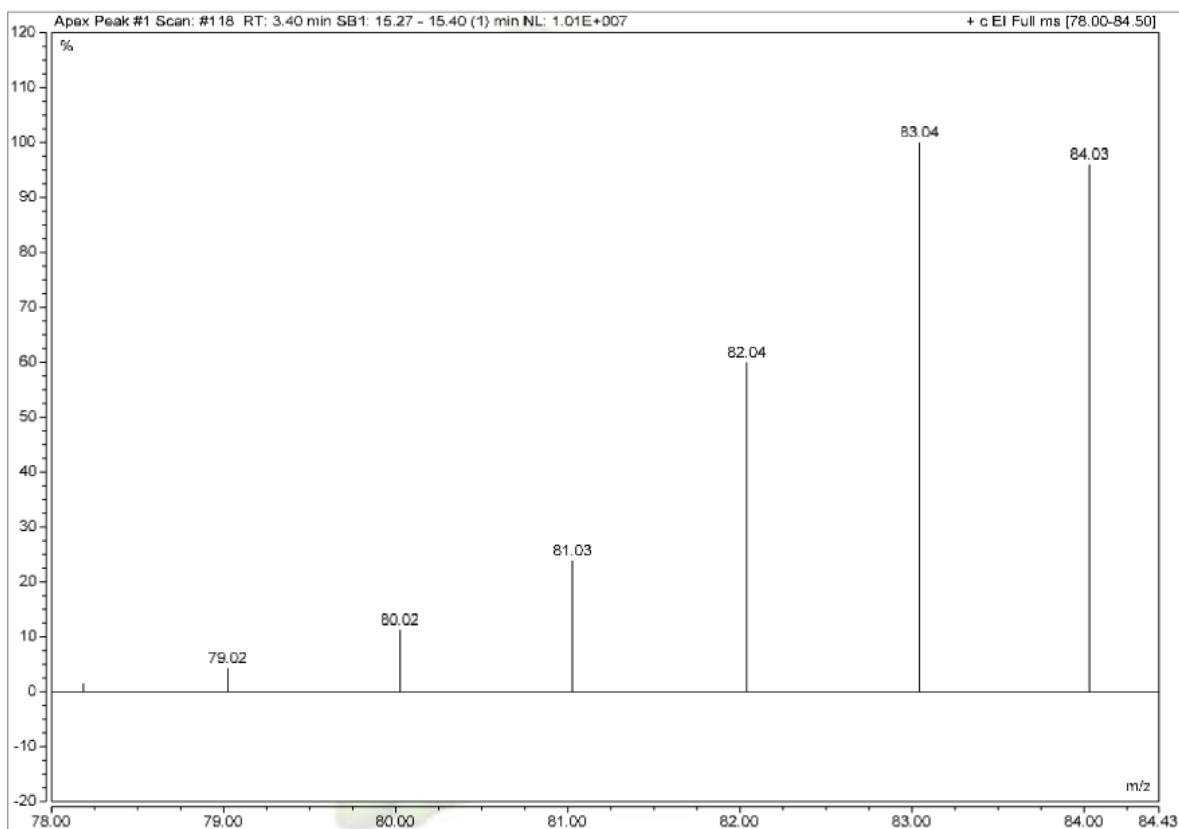
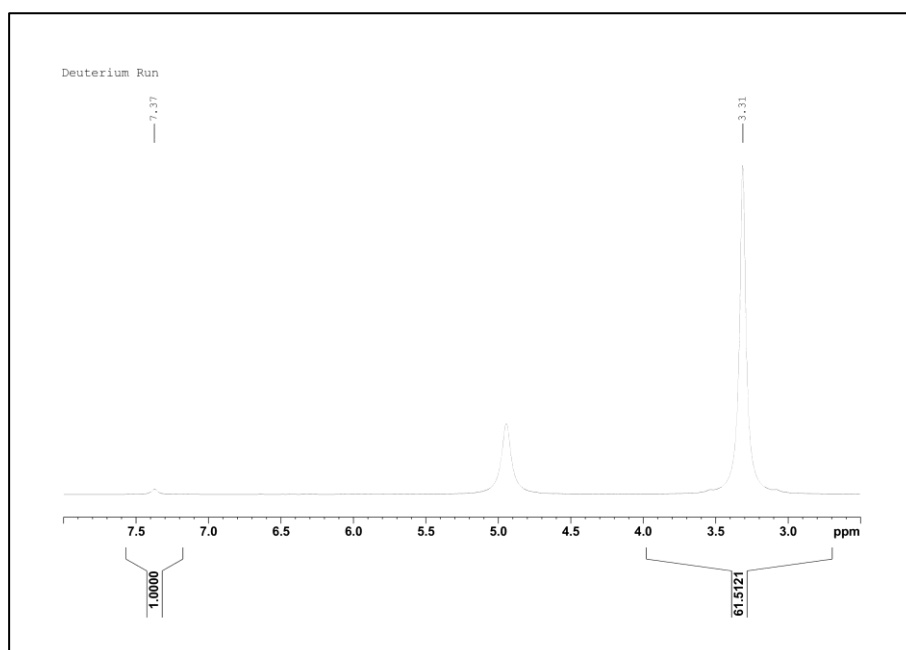
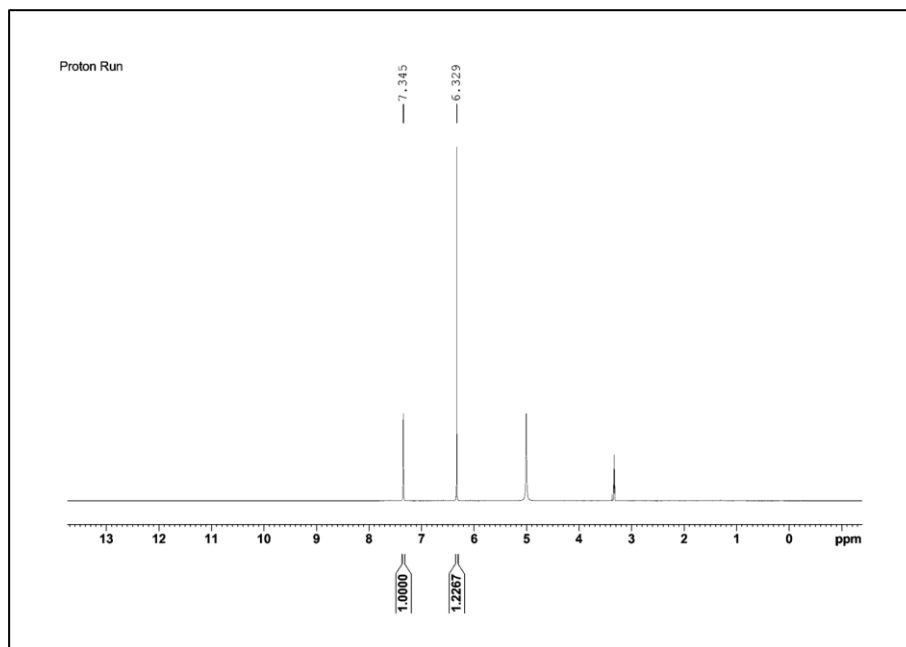


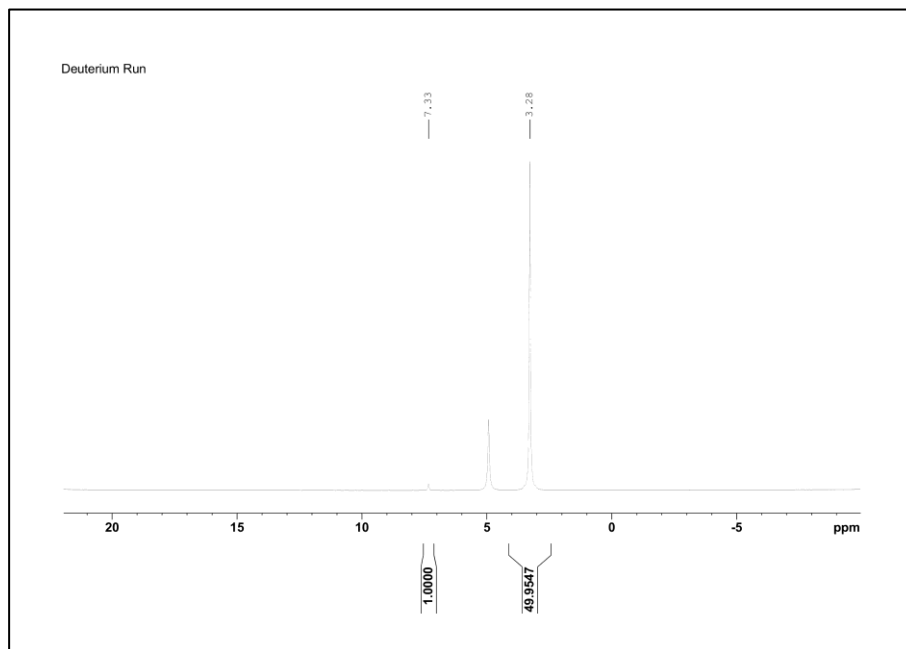
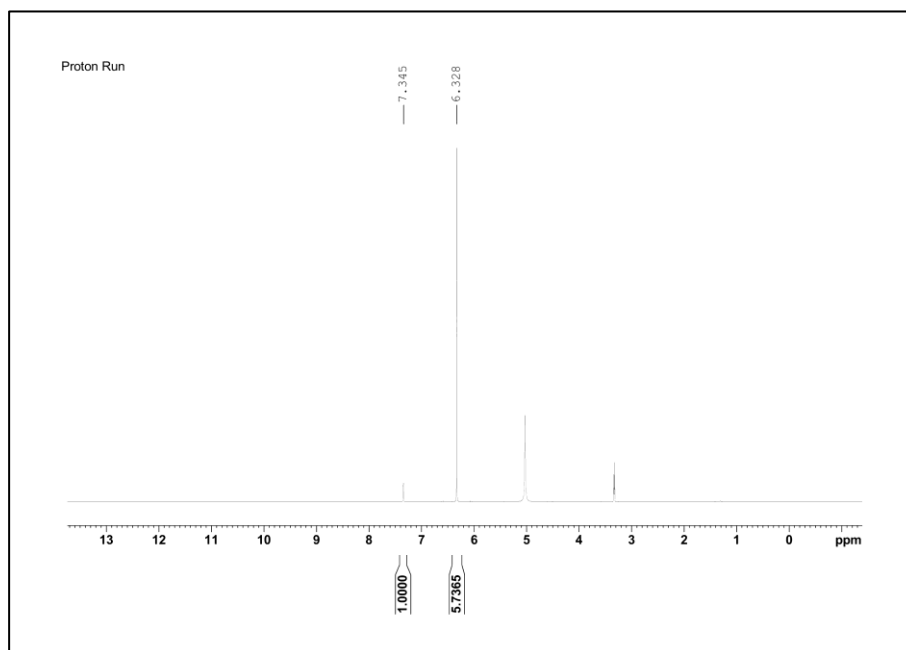
Table 2-11

Entry 1



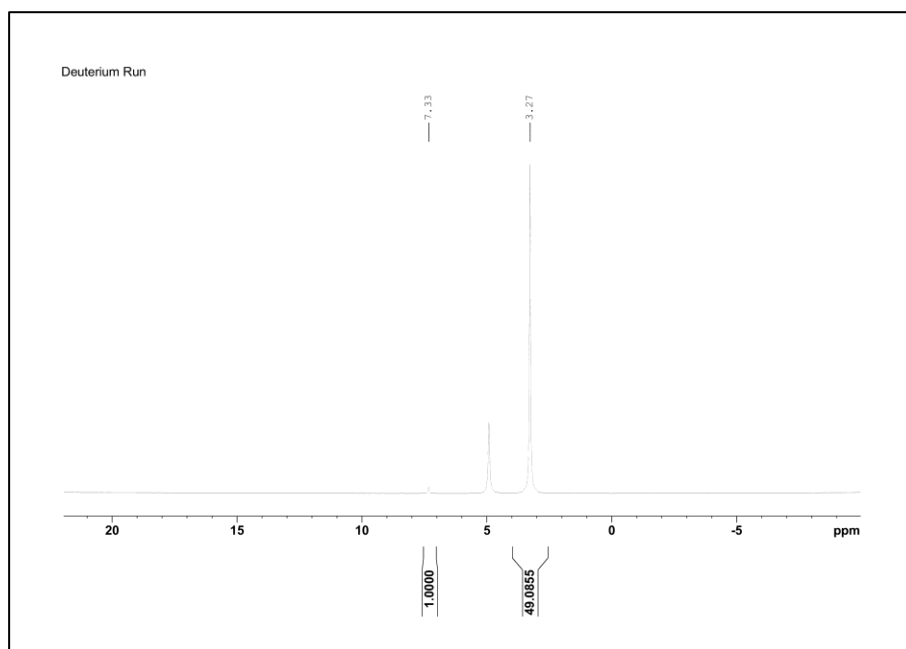
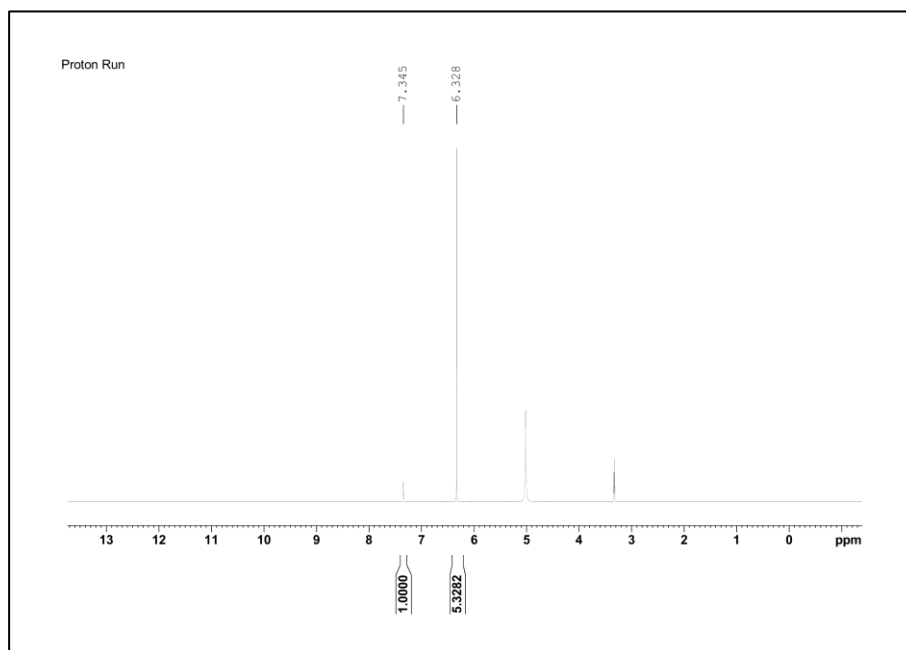
<i>Mass maleic acid (mg)</i>	<i>mmol maleic acid</i>	<i>Mass methanol- d4 (mg)</i>	<i>mmol methanol- d4</i>	<i>Mass benzene (mg)</i>
13.7	0.118	611	16.9	16

Entry 2



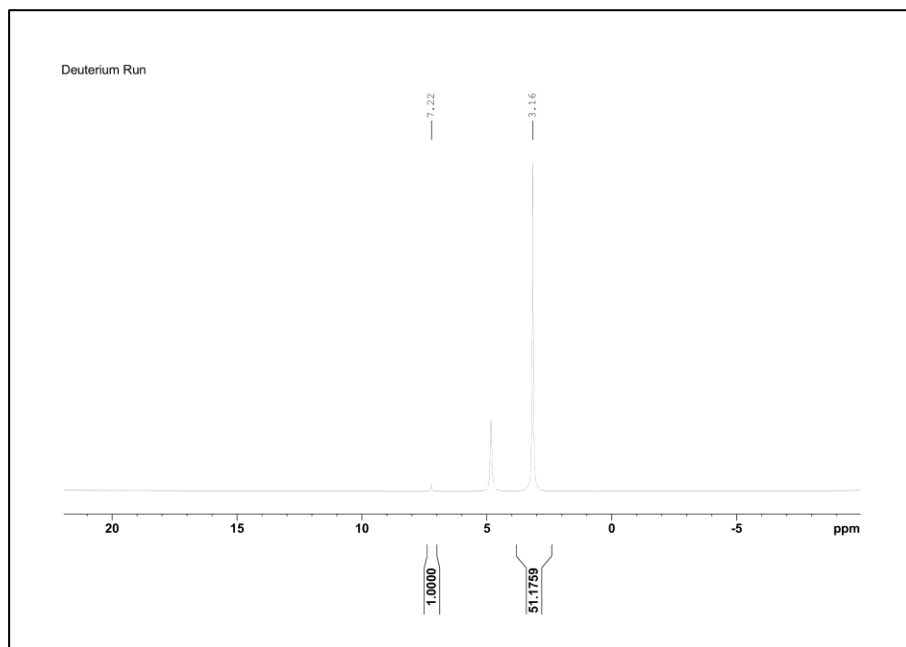
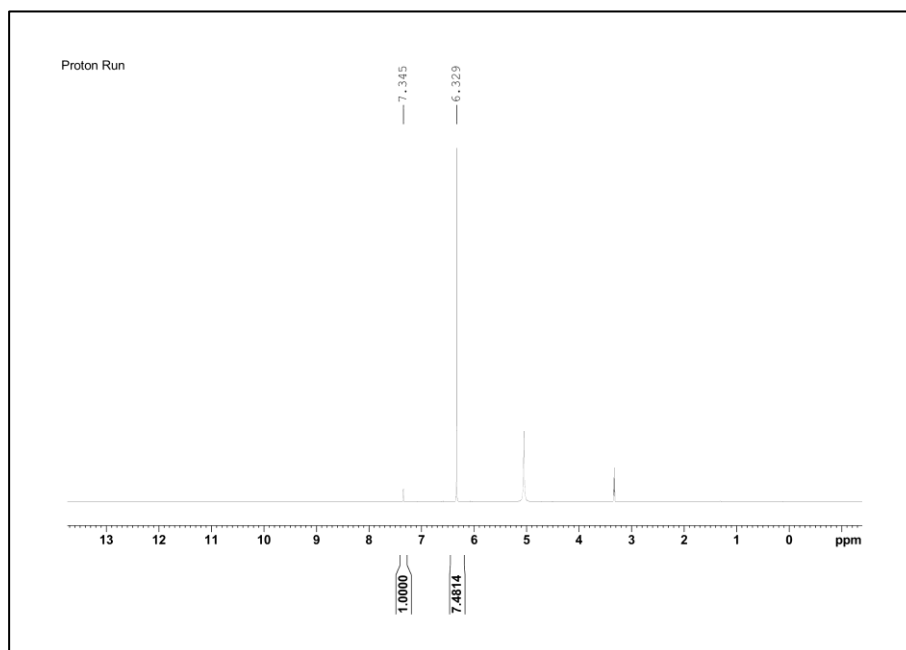
<i>Mass maleic acid (mg)</i>	<i>mmol maleic acid</i>	<i>Mass methanol- d4 (mg)</i>	<i>mmol methanol- d4</i>	<i>Mass benzene (mg)</i>
13.5	0.116	590	16.3	17.6

Entry 3



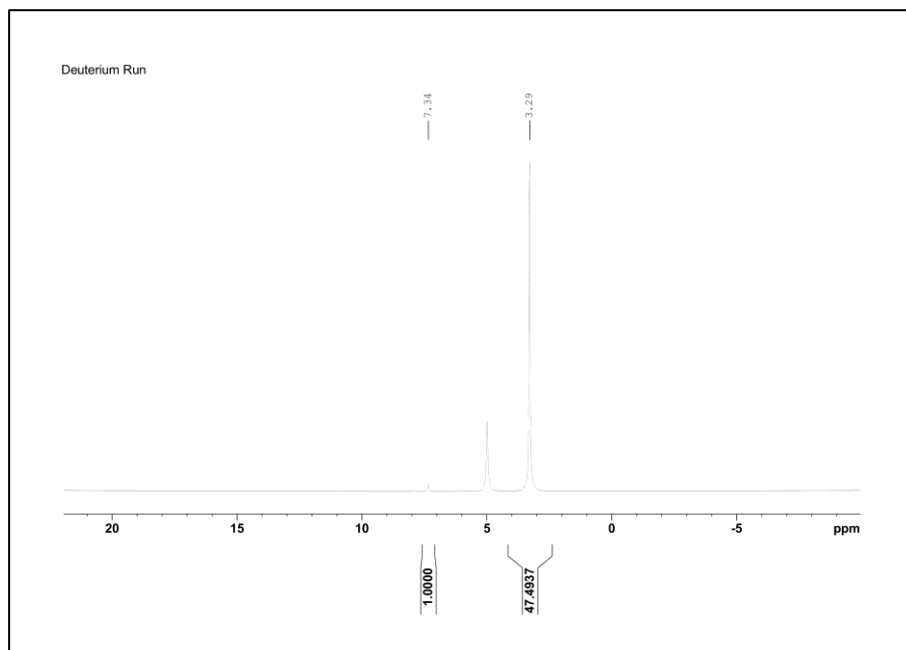
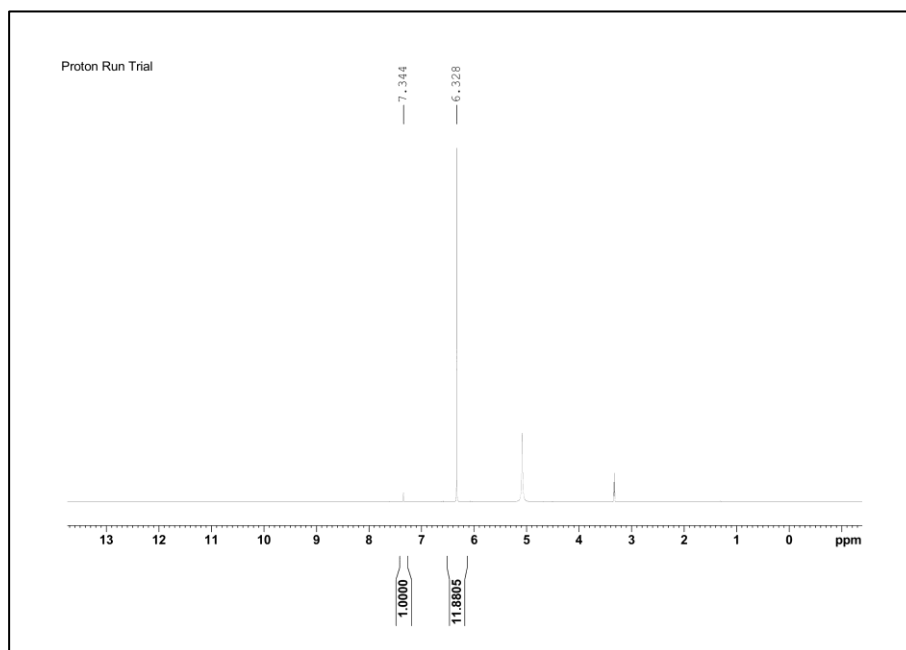
<i>Mass maleic acid (mg)</i>	<i>mmol maleic acid</i>	<i>Mass methanol- d4 (mg)</i>	<i>mmol methanol- d4</i>	<i>Mass benzene (mg)</i>
13.6	0.117	585	16.2	16.7

Entry 4



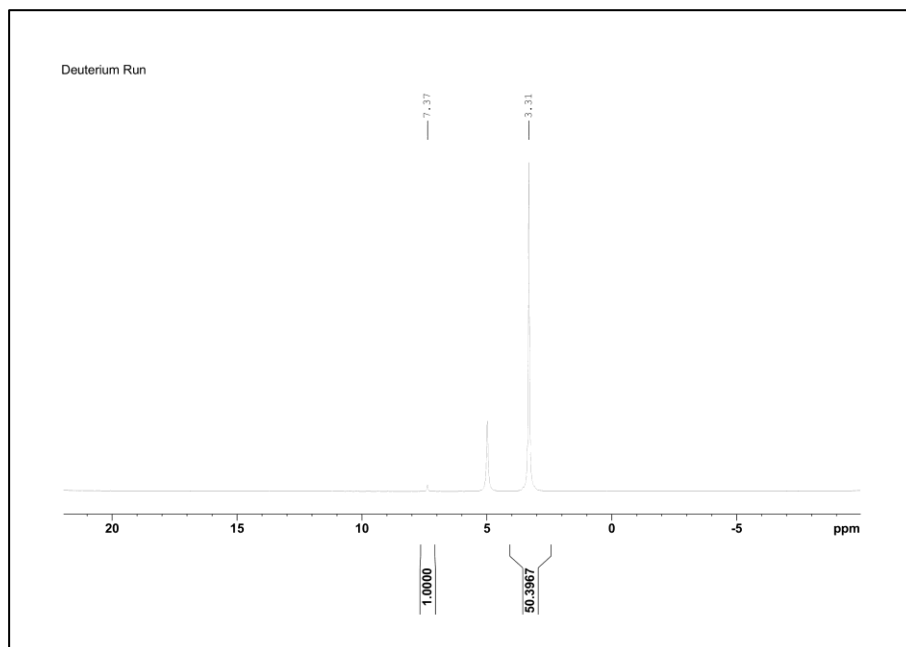
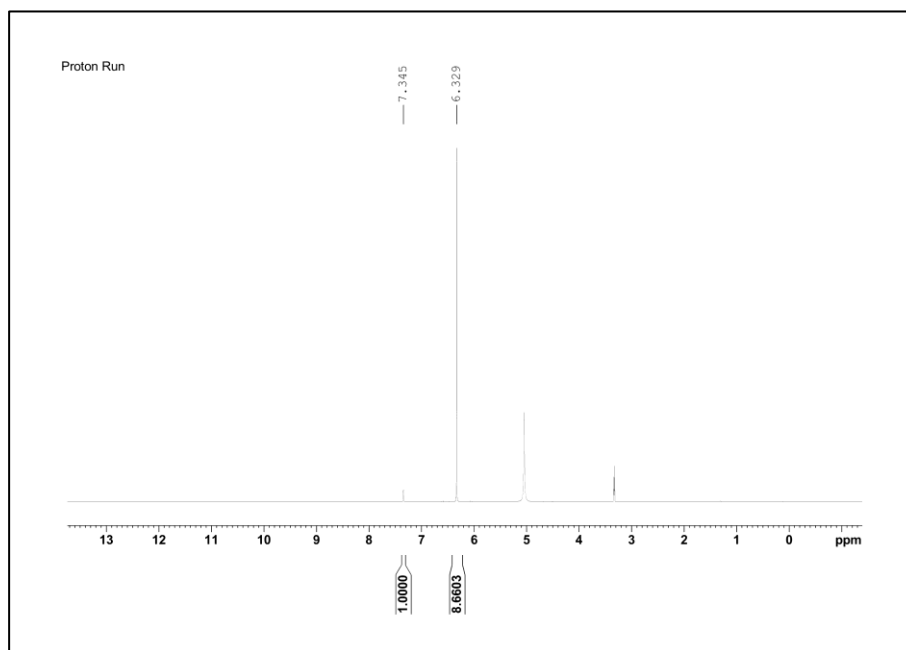
<i>Mass maleic acid (mg)</i>	<i>mmol maleic acid</i>	<i>Mass methanol- d4 (mg)</i>	<i>mmol methanol- d4</i>	<i>Mass benzene (mg)</i>
14.8	0.127	574.7	15.9	23.4

Entry 5



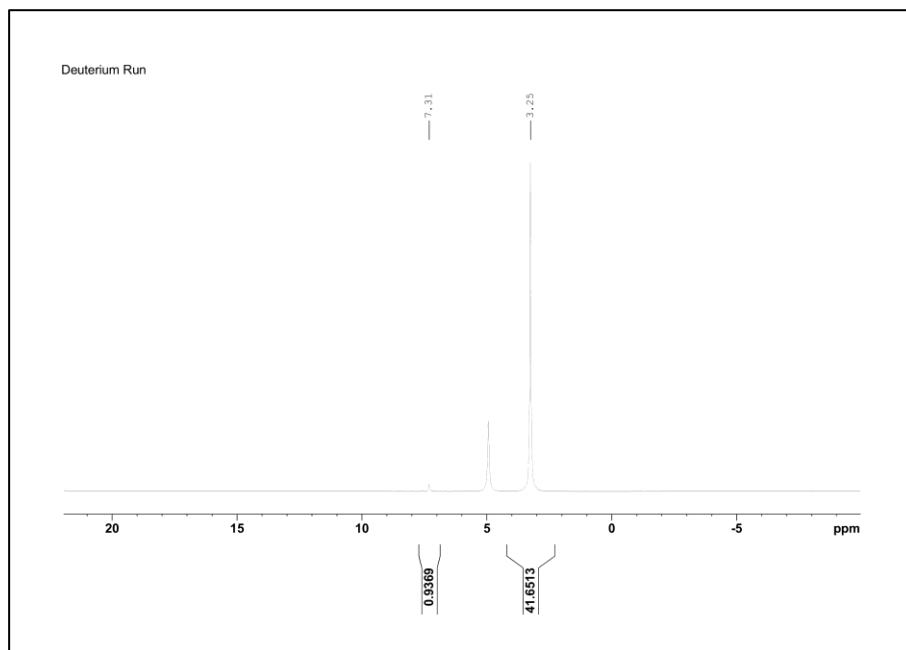
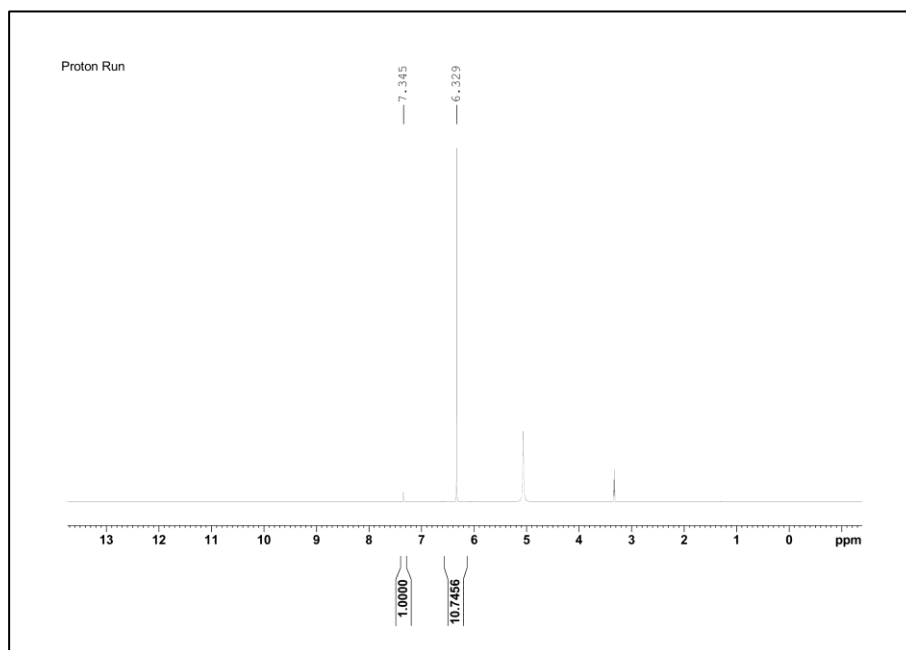
<i>Mass maleic acid (mg)</i>	<i>mmol maleic acid</i>	<i>Mass methanol- d4 (mg)</i>	<i>mmol methanol- d4</i>	<i>Mass benzene (mg)</i>
14.6	0.126	592.9	16.4	18.1

Entry 6



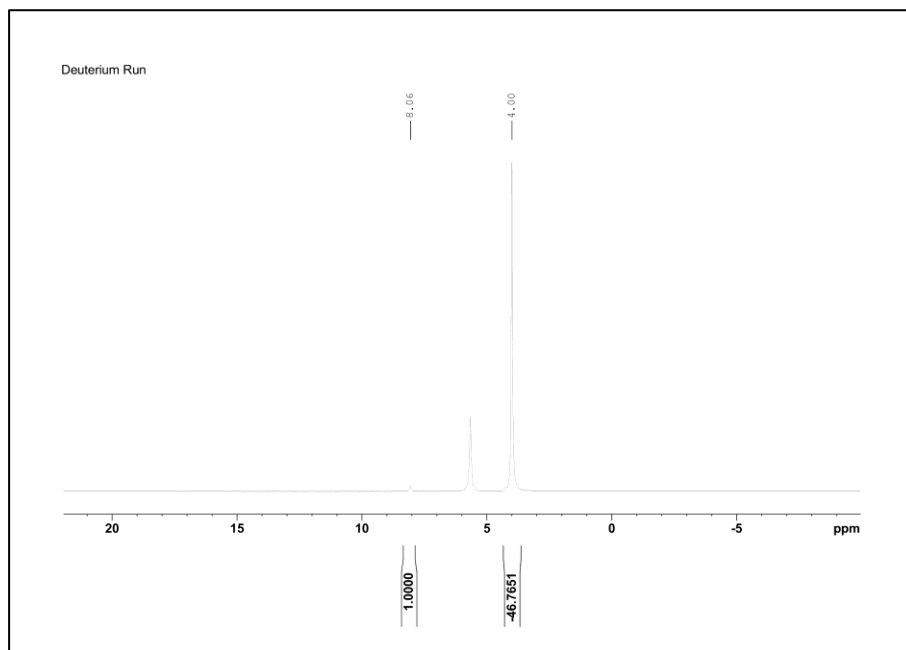
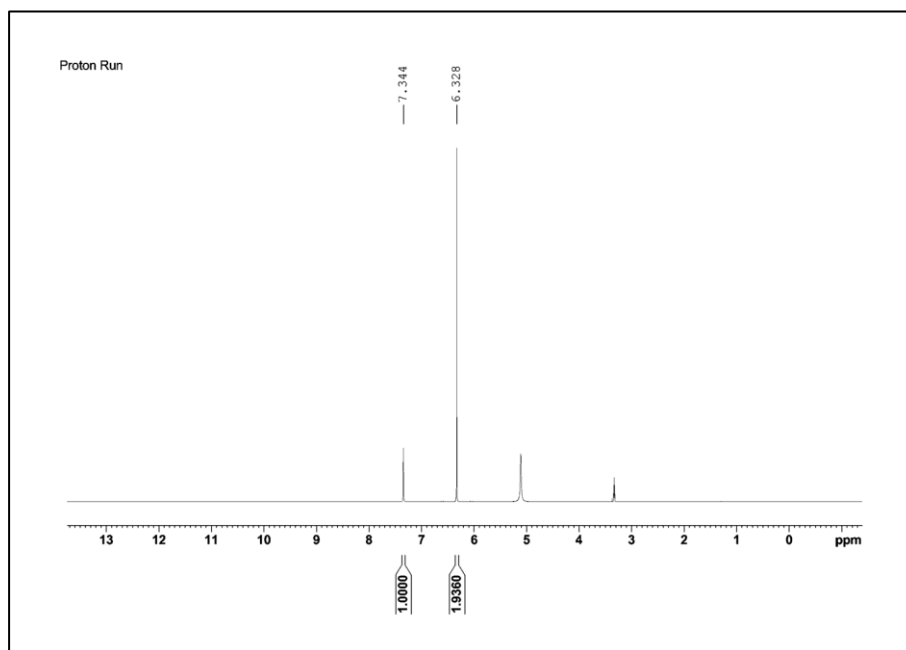
<i>Mass maleic acid (mg)</i>	<i>mmol maleic acid</i>	<i>Mass methanol- d4 (mg)</i>	<i>mmol methanol- d4</i>	<i>Mass benzene (mg)</i>
20	0.172	599	16.6	13.4

Entry 7



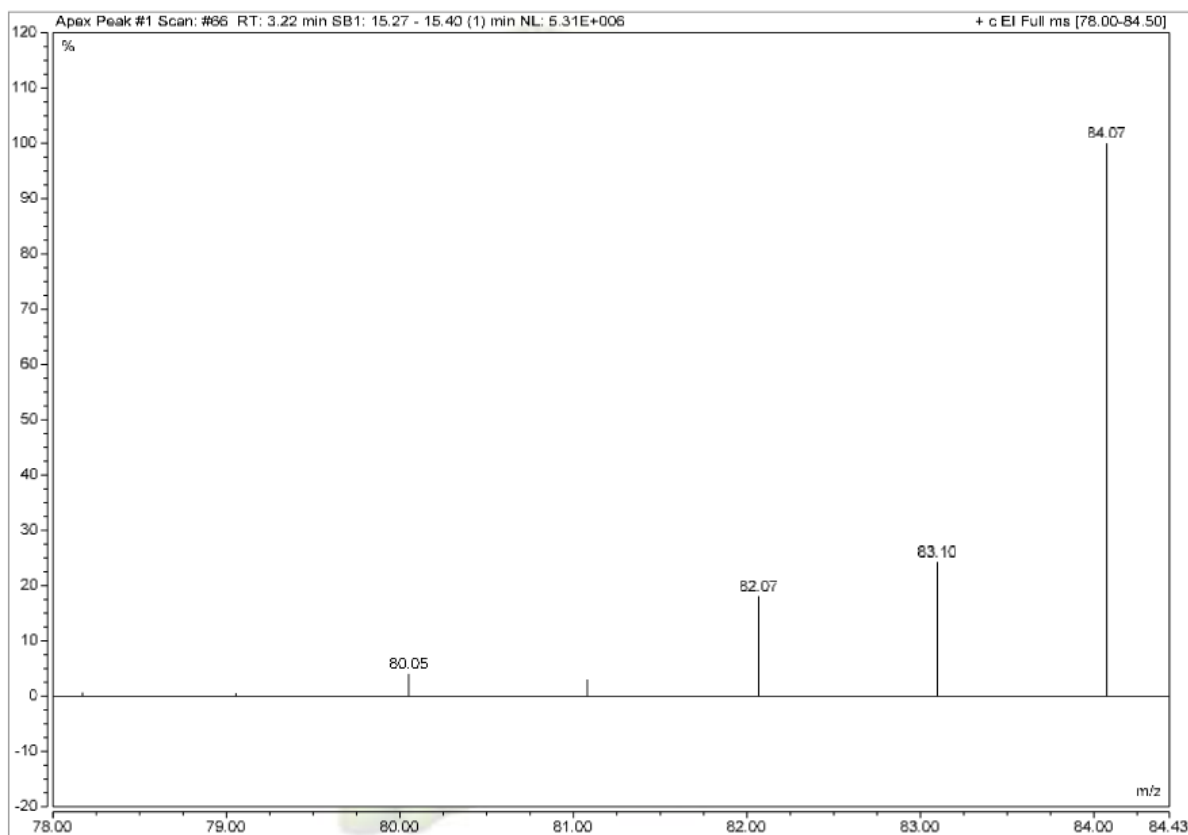
<i>Mass maleic acid (mg)</i>	<i>mmol maleic acid</i>	<i>Mass methanol- d4 (mg)</i>	<i>mmol methanol- d4</i>	<i>Mass benzene (mg)</i>
18	0.155	582	16.1	14.2

Entry 8

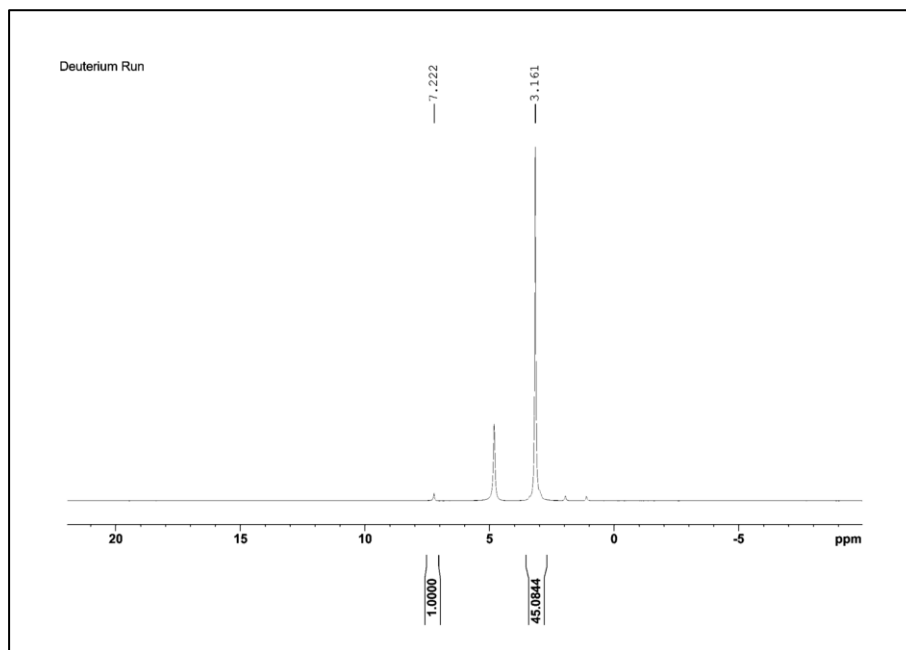
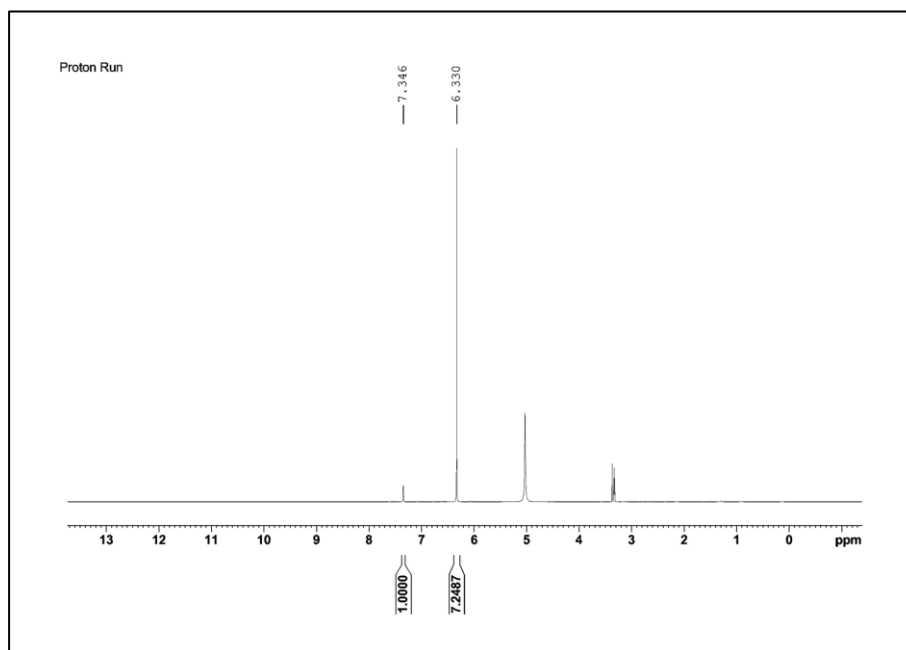


<i>Mass maleic acid (mg)</i>	<i>mmol maleic acid</i>	<i>Mass methanol- d4 (mg)</i>	<i>mmol methanol- d4</i>	<i>Mass benzene (mg)</i>
14	0.121	569	15.8	16

Entry 9



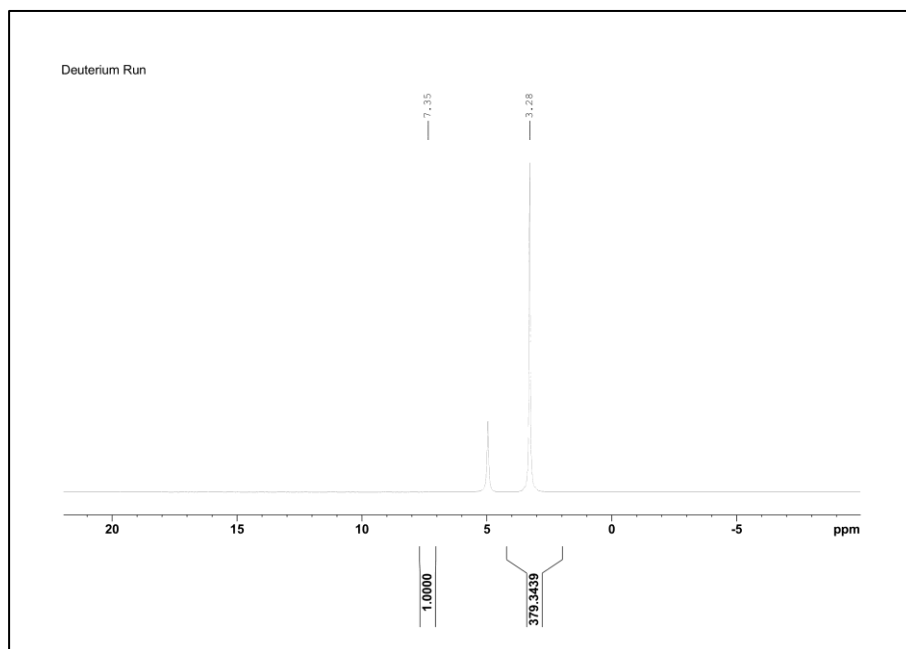
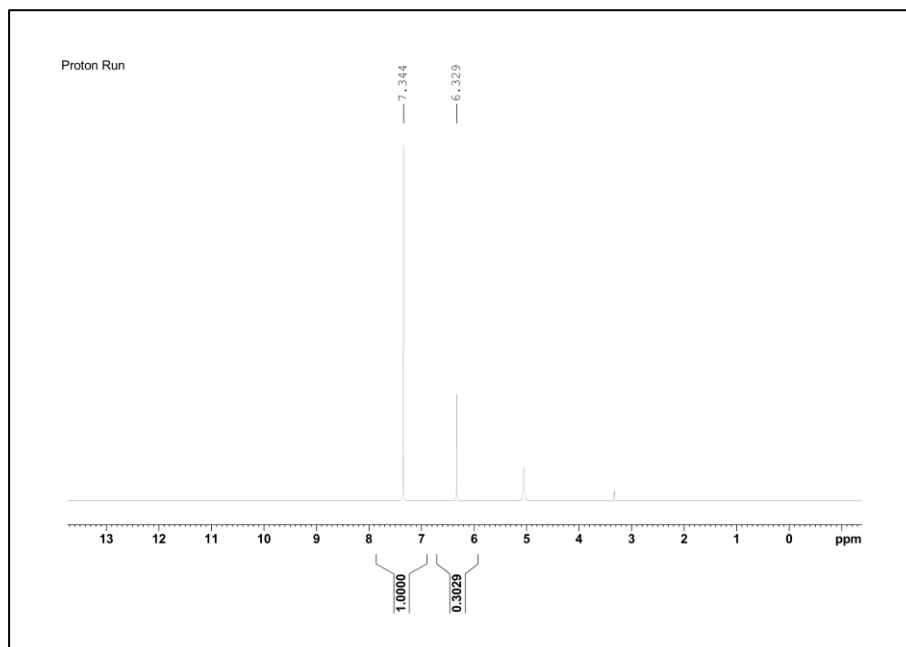
Entry 10



<i>Mass maleic acid (mg)</i>	<i>mmol maleic acid</i>	<i>Mass methanol- d4 (mg)</i>	<i>mmol methanol- d4</i>	<i>Mass benzene (mg)</i>
15.5	0.133	596.5	16.5	15

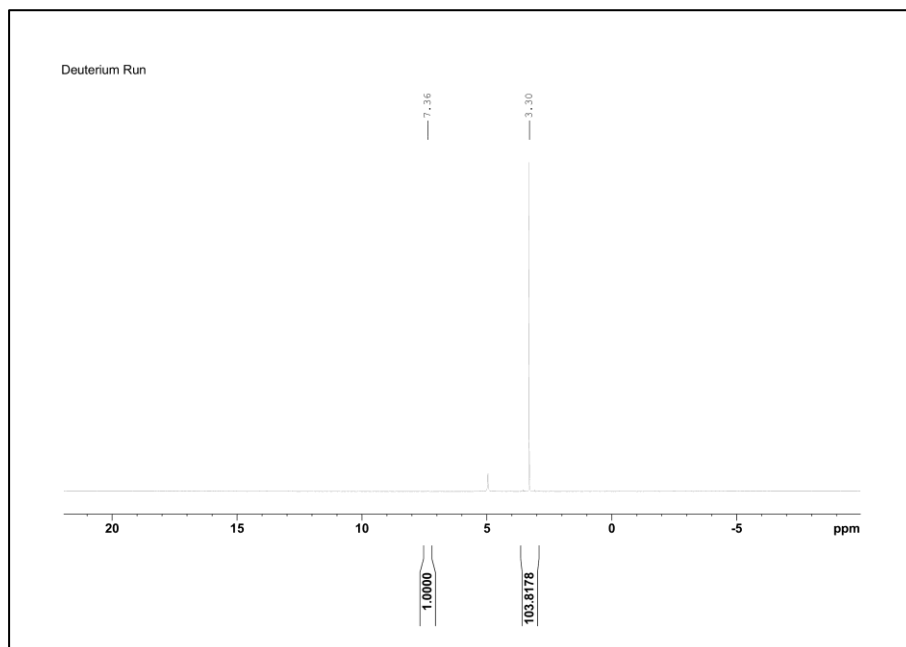
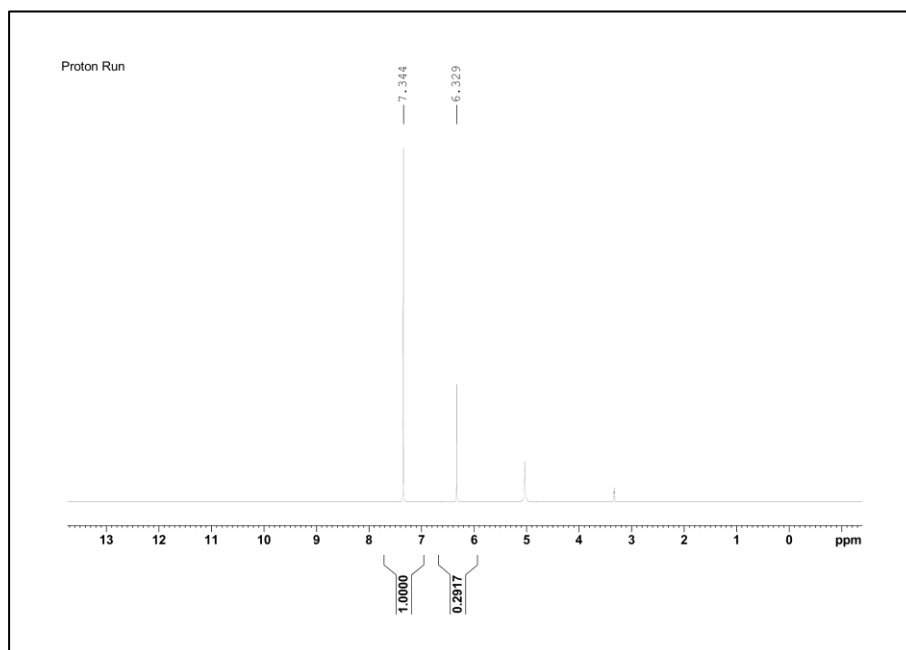
Table 2-12

Entry 1



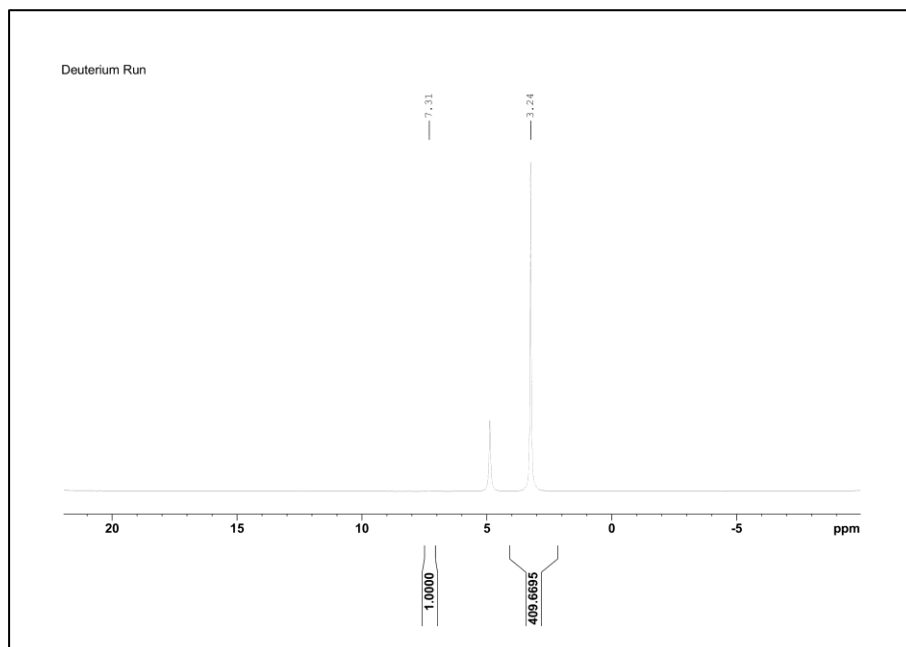
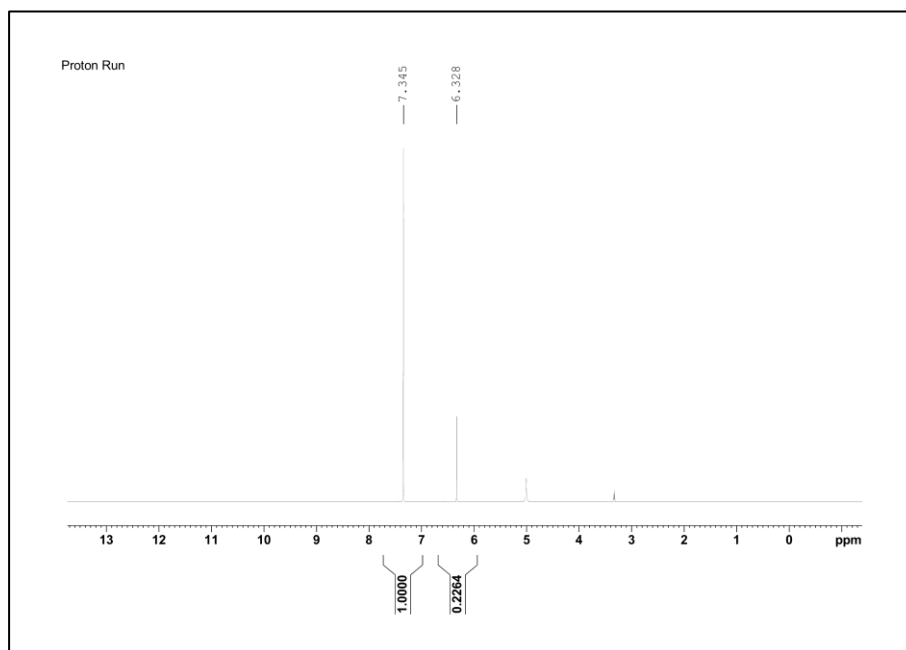
<i>Mass maleic acid (mg)</i>	<i>mmol maleic acid</i>	<i>Mass methanol- d4 (mg)</i>	<i>mmol methanol- d4</i>	<i>Mass benzene (mg)</i>
11	0.0948	588	16.3	20

Entry 2



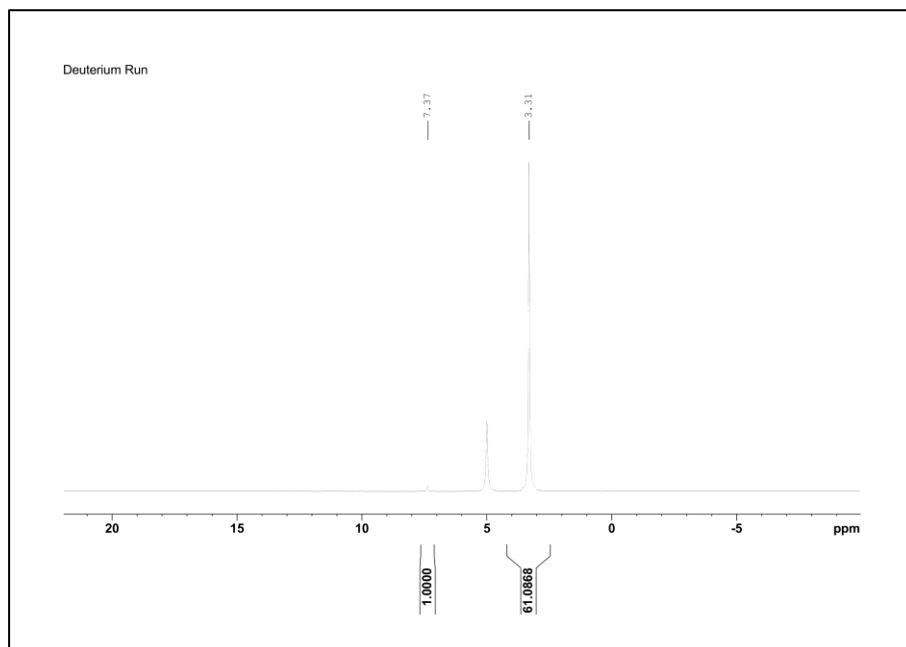
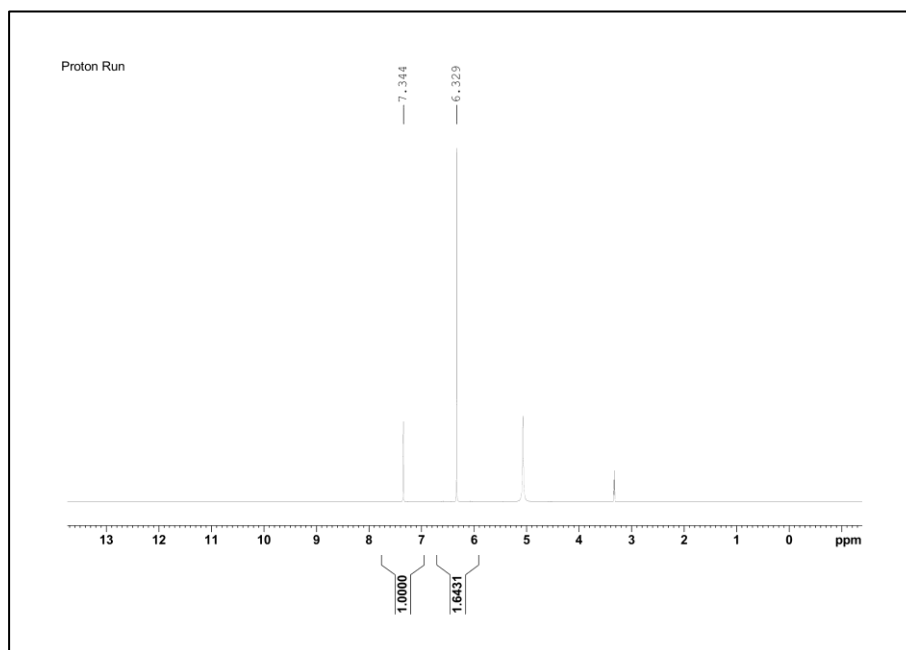
<i>Mass maleic acid (mg)</i>	<i>mmol maleic acid</i>	<i>Mass methanol- d4 (mg)</i>	<i>mmol methanol- d4</i>	<i>Mass benzene (mg)</i>
13.2	0.114	590	16.3	20

Entry 3



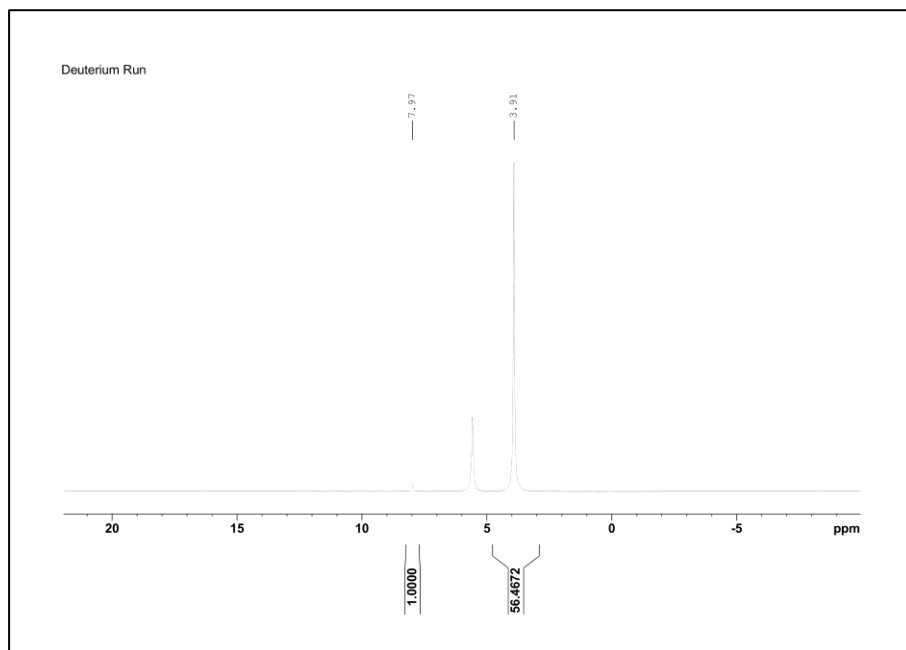
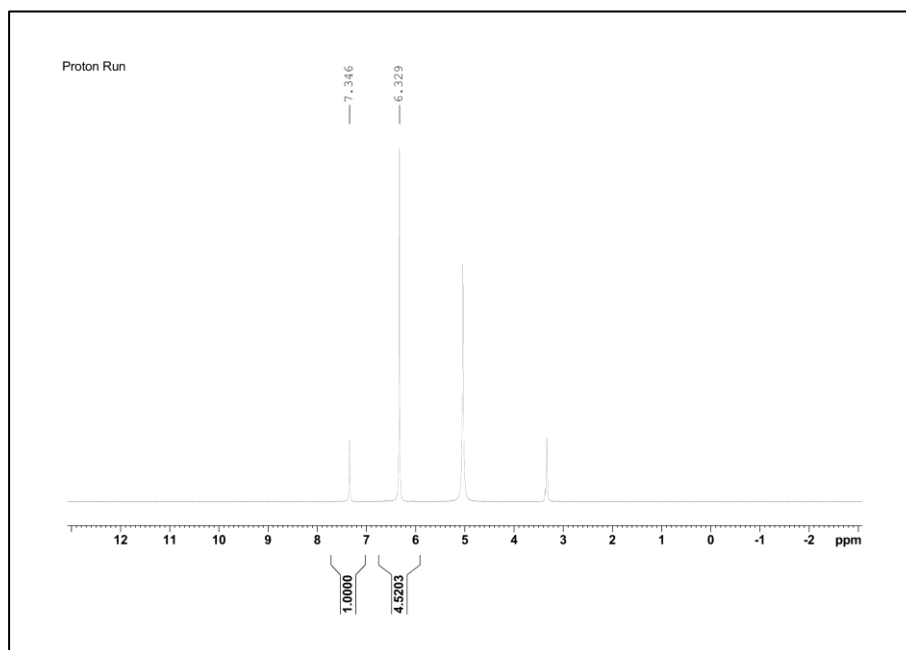
<i>Mass maleic acid (mg)</i>	<i>mmol maleic acid</i>	<i>Mass methanol- d4 (mg)</i>	<i>mmol methanol- d4</i>	<i>Mass benzene (mg)</i>
11.1	0.0956	596	16.5	17

Entry 4



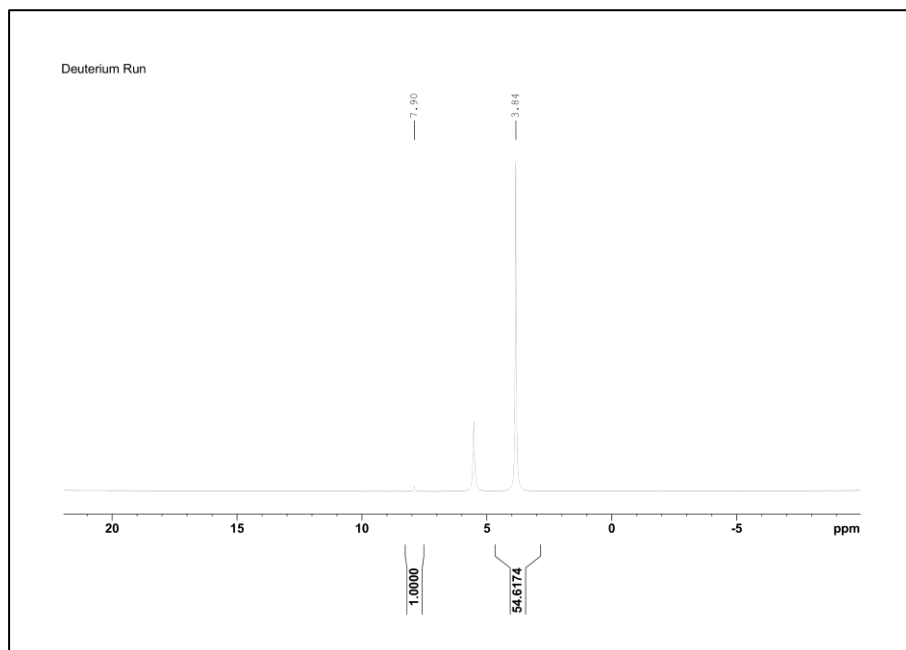
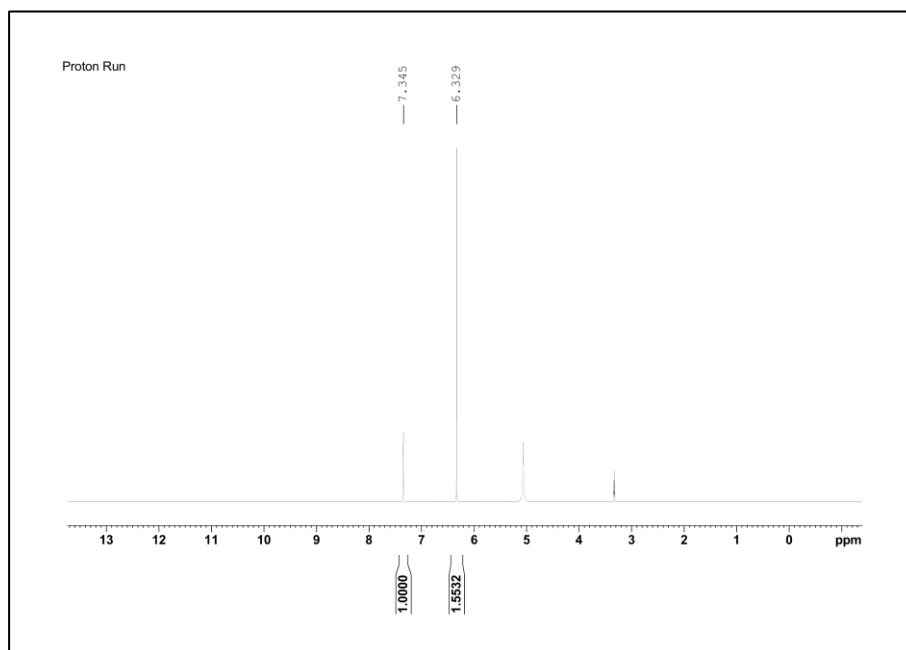
<i>Mass maleic acid (mg)</i>	<i>mmol maleic acid</i>	<i>Mass methanol- d4 (mg)</i>	<i>mmol methanol- d4</i>	<i>Mass benzene (mg)</i>
12.9	0.111	604	16.7	16

Entry 5



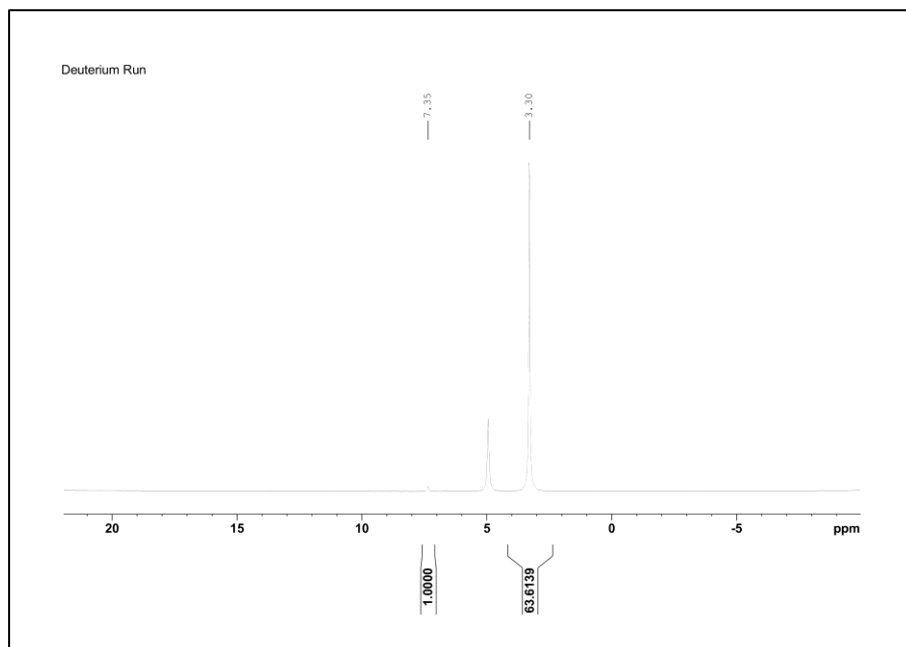
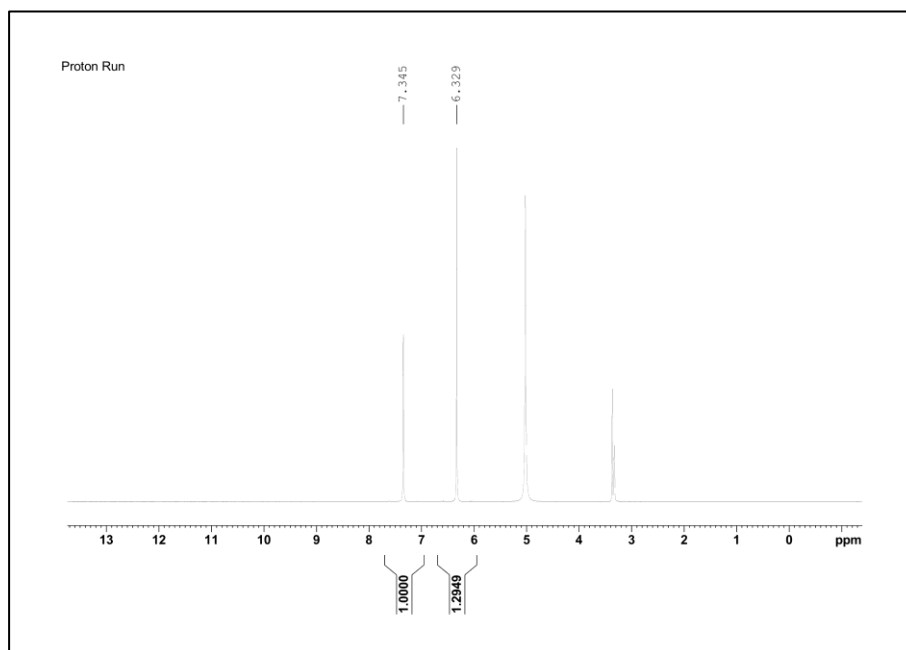
<i>Mass maleic acid (mg)</i>	<i>mmol maleic acid</i>	<i>Mass methanol- d4 (mg)</i>	<i>mmol methanol- d4</i>	<i>Mass benzene (mg)</i>
13.5	0.116	596	16.5	16

Entry 6



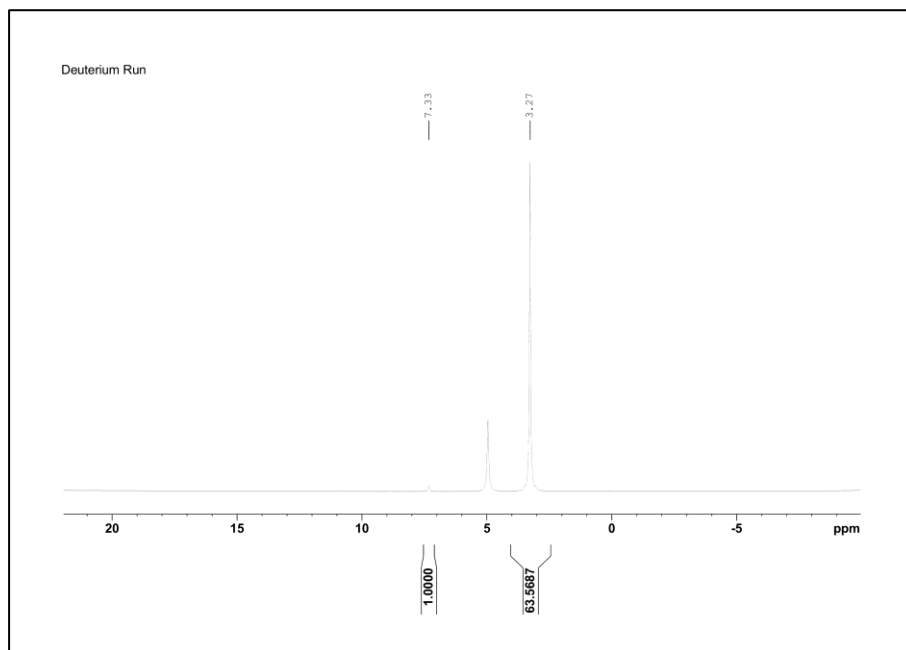
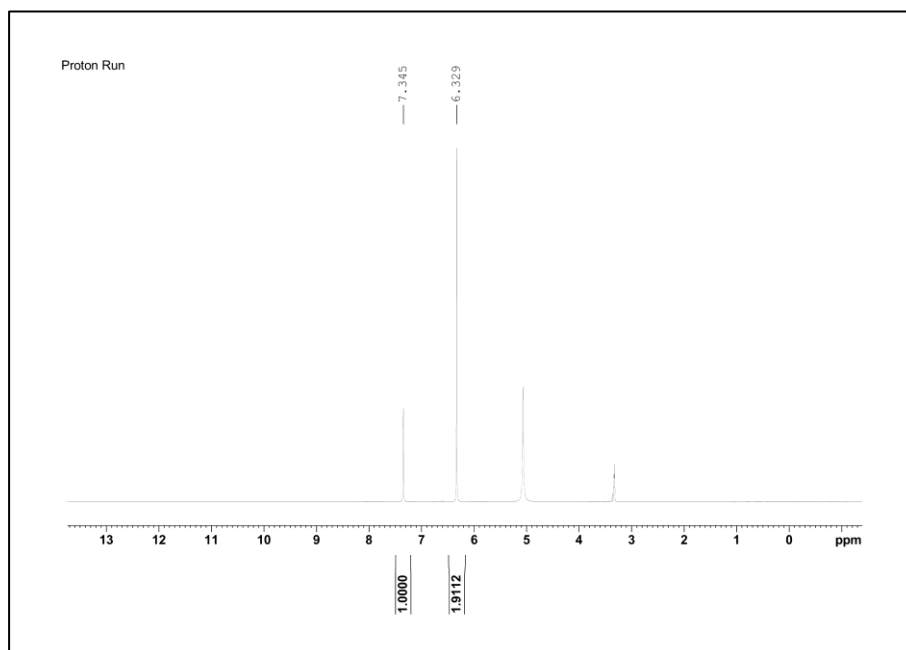
<i>Mass maleic acid (mg)</i>	<i>mmol maleic acid</i>	<i>Mass methanol- d4 (mg)</i>	<i>mmol methanol- d4</i>	<i>Mass benzene (mg)</i>
17.8	0.153	617	17.1	15

Entry 7



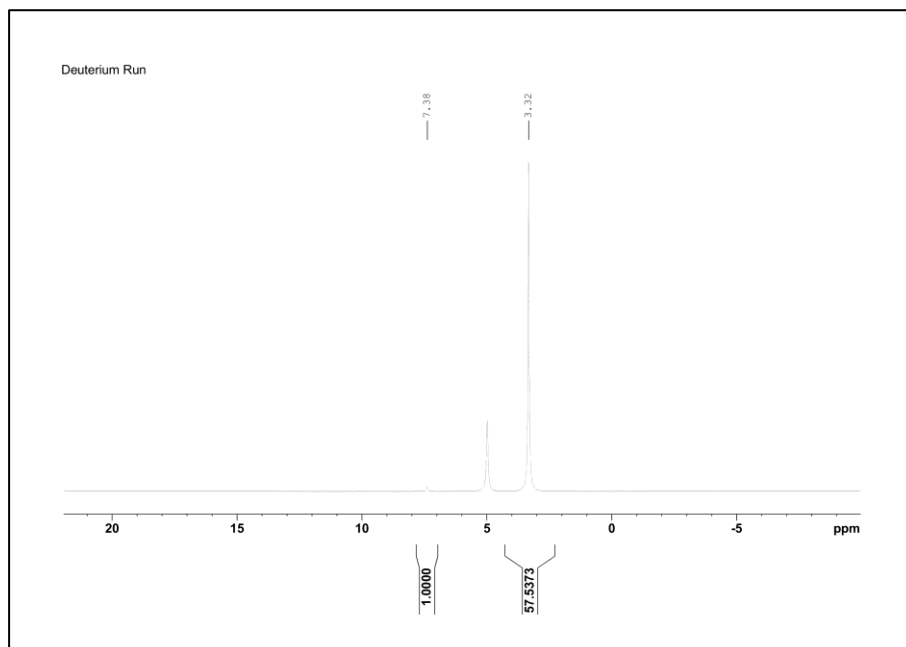
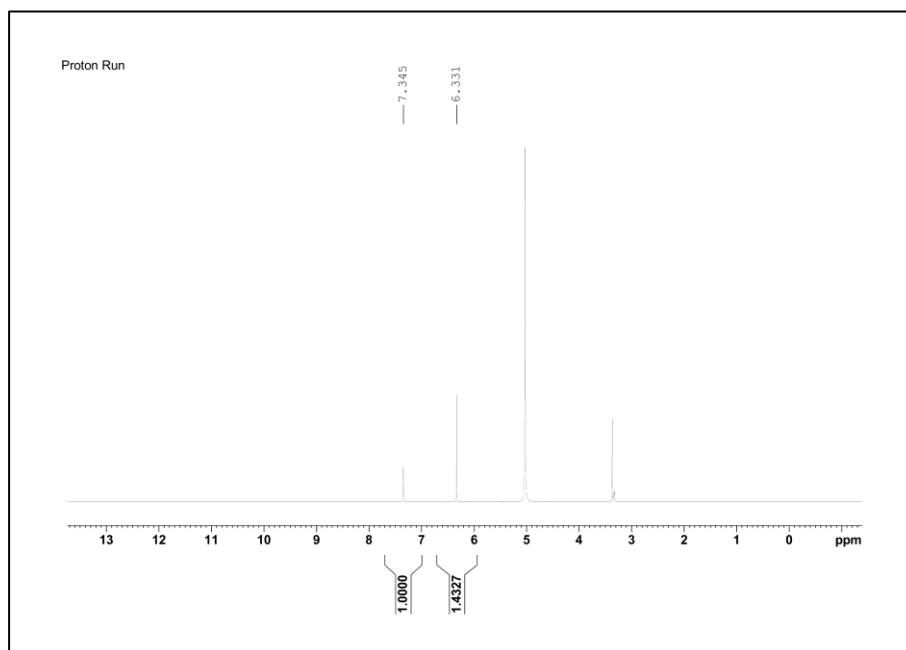
<i>Mass maleic acid (mg)</i>	<i>mmol maleic acid</i>	<i>Mass methanol- d4 (mg)</i>	<i>mmol methanol- d4</i>	<i>Mass benzene (mg)</i>
12.4	0.107	596	16.5	16

Entry 8



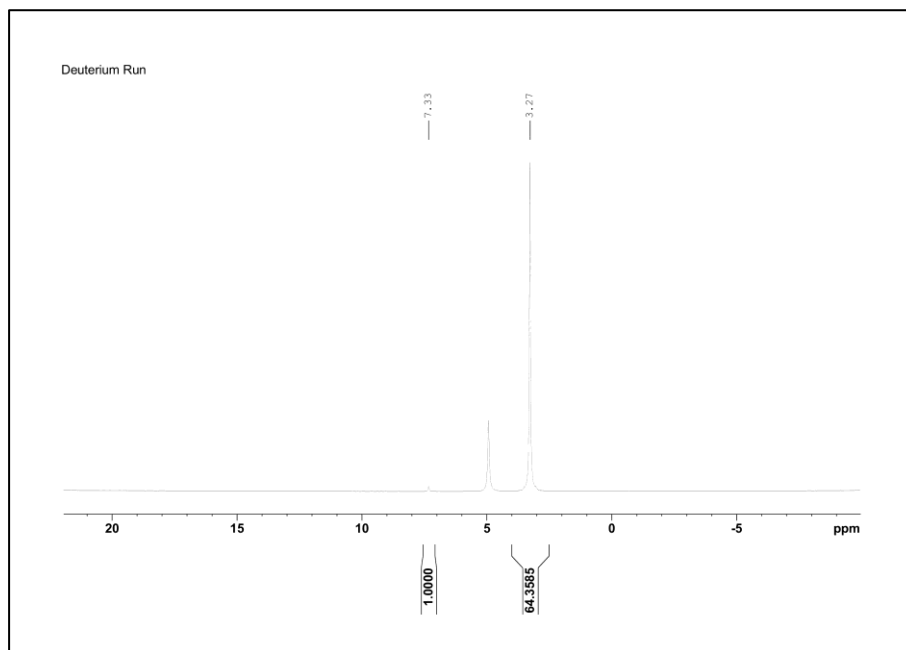
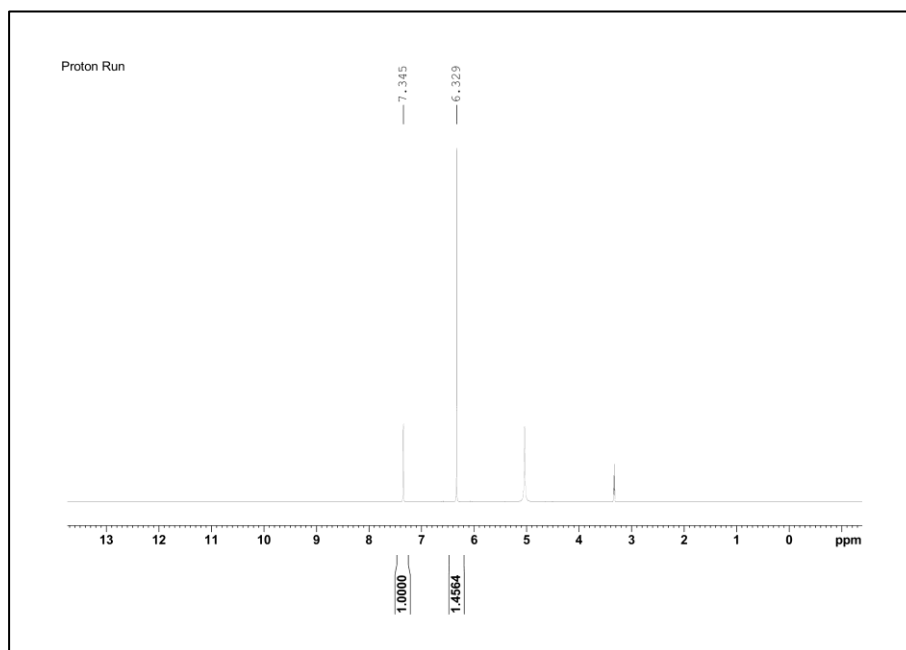
<i>Mass maleic acid (mg)</i>	<i>mmol maleic acid</i>	<i>Mass methanol- d4 (mg)</i>	<i>mmol methanol- d4</i>	<i>Mass benzene (mg)</i>
17.8	0.153	588	16.3	16

Entry 9



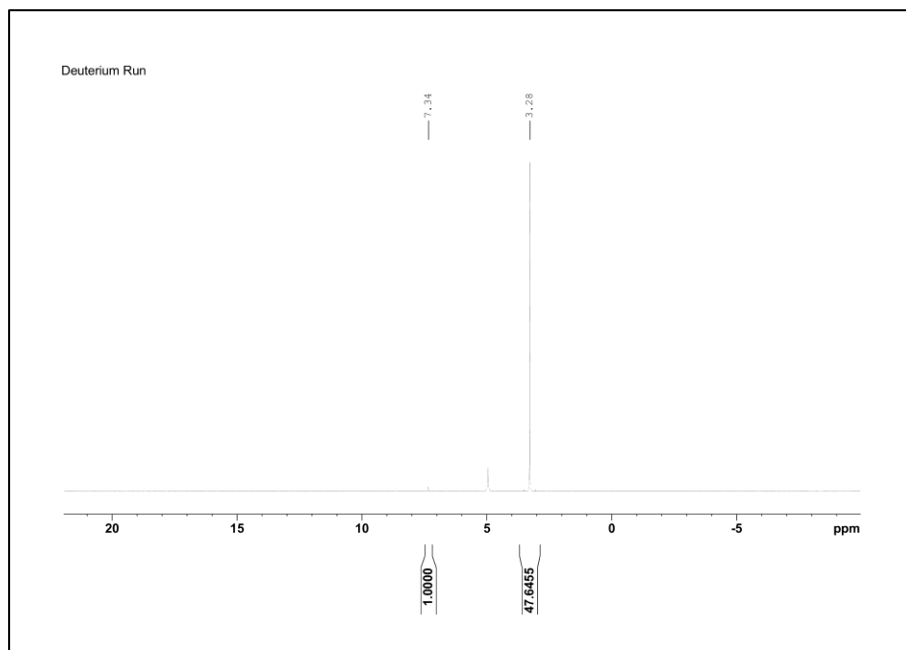
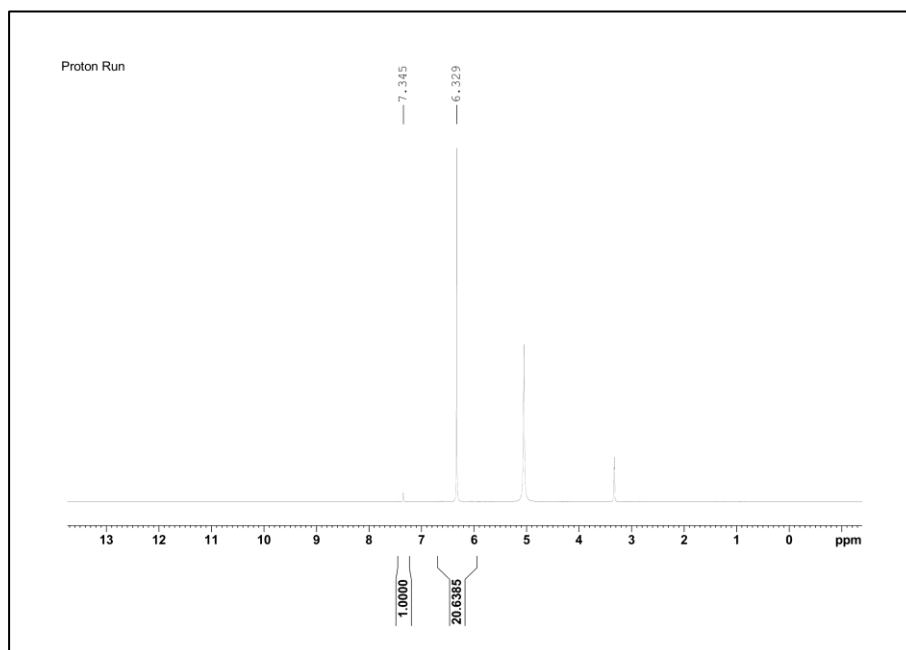
<i>Mass maleic acid (mg)</i>	<i>mmol maleic acid</i>	<i>Mass methanol- d4 (mg)</i>	<i>mmol methanol- d4</i>	<i>Mass benzene (mg)</i>
16.5	0.142	593	16.4	13

Entry 10



<i>Mass maleic acid (mg)</i>	<i>mmol maleic acid</i>	<i>Mass methanol- d4 (mg)</i>	<i>mmol methanol- d4</i>	<i>Mass benzene (mg)</i>
15.7	0.135	579	16.0	14

Scheme 2-1



<i>Mass maleic acid (mg)</i>	<i>mmol maleic acid</i>	<i>Mass methanol- d4 (mg)</i>	<i>mmol methanol- d4</i>	<i>Mass benzene (mg)</i>
13.8	0.119	600	16.6	17